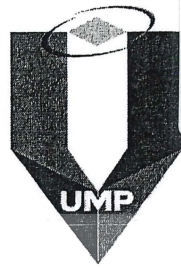


original  
13D  
RDU 0903100



PERPUSTAKAAN UMP  
0000100663

Malaysia  
**PAHANG**  
Engineering • Technology • Creativity

**HEAT TRANSFER AUGMENTATION WITH  
ALUMINIUM OXIDE NANOFLUID IN A PLAIN TUBE  
AND WITH INSERTS**

**(PENAMBAHAN KADAR PEMINDAHAN HABA MENGGUNAKAN  
BENDALIR-NANO ALUMINIUM OKSIDA DALAM TIUB BIASA DAN  
DENGAN SISIPAN)**

**PROF. DR. KORADA VISWANATHA SHARMA  
(PROJECT LEADER)**

**WAN AZMI BIN WAN HAMZAH  
PROF. DR. ROSLI ABU BAKAR  
MUHAMMAD MAT NOOR  
KUMARAN KADIRGAMA  
DR. D.M REDDY PRASAD  
MOHD IRZA PAIRUZ BIN ZAMRI**

**RESEARCH VOTE NO:  
RDU 0903100**

**Faculty of Mechanical Engineering  
Universiti Malaysia Pahang**

100663

2011



## PUSAT PENGURUSAN PENYELIDIKAN (RMC)

### BORANG PENGESAHAN LAPORAN AKHIR PENYELIDIKAN

TAJUK PROJEK : HEAT TRANSFER AUGMENTATION WITH ALUMINIUM OXIDE  
NANOFLUID IN A PLAIN TUBE AND WITH INSERTS

Saya :

**PROF. DR. KORADA VISWANATHA SHARMA**  
(HURUF BESAR)

Mengaku membenarkan **Laporan Akhir Penyelidikan** ini disimpan di Perpustakaan Universiti Malaysia Pahang dengan syarat-syarat kegunaan seperti berikut :

1. Laporan Akhir Penyelidikan ini adalah hakmilik Universiti Malaysia Pahang
2. Perpustakaan Universiti Malaysia Pahang dibenarkan membuat salinan untuk tujuan rujukan sahaja.
3. Perpustakaan dibenarkan membuat penjualan salinan Laporan Akhir Penyelidikan ini bagi kategori TIDAK TERHAD.
4. \* Sila tandakan ( / )

SULIT

(Mengandungi maklumat yang berdarjah keselamatan atau Kepentingan Malaysia seperti yang termaktub di dalam AKTA RAHSIA RASMI 1972).

TERHAD

(Mengandungi maklumat TERHAD yang telah ditentukan oleh Organisasi/badan di mana penyelidikan dijalankan).

TIDAK  
TERHAD

Tandatangan & Cop Ketua Penyelidik

*K. V. Sharma*

**DR. KORADA VISWANATHA SHARMA**  
FACULTY OF MECHANICAL ENGINEERING  
UNIVERSITI MALAYSIA PAHANG  
26060 PERANG, PAHANG MALAYSIA  
TEL: 06-424 2324 FAKS: 06-424 2202

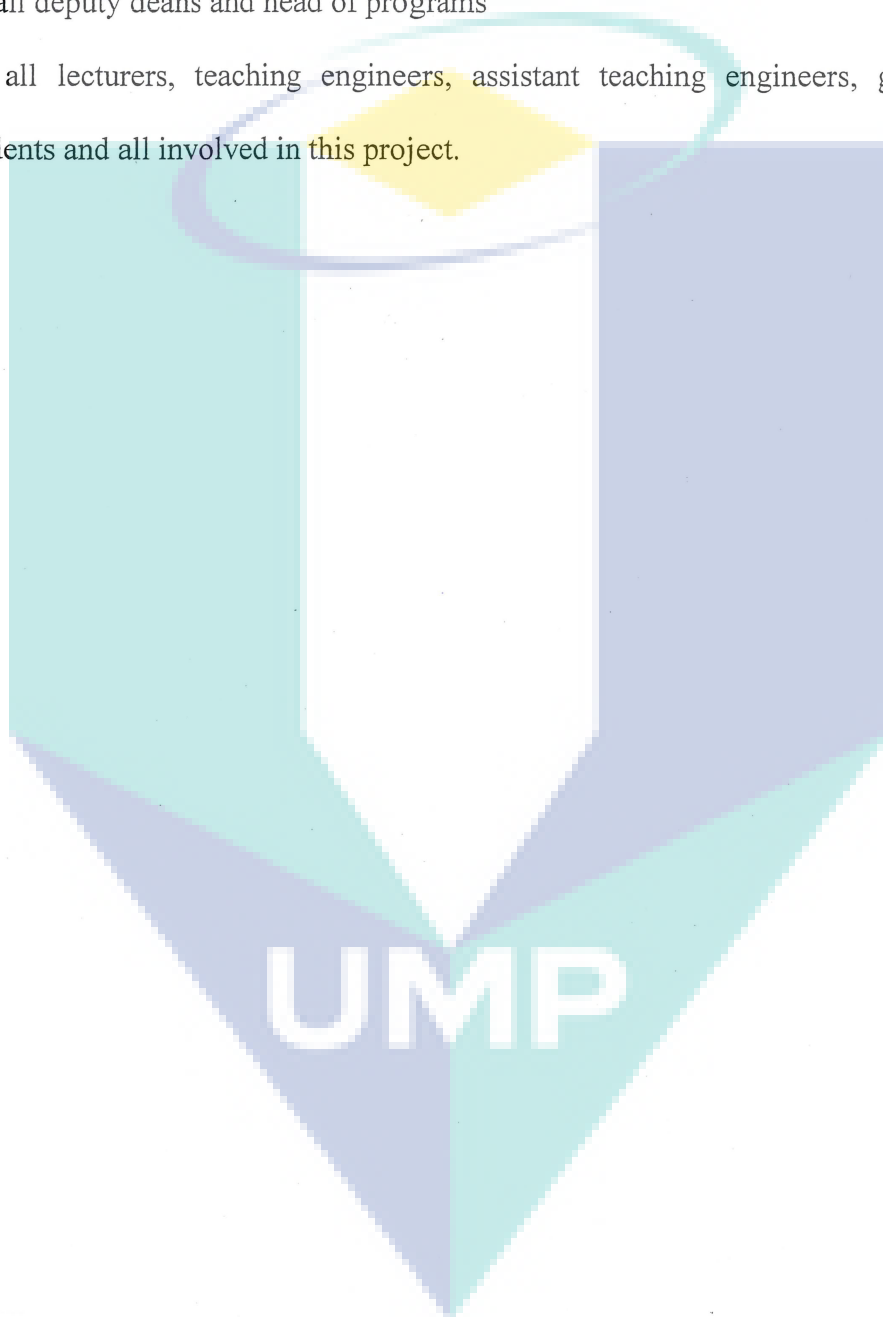
Tarikh : 3/03/2011

**CATATAN :** \* Jika Laporan Akhir Penyelidikan ini SULIT atau TERHAD, sila lampirkan surat daripada pihak berkuasa/organisasi berkenaan dengan menyatakan sekali sebab dan tempoh laporan ini perlu dikelaskan sebagai SULIT dan TERHAD.

## ACKNOWLEDGEMENTS

For the development and production of this report, we feel a deep sense of gratitude:

- To Professor Dr. Rosli Abu Bakar – Dean, Faculty of Mechanical Engineering.
- To all deputy deans and head of programs
- To all lecturers, teaching engineers, assistant teaching engineers, graduate students and all involved in this project.



## ABSTRACT

### HEAT TRANSFER AUGMENTATION WITH ALUMINIUM OXIDE NANOFLUID IN A PLAIN TUBE AND WITH INSERTS

*(Keywords: nanofluids, heat transfer augmentation, twisted tapes)*

Theoretical investigation of nanofluid heat transfer under turbulent flow in a tube has been undertaken for a wide range of Reynolds number. A model is proposed for the development of eddy diffusivity equation applicable to nanofluids. The numerical results obtained from the model are compared with the experimental data of different investigators. Equations are developed for the estimation of thermo-physical properties of nanofluids for input parameters viz., temperature, nano particle size and concentration. The viscosity of nanofluid is observed to increase with particle size and decrease with temperature, whereas the thermal conductivity decreases with particle size and increases with temperature. It is found that the values of heat transfer coefficients evaluated with the equations are in good agreement with the experimental results. The theoretical determination of Nusselt number for flow in a tube with twisted tape insert has been undertaken for the first time. The results obtained for flow in a tube with twisted tape are in good agreement with the experimental data. Relevant regression equations are developed for the estimation of Nusselt number. The Colburn type equation is developed for the prediction of Nusselt number where the friction factors are to be estimated with the Blasius equation;

$$St Pr_w^{2/3} = \frac{f}{8} (1 + \phi Pr_w)^{0.1185}$$

$$Nu = 0.0304 Re^{0.7853} Pr^{0.4} [0.001 + \phi]^{0.01398}$$

$$St Pr^{2/3} = 1.0344 \left( \frac{f_u}{8} \right) (1.0 + \phi)^{0.1479} \left( 1.0 + \frac{D}{H} \right)^{0.2445} \quad \text{where}$$

$$f_u = 0.4818 Re^{-0.2731} (0.001 + \phi)^{0.00061} (0.001 + D/H)^{0.0296}$$

The Nusselt number estimated with these equations predict are validated for water base nanofluids for  $\phi \leq 3.7\%$ ,  $3000 \leq Re \leq 70000$  and  $1.4 \leq Pr \leq 10.0$ . An experimental setup for the estimation of forced convection heat transfer coefficients is designed, commissioned and in working condition. All the three objectives envisaged in the project are achieved.

## ABSTRAK

### PENAMBAHAN KADAR PEMINDAHAN HABA MENGGUNAKAN BENDALIR-NANO ALUMINIUM OKSIDA DALAM TIUB BIASA DAN DENGAN SISIPAN

(Kata kunci: nano-bendalir, penambahan pemindahan haba, pita bengkok)

Kajian teori berkaitan pemindahan haba nano-bendalir untuk aliran gelora dalam tiub biasa telah dijalankan untuk nombor Reynolds dalam julat yang besar. Sebuah model telah dicadangkan untuk pembangunan persamaan peresapan eddy yang amat berguna kepada bendalir-nano. Keputusan berangka yang diperolehi daripada model dibandingkan dengan data eksperimen yang dihasilkan oleh penyelidik yang berlainan. Persamaan-persamaan untuk menganggar sifat-sifat termo-fizikal bendalir-nano telah dihasilkan dengan menggunakan parameter-parameter masukan berikut iaitu suhu, saiz zarah nano dan kepekatan. Kelikatan bendalir-nano didapati meningkat dengan pertambahan saiz zarah, dan menurun dengan pertambahan suhu, sedangkan konduktiviti haba menurun dengan pertambahan saiz zarah dan meningkat dengan suhu. Nilai-nilai pekali pemindahan haba yang dikira menggunakan persamaan-persamaan tadi didapati mempunyai keputusan yang sama dengan data daripada eksperimen. Penentuan nilai teori nombor Nusselt untuk aliran dalam tiub biasa bersama sisipan pita bengkok telah dilakukan untuk pertama kalinya. Keputusan yang diperolehi untuk aliran dalam tiub biasa bersama sisipan pita bengkok memberikan nilai yang menyamai dengan data eksperimen. Persamaan-persamaan regresi yang berkaitan telah dibangunkan untuk menganggar nombor Nusselt. Persamaan jenis Colburn dihasilkan untuk mengira nombor Nusselt; di mana pekali-pekali geseran dianggarkan menggunakan persamaan Blasius

$$St Pr_w^{2/3} = \frac{f}{8} (1 + \phi Pr_w)^{0.1185}$$

$$Nu = 0.0304 Re^{0.7853} Pr^{0.4} [0.001 + \phi]^{0.01398}$$

$$St Pr^{2/3} = 1.0344 \left( \frac{f_u}{8} \right) (1.0 + \phi)^{0.1479} \left( 1.0 + \frac{D}{H} \right)^{0.2445} \quad \text{di mana}$$

$$f_u = 0.4818 Re^{-0.2731} (0.001 + \phi)^{0.00061} (0.001 + D/H)^{0.0296}$$

Nombor Nusselt dikira menggunakan persamaan-persamaan anggaran ini disahkan untuk bendalir-nano berasaskan air bagi keadaan  $\phi \leq 3.7\%$ ,  $3000 \leq Re \leq 70000$  dan  $1.4 \leq Pr \leq 10.0$ . Sebuah eksperimen untuk menganggar pekali pemindahan haba olakan paksa telah direkabentuk, dipasang dan berfungsi dengan baik. Ketiga-tiga objektif yang telah disasarkan dalam projek ini semuanya telah berjaya dicapai.

A logo for the Key Researcher section, featuring a yellow diamond shape at the top, a teal oval shape below it, and a white vertical bar in the center. The background is a light blue and teal gradient.

**Key Researcher:**

Dr. Korada Viswanatha Sharma, Professor, FKM, UMP

**Co-Researcher:**

Wan Azmi bin Wan Hamzah, Lecturer, FKM, UMP  
Dr. Rosli Abu Bakar, Professor, FKM, UMP  
Muhammad Mat Noor, Senior Lecturer, FKM, UMP  
Kumaran Kadirgama, Senior Lecturer, FKM, UMP  
Dr. D.M Reddy Prasad, Senior Lecturer, FKKSA, UMP  
Mohd Irza Pairuz bin Zamri, Research Officer, AEC, UMP

E-mail : [kvsharma@ump.edu.my](mailto:kvsharma@ump.edu.my)  
Tel. No. : +6094242324  
Vote No. : RDU 0903100

**UMP**

## TABLE OF CONTENTS

		Page
<b>ACKNOWLEDGEMENTS</b>		ii
<b>ABSTRACT</b>		iii
<b>ABSTRAK</b>		iv
<b>TABLE OF CONTENTS</b>		vi
<b>LIST OF FIGURES</b>		viii
<b>LIST OF TABLES</b>		xi
<b>LIST OF SYMBOLS</b>		xii
<b>LIST OF ABBREVIATIONS</b>		xiv
<b>CHAPTER</b>		
1	<b>INTRODUCTION</b>	1
	1.1 Background	1
	1.2 Problem Statement	2
	1.3 Objectives of the Research	2
2	<b>LITERATURE REVIEW</b>	4
	2.1 Introduction	4
	2.2 Heat Transfer Coefficient In A Plain Tube	5
	2.2.1 Forced Convection in a Plain Tube - Numerical Studies	5
	2.2.2 Forced Convection in a Plain Tube – Experimental determination	6
	2.3 Heat Transfer Coefficient With Twisted Tapes	9
	2.3.1 Forced Convection With Twisted Tape – Experimental Determination	9
	2.3.2 Forced Convection With Twisted Tapes - Theoretical Analysis	11
	2.4 Analogies Between Momentum And Heat Transfer	13
3	<b>METHODOLOGY</b>	15
	3.1 Introduction	15
	3.2 Experiments With Flow In A Plain Tube	16
	3.2.1 Evaluation Of Nanofluid Friction Factor: Blasius Equation	16
	3.2.2 Equations For The Evaluation Of Nusselt Number	17
	3.3 Model For Turbulent Flow In A Plain Tube	18
	3.4 Model For Turbulent Flow With Twisted Tape Inserts	19
	3.4.1 Experiments With Tape Insert In A Tube	19
	3.4.2 Friction Factor Of Water And Nanofluid	21

4	<b>EXPERIMENTAL SETUP</b>	23
	4.1 Introduction	23
	4.2 Experiment Apparatus	25
	4.2.1 Chiller	25
	4.2.2 Reservoir	26
	4.2.3 Pump And Motor	26
	4.2.4 Flow Meter	27
	4.2.5 Heater And Copper Tube	28
	4.2.6 Control Panel	28
	4.2.7 Insulating Material	29
	4.2.8 Thermocouples	29
	4.2.9 U-Tube Manometer	30
	4.2.10 Twisted Tape Insert	30
	4.3 Nanofluid Preparation	31
	4.4 Experimentation Procedure	32
5	<b>RESULTS AND DISCUSSION</b>	34
	5.1 Validation Of Thermo-Physical Properties	34
	5.2 Development Of Regression Equation Of Colburn Type	37
	5.3 Theoretical Analysis: Nanofluid Flow In A Tube	42
	5.4 Theoretical Analysis: Nanofluid Flow With Tape Inserts	51
6	<b>CONCLUSION</b>	59
	6.1 Salient Points	59
	6.2 Recommendation And Future Work	60
	<b>REFERENCES</b>	61
	<b>LIST OF PUBLICATIONS</b>	68



UMP



## LIST OF FIGURES

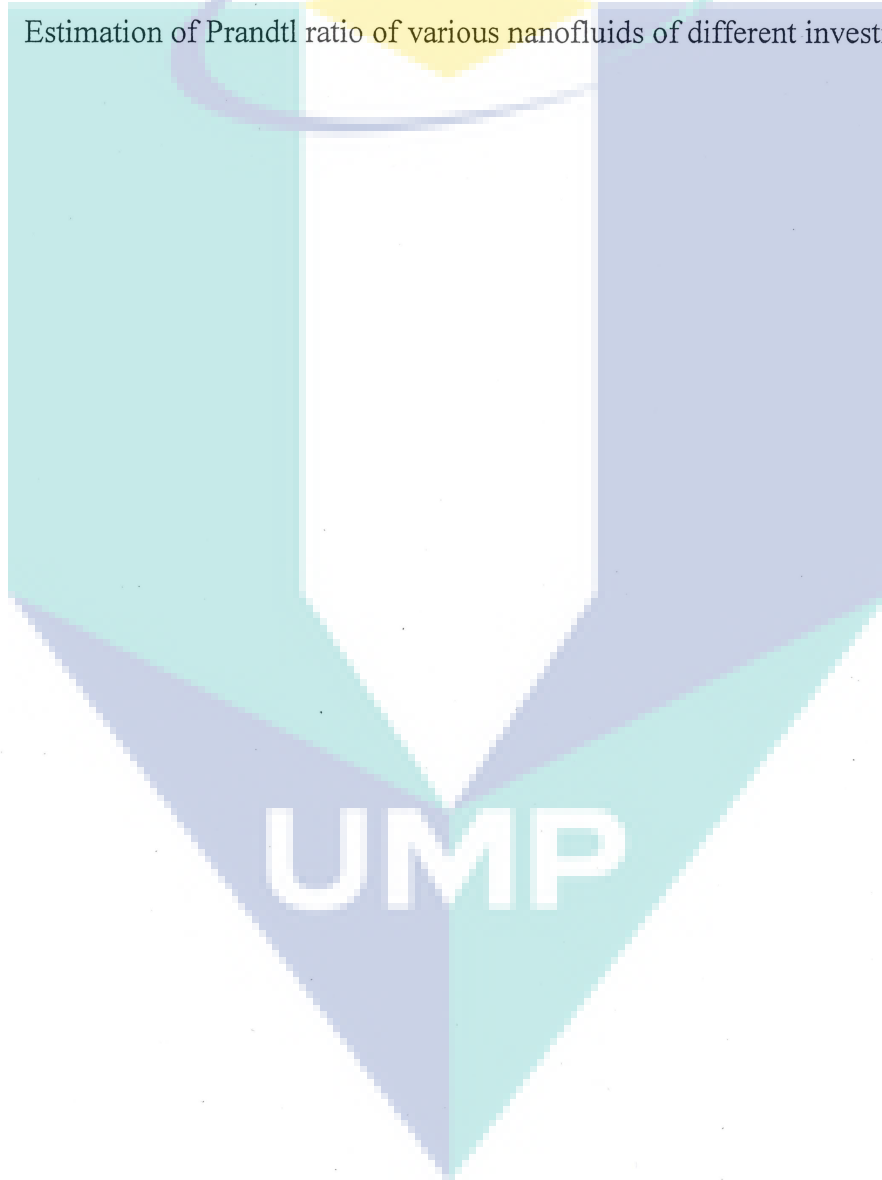
Figure No	Title	Page
3.1	Schematic diagram of twisted tape in a tube	20
4.1	Schematic diagram of the experimental setup	23
4.2	Fabricated experiment apparatus	24
4.3	Chiller	26
4.4	Reservoir	26
4.5	Pump with electric motor	27
4.6	Flow meter	27
4.7	Test Section wrapped with heating coils	28
4.8	Control Panel	29
4.9	Thermocouple	30
4.10	U-Tube Manometer	30
4.11	Full-length twisted tape and insert	31
4.12	Nanofluid prepared for various concentrations	32
5.1	Validation of experimental data for thermal conductivity and viscosity with equations	35
5.2	Variation of bulk temperature with particle diameter – Effect of concentration	35
5.3	Variation of bulk temperature with particle diameter – Effect of Prandtl number	36
5.4	Variation of Prandtl number with particle diameter – Effect of $\phi$ and bulk temperature	36
5.5	Comparison of experimental data with present equation for Nusselt number	38

Figure No	Title	Page
5.6	Comparison of experimental data with present equation and other equations for water	38
5.7	Comparison of experimental Nusselt number with present equation for CuO/water nanofluid	39
5.8	2 Comparison of experimental Nusselt number with present equation for Al <sub>2</sub> O <sub>3</sub> /water nanofluids	39
5.9	Comparison of experimental Nusselt number with present equation for SiC/water nanofluids	40
5.10	Comparison of experimental Nusselt number with present equation for Al <sub>2</sub> O <sub>3</sub> /water and ZrO <sub>2</sub> /water nanofluids	40
5.11	Comparison of experimental Nusselt number with present equation for Cu/water nanofluids	41
5.12	Comparison of experimental Nusselt number with present equation for TiO <sub>2</sub> /water nanofluid	41
5.13	Comparison of experimental data with theory and other equations for water	44
5.14	Comparison of experimental Nusselt number with theory for Cu/water nanofluid	45
5.15	Comparison of experimental heat transfer coefficients with theory for Cu/water nanofluid	45
5.16	Comparison of experimental Nusselt number with theory for CuO/water nanofluid	46
5.17	Comparison of experimental heat transfer coefficients with theory for CuO/water nanofluid	46
5.18	Comparison of experimental heat transfer coefficients with theory for Al <sub>2</sub> O <sub>3</sub> /water and ZrO <sub>2</sub> /water nanofluids	47
5.19	Comparison of experimental Nusselt number with theory for Al <sub>2</sub> O <sub>3</sub> /water and ZrO <sub>2</sub> /water nanofluids	47
5.20	Comparison of experimental heat transfer coefficients with theory for SiC/water nanofluid	48
5.21	Comparison of theory with Eq.(13) of Duangthongsuk and Wongwises (2010)	48

Figure No	Title	Page
5.22	Comparison of experimental Nusselt number with theory for TiO <sub>2</sub> /water nanofluid	49
5.23	Variation of Prandtl number with temperature for different particle size and $\phi$	49
5.24	Influence of twist ratio and Prandtl number on Nusselt number of water	53
5.25	Influence of twist ratio and concentration on Nusselt number for Pr=6.2	53
5.26	Comparison of Nusselt number of various investigators with the present theory	54
5.27	Comparison of experimental data of air with the present theory for different twist	54
5.28	Comparison of experimental data of nanofluid at different concentrations and twist ratios	55
5.29	Variation of friction factor at different concentrations and twist ratios	55
5.30	Variation of eddy diffusivity coefficient for water at different twist ratios	56
5.31	Variation of Prandtl index with concentration and twist ratio	56
5.32	Variation of dimensionless temperature with distance	57
5.33	Variation of temperature gradient with concentration and twist ratio	57
5.34	Comparison of experimental data with the proposed equation for flow in a tube and for tape insert	58

**LIST OF TABLES**

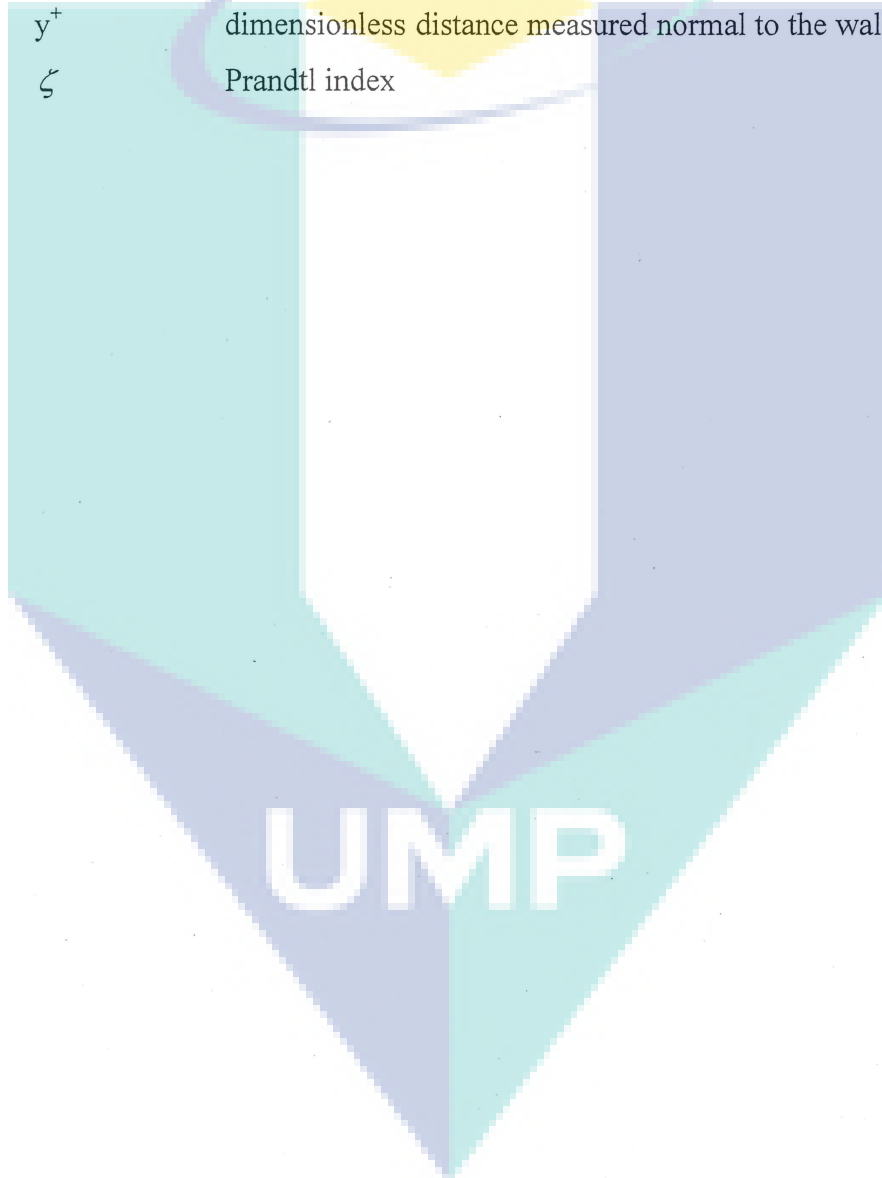
<b>Table No</b>	<b>Title</b>	<b>Page</b>
4.1	List of components used in the fabrication of the experimental setup	25
4.2	Insulators and temperature range of applicability	29
4.3	Summary of materials and equipments required for the experiment	33
5.1	Estimation of Prandtl ratio of various nanofluids of different investigators	50

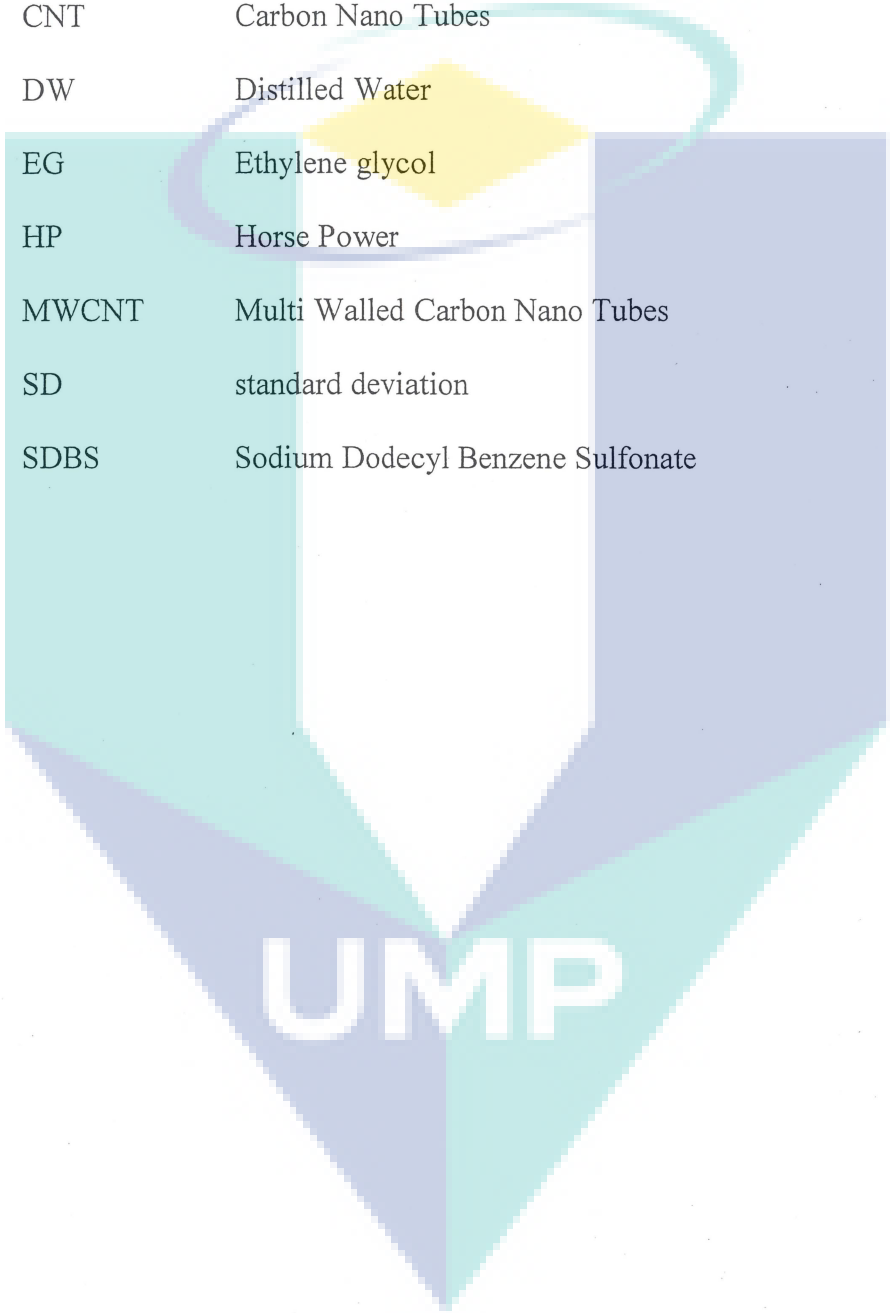


## LIST OF SYMBOLS

$B$	eddy diffusivity coefficient
$b$	bulk
$C$	specific heat, J/kg K
$C_f$	Fanning friction factor
$D$	inner diameter of the tube, m
$d$	diameter of nanoparticle, (m)
$\delta$	thickness of strip, m
$\varepsilon_H$	Thermal eddy diffusivity, ( $\text{m}^2/\text{s}$ )
$\varepsilon_m$	Momentum eddy diffusivity, ( $\text{m}^2/\text{s}$ )
$f$	friction coefficient
$\phi$	volume fraction of nanoparticles (%)
$g$	gravitational force acceleration, $\text{m}^2/\text{s}$
$H$	pitch for $180^\circ$ rotation, m
$h$	mean heat transfer coefficient, $\text{W}/(\text{m}^2\text{K})$
$H/D$	twist ratio, dimensionless
$j$	Colburn factor
$K$	thermal conductivity, $\text{J}/(\text{K m})$
$\mu$	absolute viscosity, $\text{kg}/(\text{m.s})$
$nf$	nanofluid
$Pr$	Prandtl number,
$p$	nanoparticle
$\Delta P$	pressure difference
$Re$	Reynolds number
$R^+$	dimensionless radius
$\rho$	density, ( $\text{kg}/\text{m}^3$ )
$St$	Stanton number
$T$	temperature, $^\circ\text{C}$
$\tau_{wall}$	wall shear stress
$T^+$	dimensionless temperature

$u$	velocity, (m/s)
$u^*$	shear velocity
$u^+$	dimensionless velocity, $(u/u^*)$
$V$	average fluid velocity, m/s
$\nu$	Kinematic viscosity, $(m^2/s)$
$w$	water
$y$	distance measured normal to the wall, (m)
$y^+$	dimensionless distance measured normal to the wall,
$\zeta$	Prandtl index



**LIST OF ABBREVIATIONS**

AD	average deviation
CFD	Computational Fluid Dynamic
CNT	Carbon Nano Tubes
DW	Distilled Water
EG	Ethylene glycol
HP	Horse Power
MWCNT	Multi Walled Carbon Nano Tubes
SD	standard deviation
SDBS	Sodium Dodecyl Benzene Sulfonate

## CHAPTER 1

### INTRODUCTION

#### 1.1 BACKGROUND

Heat transfer fluids such as water, mineral oils and ethylene glycol play an important role in many industrial sectors including power generation, chemical production, air-conditioning, transportation and microelectronics. The performance of these conventional heat transfer fluids is often limited by their low thermal conductivities. Driven by industrial needs of process intensification and device miniaturization, development of high performance heat transfer fluids has been a subject of numerous investigations in the past.

Various methods for heat transfer enhancements have been developed over the years either to accommodate high heat fluxes in the limited area available or to reduce the size and consequently the cost in order to compete in the global market. This augmentation of heat transfer can be achieved through active and passive methods. In the classification under active type, heat transfer enhancement is associated using external energy on the fluid through forced flow/vibration/injection/suction/jet impingement and the use of electrostatic fields. Under passive augmentation, enhancement of heat transfer can be due to artificially roughed surface, extended surface, swirl flow with twisted tape inserts, convoluted or twisted tube, use of additives in liquids and gases.

Passive method of heat transfer enhancement is advantageous to achieve high heat transfer rates with minimum pressure drop. Twisted tapes are commonly used for enhancing convective heat transfer by introducing swirl into the bulk flow. The tape disrupts the boundary layer formation and induces turbulence even at low flow rates thereby enhancing the heat transfer coefficients.



Another passive method is by adding additives to liquids. Solid particles have thermal conductivities several times higher than those of conventional fluids. Ultra fine solid particles can be used to suspend them uniformly to enhance the thermal conductivity of the fluid. Metallic, non-metallic and polymeric particles can be added to liquids to form slurries. However the usual slurries with suspended particles of the order of millimeters or even micrometers can cause severe problems such as clogging, erosion, etc. associated with higher pressure drop. Furthermore, they suffer from instability and rheological problems.

The use of nanometer size particles for use as heat transfer fluid is initiated by a research group at the Argonne National Laboratory. Choi (1995) coined the word 'nano fluids' who observed very high values of thermal conductivity compared to suspended particles of millimeter or micrometer dimension. The nanofluids showed better stability and rheological properties, dramatically higher thermal conductivities with no significant penalty on pressure drop. Most of the experiments in literature are focused on the theoretical prediction and measurement of thermal conductivity of the nanofluids.

## **1.2 PROBLEM STATEMENT**

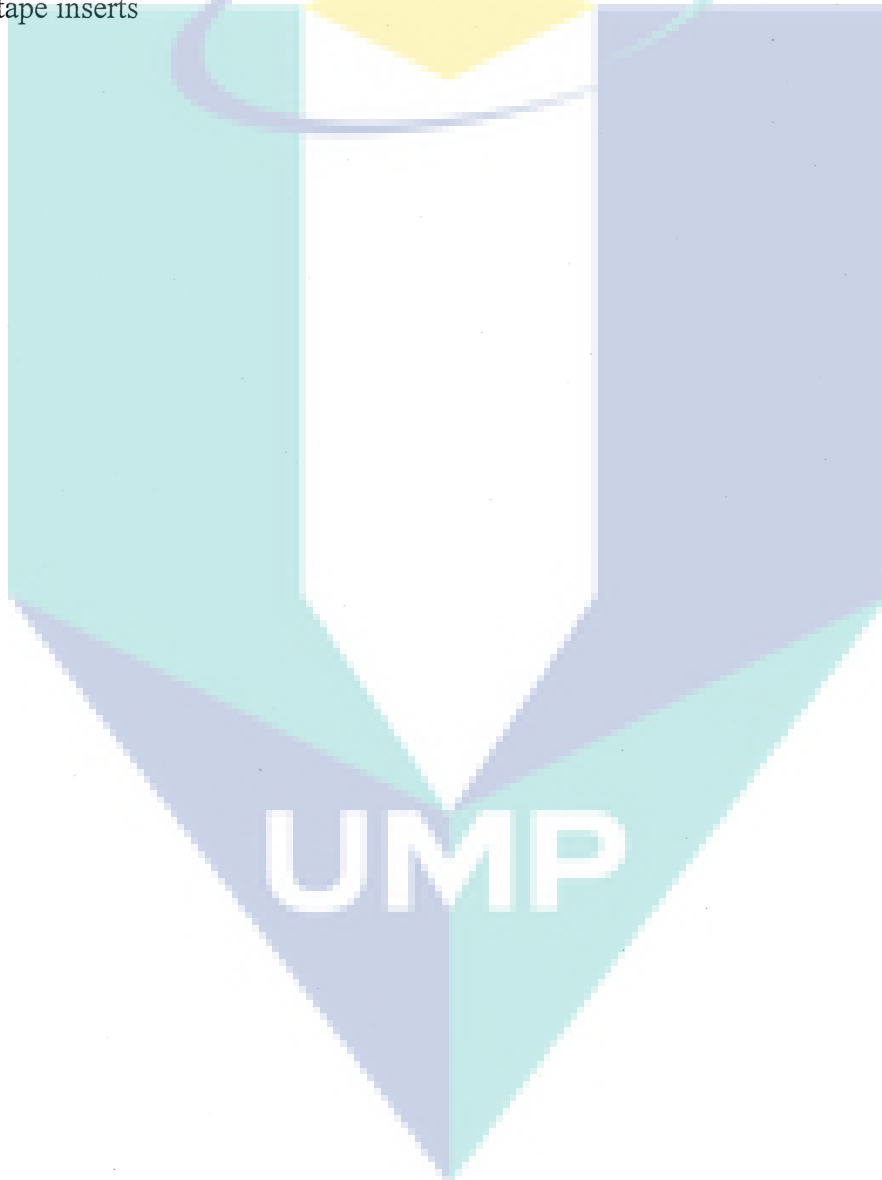
Experiments are conducted to determine the thermal conductivity, viscosity and heat transfer coefficients in the turbulent Reynolds numbers range at different temperatures, with nano materials and particle sizes in the low volume concentration. Suitable equations for the determination of thermo physical properties valid for water based nanofluid in volume concentration of less than 4% are not available in literature. Further, theoretical evaluation of nanofluid heat transfer coefficients for flow in a plain tube and with twisted tape insert is not reported till now.

## **1.3 OBJECTIVES OF THE RESEARCH**

The objectives of this project are as follows:

- i. Estimation of certain thermo-physical properties of  $\text{Al}_2\text{O}_3$  nanofluid in the volume concentration range of 0.0% to 4.0 %.

- ii. Fabrication of an experiment setup for the estimation of heat transfer coefficient and friction factor of  $\text{Al}_2\text{O}_3$  nanofluid at different volume concentrations in the Reynolds number range of 3,000 to 22,000 in a plain tube subject to constant heat flux boundary condition.
- iii. Develop equations for the estimation of Nusselt number and friction factor for comparison with other equations in literature for the case of a plain tube and with tape inserts



## CHAPTER 2

### LITERATURE REVIEW

#### 2.1 INTRODUCTION

A number of studies have been performed to investigate the transport properties of nanofluids, Eastman et al.(1997), Wang et al.(1999), Lee et al.(1999) and Xuan and Li (2000). These studies are concentrated on the evaluation of effective thermal conductivity under macroscopically stationary conditions. Limited studies on other aspects related to nanofluids such as phase change behavior has been due to Das et al.(2003), Tsai et al.(2003), You et al.(2003) and Vassallo et al.(2004).

Dittus – Boelter (1930), Gnielinski (1976), Tam and Ghajar (2006) and Churchill and Usagi (1972) developed correlations for the estimation of heat transfer coefficient of single-phase fluid flow in a circular tube under fully developed and transition flow conditions for constant heat flux boundary condition. Pak and Cho

(1998) estimated convective heat transfer coefficients in the turbulent Reynolds number range with  $\text{Al}_2\text{O}_3$  and  $\text{TiO}_2$  nanofluids dispersed in water and observed that the Nusselt number of the nanofluids increased with increasing volume fraction of the suspended nanoparticles and the Reynolds number. Xuan and Li (2003) estimated convective heat of pure water. Wen and Ding (2004), Yang et al. (2005), Heris et al. (2007) investigated the convective heat transfer of  $\text{Al}_2\text{O}_3$  nanofluid in a circular tube under laminar flow conditions subjected to constant heat flux. They observed the heat transfer rates to increase with increasing concentration of submicron particles to the base fluid.

Heris et al. (2006) conducted experiments in the laminar range with  $\text{Al}_2\text{O}_3$  and  $\text{CuO}$  nanofluids and observed  $\text{Al}_2\text{O}_3$  nanofluid to have higher heat transfer rates compared to  $\text{CuO}$  nanofluid.

Single phase heat transfer enhancement with twisted tape inserts under laminar and turbulent flow conditions have been dealt by Smithberg and Landis (1964), Manglik and Bergles (1993) and Sarma et al. (2002). Experiments with nanofluids for heat transfer enhancements in a plain tube and with twisted tape inserts is reported by Sundar and Sharma (2010) for low volume concentration in the turbulent range.

## **2.2 HEAT TRANSFER COEFFICIENT IN A PLAIN TUBE**

### **2.2.1 Forced Convection in a Plain Tube - Numerical Studies**

Maiga et al. (2005) conducted numerical investigations to determine heat transfer coefficients with  $\text{Al}_2\text{O}_3/\text{water}$  and  $\text{Al}_2\text{O}_3/\text{EG}$  nanofluids under laminar flow in a tube assuming negligible slip between the particles and the continuous phase. Correlations for the estimation of Nusselt number for the case of constant heat flux and wall temperature are presented. Numerical analysis of laminar flow heat transfer in a tube with  $\text{Al}_2\text{O}_3/\text{EG}$  and  $\text{Al}_2\text{O}_3/\text{water}$  nanofluids has been reported by Palm et al. (2004) and Roy et al. (2006). They observed the wall shear to increase with particle volume concentration and Reynolds number. Buongiorno (2006) concluded from his theoretical analysis that Brownian diffusion and thermophoresis are important mechanisms and that energy transfer by nanoparticle dispersion is negligible. The author opines that decrease in nanofluid viscosity in the boundary layer due to large temperature gradient and thermophoresis result in enhanced heat transfer. Experimental studies by Behzadmehr et al. (2007) with  $\text{Cu}$  nanoparticles in water at 1.0% vol. concentration under turbulent forced convection is found to be in good agreement with results from Computational Fluid Dynamic (CFD) mixture model. Determination of heat transfer coefficients using CFD analysis for  $\text{CuO}$ ,  $\text{Al}_2\text{O}_3$  and  $\text{SiO}_2$  nanoparticles dispersed in ethylene glycol and water mixture in 60:40 mass ratio, at 6% volume concentration has been undertaken by Namburu et al. (2008). They observed that the values of friction factor obtained in the turbulent Reynolds number range can be represented with the Blasius equation and the

heat transfer coefficients with the equation of Gnielinski (1976). Comparison of experimental values of heat transfer coefficients with TiO<sub>2</sub>/water nanofluid and CFD results by Yurong He et al. (2009) indicate close agreement in the laminar developing region. They concluded from their analysis that the variation of thermal conductivity has greater influence on heat transfer coefficient than viscosity. Izadi et al. (2009) have undertaken numerical investigations of the laminar developing flow in an annulus with the properties of Al<sub>2</sub>O<sub>3</sub> nanofluid in base liquid water. They observed the temperature profiles to be affected significantly but not the dimensionless axial velocity with changes in volume concentration. Bianco et al. (2009) conducted numerical investigation of developing flow in tubes with Al<sub>2</sub>O<sub>3</sub>/water nanofluid at 1.0 and 4.0% vol. concentration. Both single and discrete (two) phase model is employed in the analysis for a particle size of 100 nm. The results indicate a deviation of 11% between the values of heat transfer coefficient obtained from these two models. They observed higher heat transfer coefficients and lower shear stresses when thermal conductivity and viscosity are considered temperature dependent.

### **2.2.2 Forced Convection in a Plain Tube – Experimental determination**

Preliminary experiments for the determination of thermo-physical properties and forced convection heat transfer coefficients with Al<sub>2</sub>O<sub>3</sub> and TiO<sub>2</sub> submicron particles dispersed in water is due to Pak and Cho (1998). They conducted hydrodynamic and heat transfer experiments with nanofluids and obtained higher heat transfer coefficients which increased with concentration and Reynolds number. The nanofluid viscosity and thermal conductivity is observed to vary with volume concentration and temperature. However, the regression equation for Nusselt number presented is independent of volume concentration. Xuan and Roetzel (2000) proposed thermal dispersion as a major mechanism for heat transfer enhancement of a flowing nanofluid. Xuan and Li (2003) conducted experiments with Cu/water nanofluid at different particle volume concentrations of up to 2.0%. They opined that the dispersion will flatten the temperature distribution and make the temperature gradient between the fluid and the wall steeper. The regression equation for Nusselt number developed by them includes volume concentration and particle Peclet number. No significant enhancement in nanofluid friction factor is observed when compared to values of water in the

experimental range. Also, the experiments by Eastman et al. (2001) with less than 1% CuO nanofluid under turbulent flow condition showed enhancements of heat transfer coefficient by more than 15% in comparison to similar conditions obtained with water.

Forced convection experiments conducted by Nguyen et al. (2007) in the Reynolds number range of  $3000 < Re < 7000$  and volume concentration  $\phi < 6.8\%$  predicted higher heat transfer coefficients with 36nm size  $Al_2O_3$ /water nanoparticles compared to values evaluated with 47nm size particles. Heris et al. (2006) conducted experiments for the determination of convection heat transfer coefficients in the laminar flow range of  $650 < Re < 2050$  with  $Al_2O_3$  and CuO nanofluids in water at volume concentration  $\phi < 3.0\%$ . They observed the values of heat transfer coefficients with  $Al_2O_3$  nanofluid greater than CuO nanofluid at large volume fractions. However, they have not presented equation for the estimation of Nusselt number.

Experiments conducted by Yulong Ding et al. (2006) with multi walled carbon nanotubes with 0.5% weight concentration showed enhancement in convective heat transfer coefficients of over 350% at Reynolds number of 800. The authors attributed the abnormal enhancement to possible particle rearrangement, reduction of thermal boundary layer, high aspect ratio of nanotubes besides enhanced thermal conductivity. In another paper, Yulong Ding et al. (2007) observed convection heat transfer with Carbon Nanotube/water, Titanate Nanotube/water and  $TiO_2$ /water nanofluids exceed enhancements in thermal conduction. They opined that clustering of nanoparticles as a dominant mechanism responsible for enhanced heat transfer.

Yurong He et al. (2007) observed an increase in convective heat transfer coefficient of  $TiO_2$  nanofluid with volume concentration  $\phi \leq 1.0\%$  in both laminar and turbulent flow regimes. They observed the influence of nanoparticle concentration on heat transfer coefficient to be significant in the turbulent than in laminar region. Gwan Hyun Ko et al. (2007) observed that the nanofluid friction factor obtained with Multi Walled Carbon Nano Tubes (MWCNT) in water of 1400 ppm concentration and stabilized with surfactant predict higher values when compared with MWCNT nanofluid prepared by acid treatment. The nanofluids showed larger pressure drop when compared to values with distilled water in the laminar range. However, in the

turbulent range the values of pressure drop obtained with the nanofluids are close to that of water.

Williams et al. (2008) conducted experiments to estimate turbulent convective heat transfer coefficients with  $\text{Al}_2\text{O}_3$  and  $\text{ZrO}_2$  nanofluids dispersed in water for  $9000 \leq \text{Re} \leq 63000$ ,  $21 \leq T_b \leq 76^\circ\text{C}$  and maximum volume concentration of 3.6 and 0.9% respectively. They concluded that the existing correlations of single phase flow can be used to predict the convective heat transfer coefficient and pressure drop of the nanofluids. Kyo Sik Hwang et al. (2009) conducted experiments with  $\text{Al}_2\text{O}_3$  nanofluid and observed 8 % enhancement in heat transfer coefficients at a particle volume concentration of 0.3 % in the fully developed laminar range. The flattening of the velocity profiles observed by them is attributed to large gradients observed with properties responsible for enhanced heat transfer coefficients.

Doohyun Kim et al. (2009) conducted experiments with water based alumina and amorphous carbonic nanoparticles for flow in a tube under laminar and turbulent conditions. A 20% increment in convective heat transfer coefficient at 3.0% volume concentration is reported with alumina nanofluid. They concluded from their experiments that carbonic nanofluid did not show promise as an enhanced heat transfer fluid in the turbulent range. Yu et al. (2009) conducted experiments with 170 nm SiC nanoparticles in water at volume concentration of 3.7% in the range  $3300 < \text{Re} < 13000$ ,  $4.6 < \text{Pr} < 7.1$  and observed 50-60 percent enhancements in heat transfer. They concluded from their experimental analysis that SiC/water is a better heat transfer liquid and requires lower pumping power compared to  $\text{Al}_2\text{O}_3$ /water nanofluid.

$\text{TiO}_2$  nanofluid with particle size of 21nm is used to conduct heat transfer experiments in a double pipe heat exchanger in the range of  $0.2 < \phi < 2.0\%$ ,  $3000 < \text{Re} < 18000$  by Duangthongsuk and Wongwises (2010) with water as the heating medium. The heat transfer coefficients of the nanofluid are found to increase with Reynolds number and volume concentration upto 1.0%. The heat transfer coefficient decreased with further increase in volume concentration but is observed to be greater when compared to values with water. However, Pak and Cho (1998) observed the heat transfer coefficients with 3.0%  $\text{TiO}_2$  nanofluid with 27nm particle size

to be 12% lower than that of water. Fotukian and Esfahany (2010) conducted experiments in the range of  $6000 < Re < 31000$  for flow in a tube with CuO nanofluid of maximum volume concentration of 0.024%. They observed 25% enhancement in heat transfer coefficients and 20% higher pressure drop compared to values obtained with base liquid water. However most of the investigators have concluded that the pressure drop with nanofluids is close to the values of water in the turbulent range.

Estimation of heat transfer coefficients have been made mostly through experimental investigations with  $Al_2O_3$ , Cu, CuO, SiC,  $TiO_2$ , etc nanoparticles dispersed in water. The investigators used different particle sizes, concentration and temperature range in their experiments having limitation for comparison of either properties or heat transfer coefficients with others. Also the theoretical analysis for the estimation of heat transfer coefficient reported in literature is scarce.

Hence using the available experimental data, equations are developed to determine the influence of particle size, concentration and temperature on thermo-physical properties and utilize them for the theoretical estimation of heat transfer coefficients with the eddy diffusivity equations developed by Sarma et al. (2010).

## **2.3 HEAT TRANSFER COEFFICIENT WITH TWISTED TAPES**

### **2.3.1 Forced Convection with Twisted Tape – Experimental determination**

Passive heat transfer augmentation using twisted tapes, longitudinal inserts, wire coil insert, etc for a wide range of Reynolds and Prandtl numbers have been reported by Bergles (1988). The twisted tape causes the flow to swirl, providing longer path length and residence time and thereby enhancing heat transfer. However, the pressure drop with insert is higher due to the resistance offered by the additional tape surface area when compared to flow in plain tubes.

Experimental studies are conducted by Smithberg and Landis (1964) with air as the working medium. They observed that increased frictional loss is due to the vortex flow caused by the twisted tapes which continuously mixes the core flow with the



vortex flow and developed a semi-empirical model for the estimation of friction factor. Thorsen and Landis (1968) extended the analysis and developed correlation for the estimation of Nusselt number using experimental data of water. Lopina and Bergles (1969) developed a superposition model for the estimation of Nusselt number to account for the increased speed of flow due to tape insert and the centrifugal buoyancy effects in the tube. They observed an increase of 20% in the Nusselt number for tight fit tapes compared to reduced width tapes. Manglik and Bergles (1993) conducted experimental investigations on isothermal tubes with twisted-tape inserts using water and ethylene glycol in the turbulent Reynolds number range and developed correlation based on the asymptotic method. Saha and Dutta (2001) conducted thermo-hydraulic studies in a circular tube fitted with twisted tapes for a wide range of Prandtl numbers ( $205 < Pr < 518$ ) in the laminar Reynolds number range under constant wall heat flux boundary condition. They used twisted-tape inserts having short-length, regularly spaced with multiple twists in the tape module which is connected by thin circular rods and smoothly varying (gradually decreasing) pitch twisted-tapes and observed that reducing tape widths resulted in poor heat transfer where as the difference between the heated friction factor and isothermal friction factor is less for a periodic swirl flow compared to that of a plain tube.

Bandyopadhyay et al.(1991) carried out experiments with viscous oil to determine the influence of free convection on heat transfer in the laminar Reynolds number range. They classified flow regime into three types, the first with secondary flow due to swirl, the second as transition flow and the third as secondary flow due to free convection in their respective zones and compared the results with the correlation of Hong and Bergles (1976) and other free convection correlations. Agarwal and Raja Rao (1996) conducted experiments for flow with tape inserts in circular tubes under uniform wall temperature using Servotherm oil and developed correlations for the evaluation of heat transfer coefficients and friction factor. Naphon (2006) has undertaken experimental studies in plain tubes and with twisted tape inserts and developed correlations for the estimation of heat transfer and pressure drop in turbulent Reynolds number range  $7000 < Re < 23000$  and for twist ratio ( $H/D$ ) between 3.1 and 5.5. Experiments to determine heat transfer coefficient under laminar flow of water in a tube with different twisted tape inserts in vertical and horizontal orientations were

carried out by Klaczak (2001). At low flow rates, it is observed that natural convection effects dominated and heat transfer rates are higher with twisted tape insert in vertical compared to horizontal orientation. Herwig and Kock (2006) developed a tool from thermodynamic point of view for evaluating heat transfer performance under turbulent flow in a pipe with twisted tape inserts. Turbulence modelling of the flow phenomenon indicated a reduction in overall entropy production for a certain range of twist ratio when compared to flow in a plain tube. Mazen Abu-Khader (2006) investigated the behavior of heat transfer in a shell and tube heat exchanger for different twist ratios for a wide range of flow Reynolds number. It is observed that pressure drop increased sharply with decrease in tube diameter. However, the Nusselt number increased significantly with twist ratio in the laminar Reynolds number range. Akhavan-Behabadi et al. (2008) conducted experiments at different mass flow rates and developed correlations and determined heat transfer coefficients during condensation of R-134a refrigerant in a plain tube and with twisted tape inserts. Ayub and Al-Fahed (1993) observed experimentally the effect of gap between the tube and tape insert on pressure drop for turbulent flow of water. The pressure drop increased with decrease of gap width and increase of tape width.

Experiments with nanofluid are conducted by Sharma et al. (2009) and Sundar and Sharma (2010) for the determination of heat transfer coefficients in a tube and with tape inserts applicable in the transition and turbulent range of Reynolds number, respectively. The values of Nusselt number is compared for water with the equation of Gnielinski (1976) and for nanofluid with the equation of Pak and Cho (1998) under turbulent flow conditions for flow in a plain tube. A satisfactory agreement of the experimental data with these equations has been observed. Hence, based on the reliability of the values obtained, experiments are carried out with water and nanofluid with tape inserts in a tube at different flow conditions.

### **2.3.2 Forced Convection with Twisted Tapes - Theoretical Analysis**

Theoretical analysis for the estimation of heat transfer coefficient of pure fluids with twisted tape insert has been documented. The theoretical modelling considers the effect of turbulence due to spiralling flow and heat conduction in the tape. Date (1974)

undertook numerical analysis to predict friction factor and heat transfer for fully developed laminar and turbulent flows with twisted tape insert. It is observed that the numerical procedure of Gosman et al. (1969) has to be modified suitably for results to converge. DuPlessis and Kroger (1984) developed friction factor correlation for laminar flows based on numerical studies considering finite thickness of the tape.

Marnier and Bergles (1989) performed experimental investigations for pressure drop and heat transfer rates under laminar flow for three test cases like plain tube, internally finned tube and with twisted tape inserts for highly viscous fluids under uniform wall temperature boundary condition. The friction factors were higher for tubes with internal fins and twisted tape inserts compared to a plain tube. Nusselt number was higher for internally finned tube and for tape inserts under heating and cooling conditions when compared to a plain tube. Sarma et al. (2002) proposed that enhancement in heat transfer due to twisted tape insert is reflected in enhanced eddy thermal diffusivity. They showed that the Van Driest (1972) equation can be used to predict the heat transfer coefficients if the universal constant in the equation is modified to accommodate the influence of swirl flow caused by the tape. They employed Smithberg and Landis equation for friction factor and developed expression for the estimation of heat transfer coefficient of water. Chang et al. (2007) developed a set of empirical equations for turbulent heat transfer and pressure drop in a tube fitted with smooth and serrated twisted tapes. They found that for the same twist ratio, smooth walled tapes performed better in heat transfer enhancement than serrated tapes and decrease in twist ratio increased the thermal performance for both smooth and serrated tapes. Chiu and Jang (2009) had performed 3-D flow Numerical analysis and experiments with air having tapes of three different twist angles and horizontal longitudinal strips with and without holes. They performed the experiments with air and observed enhancement in heat transfer coefficient with increasing pressure drop with longitudinal and twisted tapes. But, the twisted tapes performed better than the longitudinal tapes with and without holes with regard to heat transfer enhancement. All these studies are directed for the estimation of friction factor and heat transfer coefficient of pure fluids.

Theoretical analysis of twisted tape inserts for flow of nanofluid has been undertaken for the first time. An eddy diffusivity model is proposed for the determination of nanofluid Nusselt number for flow in the turbulent range. The theoretical analysis is observed to be in good agreement with the available experimental data in literature. Numerical analysis for the determination of nanofluid Nusselt number at higher concentrations is undertaken and the results presented in the form of graphs.

#### 2.4 ANALOGIES BETWEEN MOMENTUM AND HEAT TRANSFER

The study of heat and mass transfer in turbulent flows have been heavily influenced by the formulation of an analogy with the better known law for momentum transfer by Reynolds (1874).

$$St = \frac{C_f}{2} \quad (1)$$

Where;

$$St \quad \text{Stanton number, } h/(\rho C_p V) \quad (2)$$

$$C_f \quad \text{Fanning friction factor, } 2\tau_{wall}/(\rho V^2) \quad (3)$$

$C_p$  specific heat, J/kg K

$V$  average fluid velocity, m/s

$h$  mean heat transfer coefficient, W/(m<sup>2</sup>K)

The analogy works well for the region outside the relatively thin layer where from the wall diffusion is important but the exact connection between the wall and the outer region has been elusive (Trinh, 2010). A number of empirical correlations were proposed to provide useful tools for engineering design. The most widely referred is perhaps the modified Reynolds analogy or Chilton-Colburn analogy (1964).

$$St Pr^{-2/3} = \frac{C_f}{2} \quad (4)$$

$$j = St Pr^{2/3} = \frac{C_f}{2} \quad (5)$$

Where;

$j$  Colburn factor

Pr Prandtl number,  $(C_p \mu) / K$  (6)

Though certain semi-theoretical correlations were later derived, (Metzner and Friend, 1958, and Trinh, 1969) the Colburn analogy is often quoted and the  $j$  factor is used commonly. Among other analogies such as Reynolds and Prandtl-Taylor, Colburn was developed to relate heat transfer coefficients with Darcy friction factor ' $f$ ' for flow in a tube.

$$St Pr^{2/3} = \frac{f}{8} \quad (7)$$

Where;

$$f = \frac{d}{L} \frac{(\Delta P)}{(\rho V^2 / 2)} \quad (8)$$

The experimental data of heat transfer coefficient and friction factor of water and nanofluids in the volume concentration of less than 4.0% is available in literature. It is fairly established by various investigators that the friction factor of water and nanofluid can be estimated using Blasius equation in the turbulent range of Reynolds number. Hence an equation for the determination of nanofluid heat transfer coefficient has been developed with the consideration of volume concentration of the nanofluid in a similar structure of the Colburn's equation given by Eqn. (7). The equation has the flexibility to evaluate the heat transfer coefficients of both water and nanofluids, if the friction factor is known. In other words, experiments with fluid flow need be conducted to evaluate heat transfer coefficients. However, the equation developed can be used to determine the Nusselt number, with the friction factor evaluated with Blasius equation.

## CHAPTER 3

### METHODOLOGY

#### 3.1 INTRODUCTION

Theoretical analysis of forced convection heat transfer has been undertaken by Sarma et al. (2010). They established the validity of the theoretical model for nanofluid heat transfer coefficients for the volume concentration  $\phi < 0.5$ . However, experiments have been undertaken by other investigators to determine heat transfer coefficients with different nanofluids in the volume concentration range of  $0.5 < \phi < 4.0\%$ . Validation of the theoretical model requires thermo-physical properties at different concentrations, temperatures and particle sizes. Hence, equations are developed based on the observation of Vajjha et al.(2009), Nguyen et al. (2007), Namburu et al. (2007) that the values of viscosity do not show significant variation with particle size and material for volume concentration less than 4%. It is also assumed that thermal conductivity depends on temperature, volume concentration in addition to particle size. Based on the observations and assumption, regression equations are developed for the estimation of the thermo-physical properties of nanofluids based on the experimental data of various authors. The equations (9) – (12) are valid for nanofluids having  $\phi \leq 4.0\%$ ,  $T_{\max} \leq 70^\circ\text{C}$  and  $d_{\max} \leq 150\text{ nm}$  with deviation from experimental values by a maximum of 14% are used for the theoretical estimation of heat transfer coefficients.

$$\frac{\rho_{nf}}{\rho_w} = (0.9973 + 0.03479 \times \phi + 0.0000619 \times T_b) \quad (9)$$

$$\frac{C_{nf}}{C_w} = (1.036 - 0.0298 \times \phi - 0.001037 \times T_b) \quad (10)$$

$$\frac{\mu_{nf}}{\mu_w} = (0.9042 + 0.1245 \times \phi + 0.0043 \times d_p - 0.001206 \times T_b) \quad (11)$$

$$\frac{K_{nf}}{K_w} = (0.9808 + 0.0142 \times \phi + 0.003883 \times T_b - 0.00068 \times d_p) \quad (12)$$

The properties of water are estimated with the aid of Eqs. (13) – (16) applicable in the range  $5 \leq T_b \leq 70$  where  $T_b$  in °C is obtained with a maximum deviation of 2.6 %.

$$\rho_w = 1000 \times \left[ 1.0 - \frac{(T_b - 4.0)^2}{119000 + 1365 \times T_b - 4 \times (T_b)^2} \right] \quad (13)$$

$$C_w = 4217.629 - 3.20888 \times T_b + 0.09503 \times (T_b)^2 - 0.00132 \times (T_b)^3 + 9.415e-6 \times (T_b)^4 - 2.5479 \times 10^{-8} (T_b)^5 \quad (14)$$

$$\mu_w = 0.00169 - 4.25263e-5 \times T_b + 4.9255e-7 \times (T_b)^2 - 2.0993504e-9 \times (T_b)^3 \quad (15)$$

$$k_w = 0.56112 + 0.00193 \times T_b - 2.60152749e-6 \times (T_b)^2 - 6.08803e-8 \times (T_b)^3 \quad (16)$$

## 3.2 EXPERIMENTS WITH FLOW IN A PLAIN TUBE

Experiments in the turbulent range of Reynolds number are undertaken by various investigators with water and oxide nanoparticles dispersed in water. The properties are evaluated by conducting experiments or estimated with equations available in the literature.

### 3.2.1 Evaluation of nanofluid friction factor: Blasius equation

The investigations conducted so far revealed that the nanofluid friction factor, estimated using the equation for pressure drop, can be represented with the Blasius equation given by

$$f = 0.3164 / \text{Re}^{0.25} \text{ where } \Delta P = \rho gh = f \left( \frac{L}{D} \right) \left( \frac{\rho V^2}{2} \right) \quad (17)$$

### 3.2.2 Equations for the evaluation of Nusselt number

#### a) Equation of Gnielinski (1976) applicable for pure fluids

$$Nu = \frac{\left(\frac{f}{2}\right)(Re-1000)Pr}{1 + 12.7\left(\frac{f}{2}\right)^{0.5}\left(Pr^{\frac{2}{3}}-1\right)} \quad \text{where } f = (1.58 \ln Re - 3.82)^{-2} \quad (18)$$

valid in the range of  $2300 < Re < 5 \times 10^6$  and  $0.5 < Pr < 2000$ .

#### b) Equation of Dittus-Boelter (1930) applicable for pure fluids

$$Nu = 0.023 Re^{0.8} Pr^{0.4} \quad (19)$$

valid for  $Re > 10^4$  and  $0.6 < Pr < 200$

#### c) Equation of Tam and Ghajar (2006) applicable for pure fluids

$$Nu = 0.023 Re^{0.8} Pr^{0.385} \left(\frac{X}{D}\right)^{-0.0054} \left(\frac{\mu_b}{\mu_w}\right)^{0.14}$$

Valid for  $3 < (X/D) < 192$ ,  $7000 < Re < 49,000$ ,  $4 < Pr < 34$  and

$$1.1 < (\mu_b/\mu_w) < 5 \times 10^6 \quad (20)$$

#### d) Equation applicable for water and nanofluids

Experimental Nusselt numbers obtained for water and nanofluids by different investigators (Sundar and Sharma (2010), Sharma et al. (2009), Fotukian and Esfahany (2010), Xuan and Li (2003), Yu et al. (2009) and Williams et al. (2008)) valid in the range  $3600 \leq Re \leq 63000$ ,  $2.0 \leq Pr \leq 9.5$ ,  $0 \leq \phi \leq 3.7\%$  can be presented in a form similar to Eq. (19) of Dittus-Boelter

$$Nu = 0.027 Re^{0.8} Pr^{0.4} [0.001 + \phi]^{0.0153} \quad (21)$$

or,  $Nu = 0.0304 Re^{0.7853} Pr^{0.4} [0.001 + \phi]^{0.01398}$  ( $\phi = 0$  refers to water).

The data is also transformed to the structure of Colburn's equation given by

$$St Pr_w^{2/3} = \frac{f}{8} (1 + \phi Pr_w)^{0.1185} \quad (22)$$



### 3.3 MODEL FOR TURBULENT FLOW IN A PLAIN TUBE

A theoretical model for the evaluation of nanofluid heat transfer coefficient under turbulent flow has been presented by Sarma et al. (2010). Making certain simplifications and introducing a correction factor for the mixing length, expressions for eddy diffusivity of momentum ( $\varepsilon_{nf}/\nu_{nf}$ ) and heat ( $\varepsilon_H/\alpha_{nf}$ ) are developed. The assumptions made in the analysis by Sarma et al. (2010) are

1. The nanoparticles do not agglomerate but disperse uniformly in the base liquid water.
2. The total momentum exchange is due to sum of the molecular and eddy viscous

forces,  $\tau = \mu_{nf} \left[ 1 + \frac{\varepsilon_m}{\nu_{nf}} \right] \frac{\partial u}{\partial y}$

3. The nanofluid is assumed Newtonian for concentration  $\phi < 0.5\%$ . Hence, the shear distribution across the tube is assumed linear as  $\frac{\tau}{\tau_w} = \left[ 1 - \frac{y^+}{R^+} \right]$  where  $R^+ = \left( \frac{R}{\nu} \sqrt{\frac{\tau_w}{\rho}} \right)$ ,

$$y^+ = \frac{yu^*}{\nu} \quad \text{and} \quad u^* = \left( \sqrt{\frac{\tau_w}{\rho}} \right)$$

4. The thermal exchange due to combination of molecular and eddy diffusivity is given by

$$q = \rho_{nf} C_{Pnf} (\alpha_{nf} + \varepsilon_H) \frac{\partial T}{\partial y} = k_{nf} \left( 1 + \frac{\varepsilon_H}{\alpha_{nf}} \right) \frac{\partial T}{\partial y}$$

5. By dimensional reasoning, the momentum eddy diffusivity equation is assumed

$$\text{as } \frac{\varepsilon_m}{\nu_{nf}} = B u^+ y^+ \left[ 1 - \exp \left( -\frac{y^+}{15} \right) \right]^2 \quad \text{where } u^+ = \frac{u}{u^*} \quad (23)$$

The value of B has been obtained as a constant and equal to 0.0213.

6. The thermal eddy diffusivity is related to momentum eddy diffusivity through the relationship  $\frac{\varepsilon_H}{\alpha_{nf}} = \left[ \frac{\varepsilon_m}{\nu_{nf}} \right] (\text{Pr}_{nf})^\zeta$ . Sarma et al. (2010) obtained the relation for the

$$\text{Prandtl index } \zeta = 7.45 (R^+)^{0.236} [0.5 + \phi]^{0.448} \quad (24)$$

The eddy diffusivity equations along with the equation of Blasius for friction factor are employed in the evaluation of the Nusselt number and validated with Eqs. (18) to (21). This approach to the evaluation of turbulent heat transfer coefficients employing eddy diffusivity equations and validating experimental values with properties estimated with regression equations (9) - (16) for different nanofluids and concentrations has not been reported in literature till now.

### 3.4 MODEL FOR TURBULENT FLOW WITH TWISTED TAPE INSERTS

Theoretical analysis for the determination of nanofluid heat transfer coefficients with twisted tape insert in a tube has not been reported. The eddy diffusivity model of Sarma et al. (2010) for turbulent flow as briefed in Section 3.3 is used for the analysis with tape inserts. The presence of tape in the flow path induces more turbulence and consequently greater heat transfer coefficients and pressure drop are expected compared to flow in a plain tube. Lower temperature gradients at the wall are expected as the mixing of the fluid is enhanced due to the presence of the tape. Nanofluid heat transfer coefficients at different twist ratios are evaluated using Eqs. (9) – (16) and compared with the limited experimental data available in literature.

#### 3.4.1 Experiments with tape insert in a tube

Equations for the estimation of Nusselt number and friction factor for flow in a tube with twisted tape inserts are undertaken by many. Reference to the works of Smithberg and Landis (1964), Lopina and Bergles (1969), Watanabe et al (1983), Lecjacks et al. (1984), DuPlessis and Kröger (1984), Manglik (1991), Manglik and Bergles (1993), and Sarma et al. (2002, 2005) are commonly cited in literature.

Experiments are conducted by Sharma et al. (2009) and Sundar and Sharma (2010) with twisted tape insert having twist ratio  $H/D$  of 5, 10, 15 and 83 with water and nanofluid and in a tube as shown in Figure 3.1.

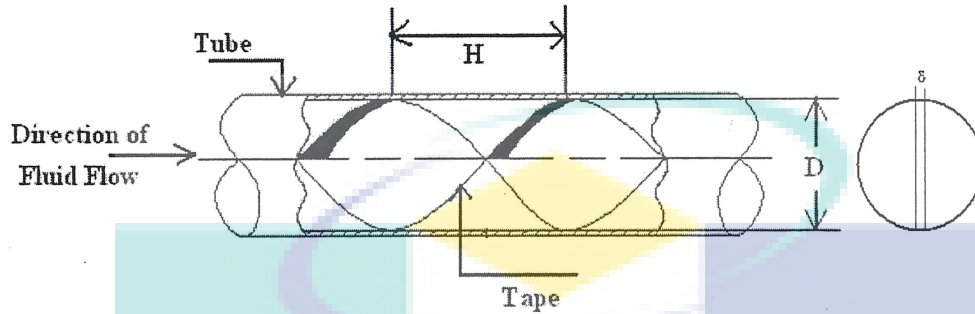


**Figure 3.1:** Schematic diagram of twisted tape in a tube

The following equations for Nusselt and friction factors are frequently cited by various authors.

**a. Equation of Manglik (1991)** valid in the range of  $10^4 < Re < 1.3 \times 10^5$ ,  $3 < Pr < 5$

$$Nu = 0.023 Re^{0.8} Pr^{0.4} \left[ 1 + 0.769 \frac{D}{H} \right] \left[ \frac{\pi}{\pi - 4\delta/D} \right]^{0.8} \left[ \frac{\pi + 2 - 2\delta/D}{\pi - 4\delta/D} \right]^{0.2} \phi \quad (25)$$

where  $\phi = (\mu_b/\mu_w)^n$  or  $(T_b/T_w)^m$  and

$$n = \begin{cases} 0.18 & \text{for liquid heating} \\ 0.30 & \text{for liquid cooling} \end{cases} \quad \text{and} \quad m = \begin{cases} 0.45 & \text{for gas heating} \\ 0.15 & \text{for gas cooling} \end{cases}$$

**b. Equation of Sarma et al. (2005)** valid for  $90 < Re < 1,30,000$ ,  $4 < Pr < 460$ ,  $2.5 < H/D < 10$

$$\log_{10} \frac{Nu}{Pr^{1/3} [1 + D/H]^2} = 0.974 - 0.783 \log_{10} \{Re\} + 0.35 \{\log_{10} [Re]\}^2 - 0.0273 \{\log_{10} [Re]\}^3 \quad (26)$$

**c. Present analysis**

The Nusselt number of water and nanofluid obtained by various investigators (Sundar and Sharma (2010), Sharma et al. (2009), Fotukian and Esfahany (2010), Xuan and Li (2003), Yu et al. (2009) and Williams et al. (2008)) and the present data is used in obtaining regression equation encompassing a wide range of operating parameters available in literature for water based nanofluids. The equations are developed and presented in different forms

$$Nu = 0.084 Re^{0.7258} Pr^{0.2486} [0.001 + \phi]^{0.0345} [0.001 + D/H]^{0.0302} \quad (27a)$$

$$Nu = 0.02954 Re^{0.8} Pr^{0.4} [0.001 + \phi]^{0.0278} [0.001 + HD]^{0.0093} \quad (27b)$$

$$St Pr^{2/3} = 1.0344 \left(\frac{f}{8}\right) (1.0 + \phi)^{0.1479} \left(1.0 + \frac{D}{H}\right)^{0.2445} \quad (27c)$$

valid for the range  $3600 \leq Re \leq 63000$ ,  $2.0 \leq Pr \leq 9.5$ ,  $0 \leq \phi \leq 3.7\%$  ( $\phi = 0$  refers to water) and  $5 \leq (H/D) \leq 83$

### 3.4.2 Friction factor of water and nanofluid

The pressure drop across the length of the test section is obtained and Darcy friction factor  $f$  estimated from the relation,

$$\Delta P = \rho gh = f \left(\frac{L}{D}\right) \left(\frac{\rho V^2}{2}\right) \text{ or } f = \frac{\Delta P}{\left(\frac{L}{D}\right) \left(\frac{\rho V^2}{2}\right)} \quad (28)$$

#### a. Equation of Smithberg and Landis (1964)

$$f = \left\{ 0.046 + 2.1 \left[ \frac{H}{D} - 0.5 \right]^{-1.2} \right\} \left[ \frac{Re}{1 + 2/\pi} \right]^{-n} \text{ where } n = 0.2 \left[ 1 + 1.7 \left( \frac{H}{D} \right)^{-0.5} \right] \quad (29)$$

#### b. Equation of Lopina and Bergles (1969)

$$\left(\frac{f}{f_s}\right)_h = 2.75(H/D)^{-0.406} \text{ where } f_s = 0.046 / Re^{0.2} \quad (30)$$

$f_s$  is the friction factor for single phase flow in a plain tube and  $D$  is based on hydraulic diameter

#### c. Equation of Manglik (1991)

$$f = \left[ \frac{0.0791}{Re^{0.25}} \right] \left[ \frac{\pi}{\pi - 4\delta/D} \right]^{1.75} \left[ \frac{\pi + 2 - 2\delta/D}{\pi - 4\delta/D} \right]^{1.25} \left[ 1 + 2.752 \left( \frac{D}{H} \right)^{1.29} \right] \quad (31)$$

#### d. Equation of Petukhov (1970) valid in the range $3000 \leq Re \leq 5 \times 10^6$

$$f = (0.790 \ln(Re)_h - 1.64)^{-2} \quad (32)$$

e. Equation of Sarma et al. (2005) valid in the range of  $400 < Re < 1,30,000$ ,  
 $3 < Pr < 5$ ,  $4 < Pr < 460$ ,  $2.5 < H/D < 10$

$$\frac{f}{[1 + D/H]^{3.378}} = 0.474 - 0.3 \log_{10}(Re) + 0.065 [\log_{10}(Re)]^2 - 4.66 \times 10^{-3} [\log_{10}(Re)]^3 \quad (33)$$

f. Equation of Sundar and Sharma (2010) valid for  $3000 < Re < 22000$ ,  
 $4.4 < Pr < 6.2$ ,  $0 < \phi < 0.5$ ,  $0 < H/D < 83$ . ( $\phi = 0$  for water,  $H/D = 0$  for plain tube)

$$f = 0.3124 Re^{-0.2414} \left(1.0 + \frac{D}{H}\right)^{-0.5405} (1.0 + \phi)^{0.1061} \quad (34)$$

g. The experimental friction factor data is estimated with Eq. (28) for water and nanofluid for flow in tube and with tape insert. The friction factor estimated in this manner is subjected to regression with the assumption that nanofluid behaves as single phase fluid and is given by

$$f = 0.4818 Re^{-0.2731} (0.001 + \phi)^{0.00061} (0.001 + D/H)^{0.0296} \quad (35)$$

Equation (35) is valid in the range  $3600 \leq Re \leq 63000$ ,  $2.0 \leq Pr \leq 9.5$ ,  $0 \leq \phi \leq 3.7\%$  ( $\phi = 0$  refers to water) and  $5 \leq (H/D) \leq 83$ , obtained with an average deviation (AD) of 4% and standard deviation (SD) of 5%.

UMP

## CHAPTER 4

### EXPERIMENTAL SETUP

#### 4.1 INTRODUCTION

The experimental set up consists of a circulating pump, flow meter, heater, control panel, thermocouples, chiller, receiving tank, collecting tank and 10mm diameter copper tube of 1.5m length. The total length of fluid flow in the tube is more than 5.0m to ensure turbulent flow at the entry of the test section. The schematic diagram of the experimental set up is shown in Figure 4.1.

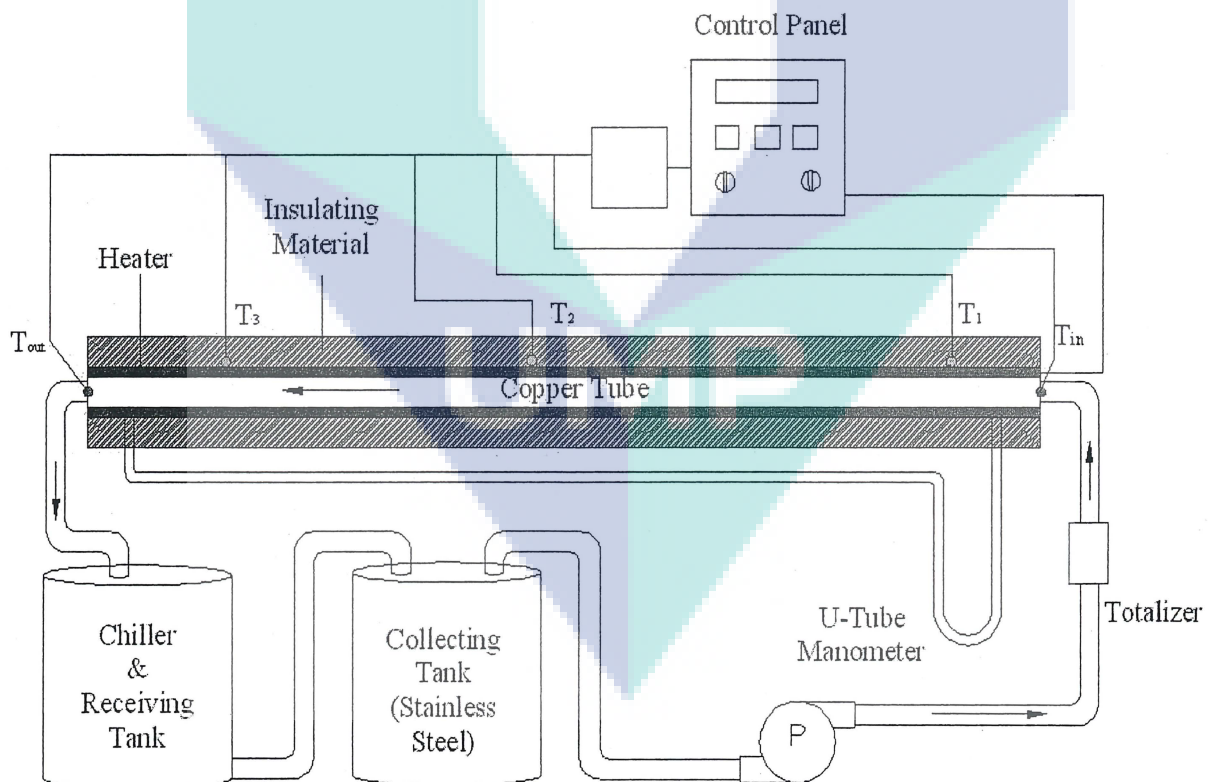
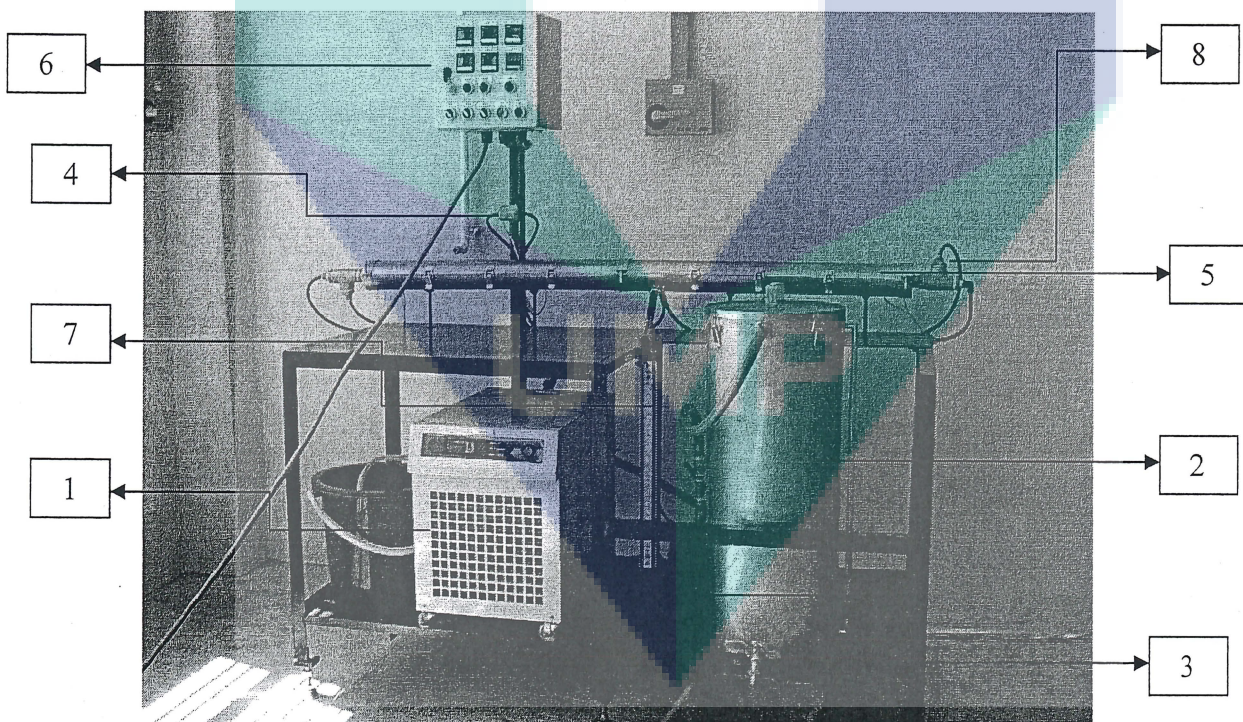


Figure 4.1: Schematic diagram of the experimental setup

The working fluid is circulated using a pump to force the fluid through the test section in this study. The working fluid is stored in the collecting tank made of stainless steel having 30 liter capacity.

The tube is heated uniformly for a length of 1.5m by wrapping with two nichrome heaters of 20 gauge with 1000W electric rating. The tube is enclosed with rock wool insulation to minimize heat loss to atmosphere. Five thermocouples are located on varies locations, three on the surface of the tube wall at 0.375, 0.75, 1.125 m from the inlet and the other two are measure inlet and outlet temperatures of the fluid. A flow meter is located before the working fluid enters the test section to determine the flow rate. When the system attains steady state, the temperatures at different locations, electric heat input and the flow rate is noted. The provision of chiller between the test section and the collecting tank helped to achieve steady state condition faster. U-tube manometer is connected to pressure taps located on either side of the test section to measure the pressure drop of fluid flow across the length of the test section as shown in Figure 4.2. Table 4.1 gives the list of major components used in the fabrication.



**Figure 4.2:** Fabricated experiment apparatus

**Table 4.1** List of components used in the fabrication of the experimental setup

[1] Chiller	[5] Copper Tube
[2] Reservoir Tank	[6] Control Panel
[3] Pump	[7] U-tube manometer
[4] Flow meter	[8] Thermocouple

Experiments are initially conducted with water and checked for consistency of results. The experiment is repeated with nanofluid at different concentrations and heat transfer coefficients estimated at various Reynolds number. It is assumed that heat loss to atmosphere is negligible. In the range of nanofluid concentration, it is also assumed that Newton's convective law is applicable.

## 4.2 EXPERIMENT APPARATUS

The apparatus is designed and fabricated for flow of fluid in a tube and with twisted tape as shown in Figure 4.2. The functions of the various components listed in Table 4.1 are explained item wise.

### 4.2.1 Chiller

Chiller shown in Figure 4.3 is used to cool the fluid which is heated in the test section. Provision is available for display of outlet temperature from the chiller. The function of the chiller is something like a radiator in a car to cool down the working fluid. The advantage of providing the chiller is to remove the heat added in the test section and regulate the temperature of the circulating fluid at its original value. This will enable to achieve steady state condition faster.



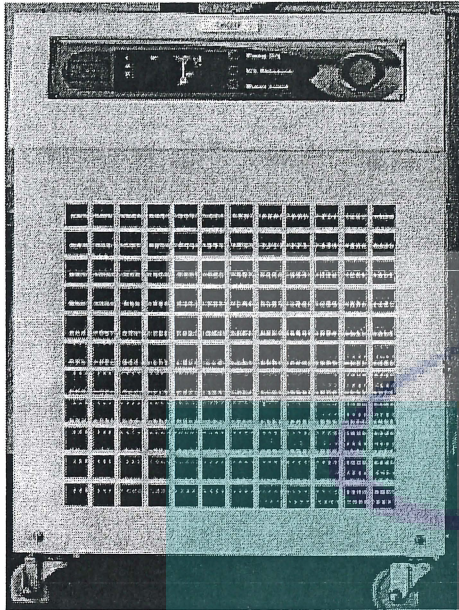


**Figure 4.3: Chiller**



**Figure 4.4: Reservoir**

#### 4.2.2 Reservoir

Fluid flowing through the chiller enters the stainless steel tank or reservoir shown as Figure 4.4. The liquid mixed with the liquid in the tank and consequently the temperature of the fluid decreases due to higher residence time. This will enable one to view, if sufficient liquid is available in the tank in the process of altering the flow rate through the test section and prevent the pump from running dry. The stainless steel tank has a capacity of 30 liter sufficient for fluid circulation even at very high Reynolds number

#### 4.2.3 Pump and Motor

A pump is used as an external means to force a fluid flow through the tube. Since the experiment is designed for a closed circuit, this type of pump is very suitable because the amount of effort required to overcome friction within the piping system is significantly less. An electric motor of 0.5 HP is used for circulation of the fluid. Figure 4.5 shows the pump used in this experiment with electric motor.

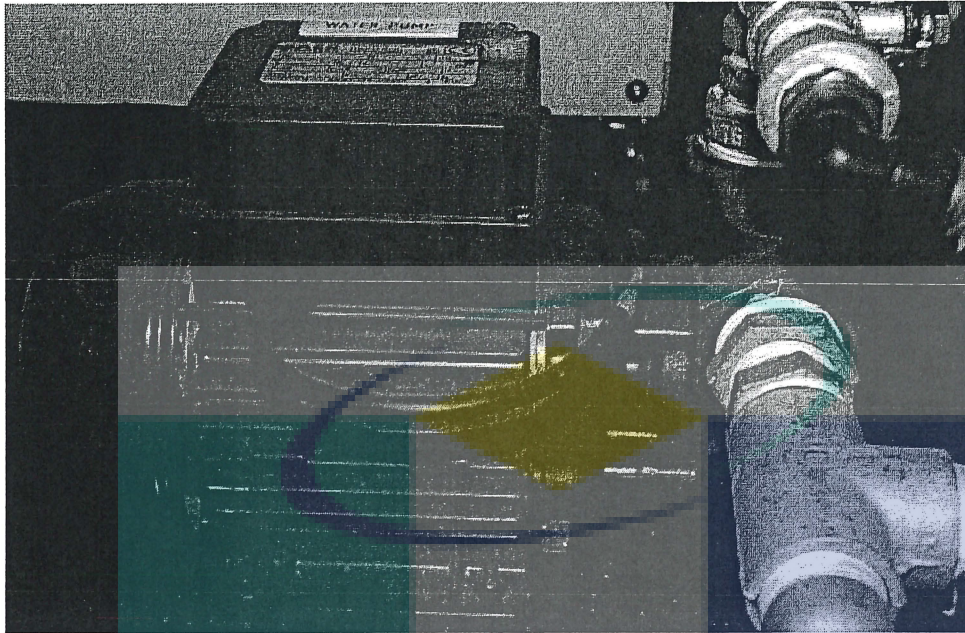


**Figure 4.5:** Pump with electric motor

#### 4.2.4 Flow meter

Flow meter shown in Figure 4.6 is located after the pump to measure the flow rate of the fluid through the tube. It is one of the important parameters required for the evaluation of Reynolds number. Digital flow meter is used for convenience which measures the velocity to one significant digit.

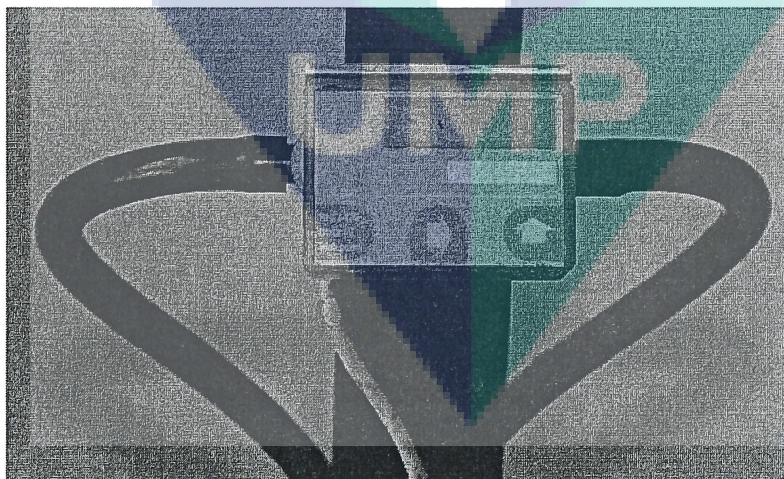


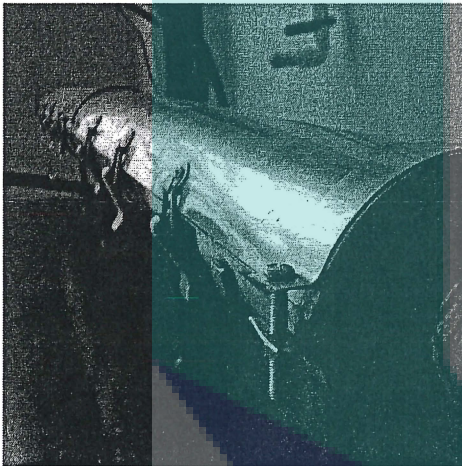
**Figure 4.6:** Flow meter

#### 4.2.5 Heater and Copper Tube

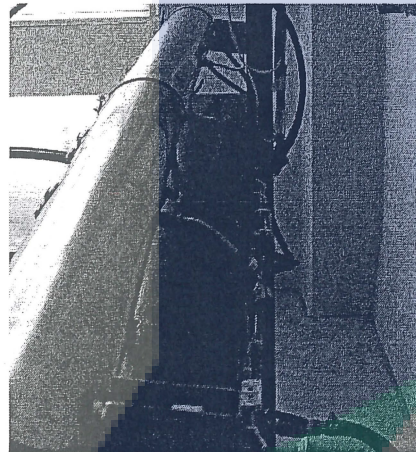
Two nichrome heaters of 20 gauge having a resistance of  $53.5 \Omega$  per meter length and 1000 W maximum electrical rating wrapped to a copper tube (plain tube) shown as Figure 4.7 is subjected to constant heat flux boundary condition.

#### 4.2.6 Control Panel

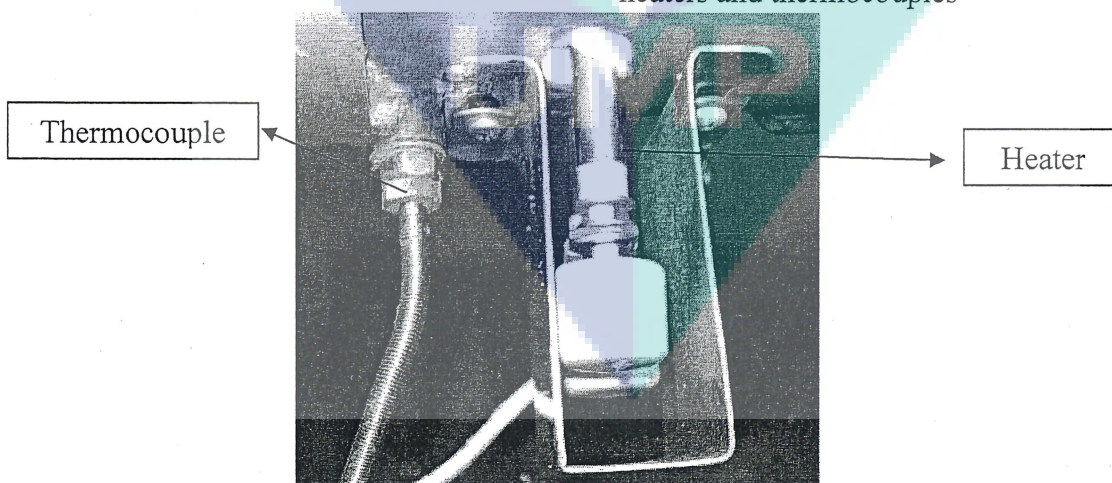
A panel is used to facilitate all controls such as the power supply to the heater, chiller, pump and the temperature display unit. All thermocouples are connected to the digital temperature indicator located on the control panel to enable monitor the experiment as shown in Figure 4.8.



(a) Front view of test section



(b) Rear view of test section with heaters and thermocouples



(c) Top view of heater and thermocouple attached to test section

**Figure 4.7:** Test Section wrapped with heating coils

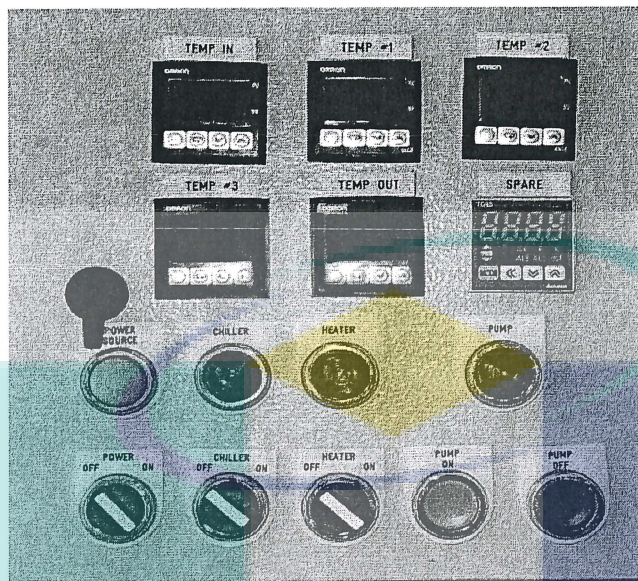


Figure 4.8: Control Panel

#### 4.2.7 Insulating Material

In order to minimize heat loss to the atmosphere, rock wool insulation is wrapped between the test section and the outer casing. Rock wool is used since their ability to partition air makes it an excellent heat insulator. Table 4.2, gives the temperature range of applicability of the various insulating materials.

Table 4.2: Insulators and temperature range of applicability

Material	Temperature ( $^{\circ}$ C)
Glass Wool	230-250
Stone/rock Wool	700-850
Ceramic Fiber Wool	1200

#### 4.2.8 Thermocouples

Five K- type thermocouples is provided to the test section as shown in Figure 4.7 (b), three are brazed to the surface at distances of 0.375, 0.75 and 1.125m from the location

of fluid entry and two others located at the inlet and outlet test section to measure the temperature of the working fluid. All these thermocouples have  $0.1^{\circ}\text{C}$  resolution and need to be calibrated before fixing them at the specified locations.

#### 4.2.9 U-Tube Manometer

U-tube manometer is connected to pressure taps located at either ends of the test section to measure the pressure drop over the length for various flow rates of the liquid. Carbon tetra chloride is used as the manometer liquid. The liquid level in the U tube will be lower which is connected to the tap at fluid entry and will be higher in the other. The difference between the levels as obtained from the manometer shown in Figure 4.10 is a function of the applied pressure, density of the pressurizing and manometer fluid.

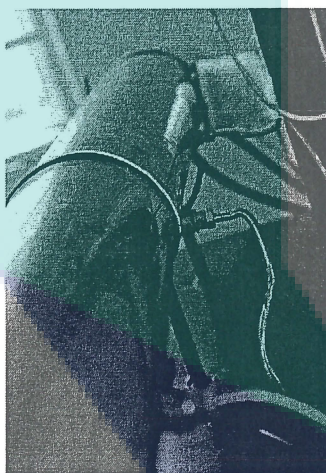


Figure 4.9: Thermocouple

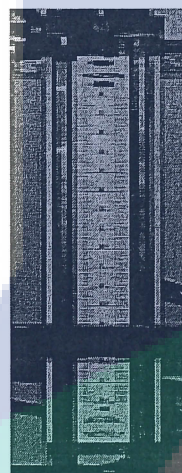
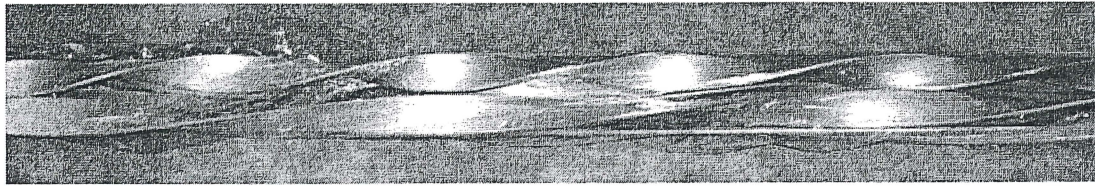


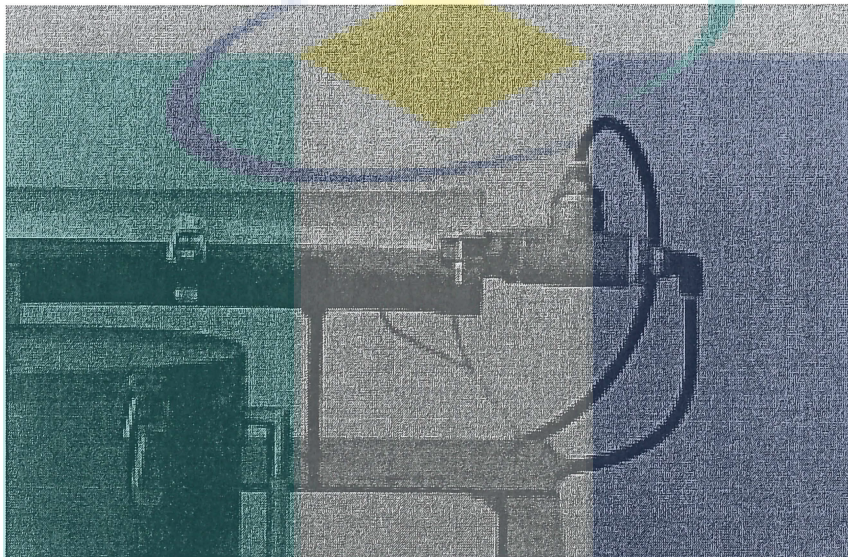
Figure 4.10: U-Tube Manometer

#### 4.2.10 Twisted tape Insert

The twisted tape is made of aluminum of 1.0mm of thick and 18mm wide as shown in Figure 4.11 (a). It is fabricated in the laboratory by fixing the ends of the strip to lathe, one in the headstock and the other in the tail stock. The strip is then twisted manually by turning the chuck to obtain various twist ratios. The strip can then be inserted from one end of the test section which can be opened with a wrench as shown in Figure 4.11 (b). The twist ratio of the tape is one of parameters considered in the study for heat transfer enhancement.



(a)



(b)

**Figure 4.11** Full-length twisted tape and insert

### 4.3 NANOFUID PREPARATION

$\text{Al}_2\text{O}_3$  nanoparticles, spherical in shape, having an average diameter of 50nm supplied by Sigma-Aldrich and Distilled Water (DW) are used to prepare the nanofluid. Nanoparticles are weighed in an electronic balance accurately to obtain the desired concentration. Sodium Dodecyl Benzene Sulfonate (SDBS) weighing one tenth the weight of nanoparticles is mixed with DW and stirred for ten to fifteen minutes. It is used as a surfactant to disperse the nanoparticles in the base fluid to prevent agglomeration. The nanoparticles are added and the mixture is stirred with magnetic/mechanical stirrer continuously for 10 hours. The preparation of nanofluid in this manner is referred as two step method.



**Figure 4.12:** Nanofluid prepared for various concentrations

The pH value changes depending on the material and concentration of the nanoparticles. The pH value is significant as it can react with the container material if its value is low (acidic range). To ensure that the particles do not agglomerate, a high value of zeta potential is preferred. In this manner different concentrations of nanofluid are prepared and tested for stability.

#### 4.4 EXPERIMENTATION PROCEDURE

- i. Distilled water is filled in the storage tank and experiments conducted for the evaluation of pressure drop and heat transfer coefficient.
- ii. Data is obtained at different flow rates and outlet temperatures. The flow rate, the pressure drop across the length of the tube, the temperatures of the fluid at the inlet and outlet, the surface temperatures are noted under steady state condition
- iii. The experimental values of friction factor and heat transfer coefficient are evaluated using equations (8) and Newton's law of cooling respectively.
- iv. The experimental data is compared with values evaluated with Blasius and Gnielinski equations for friction factor and Nusselt number respectively for

water. The reliability of the data obtained for water from the experimental setup is ensured before conducting experiments with nanofluid.

- v. Based on the reliability of the data with water, procedure i to iii is followed and experiments conducted with nanofluids prepared as explained in Section 4.3.

**Table 4.3:** Summary of materials and equipments required for the experiment

Equipment	Description
Nanofluids	Al <sub>2</sub> O <sub>3</sub> , CuO and TiO <sub>2</sub> are use as the working fluid that will be carrier for the thermal heat from the test section. The working fluid will be cooled by chiller.
Copper tube	Copper tube with 1.5 m in length and 0.019m in diameter.
Collecting Tank	The tank is stainless steel with a capacity of 30litres.
Thermocouple	5 calibrated thermocouples will be used with 0.1°C resolution.
Flow meter	The flow rate of working fluid in the test section will be determine by the flow meter
U-tube manometer	The manometer will take the pressure drop across the test section.
Pump	The pump will circulate the working fluid.

UMP



## CHAPTER 5

### RESULTS AND DISCUSSION

#### 5.1 VALIDATION OF THERMO-PHYSICAL PROPERTIES

The experimental data of viscosity and thermal conductivity ratios are shown in comparison with the values evaluated with Eqs. (11) and (12) in **Fig. 5.1**. The effect of volume concentration and Prandtl number with particle diameter on bulk temperature is shown in **Figs. 5.2 and 5.3** respectively. The bulk temperature increases with particle diameter for different values of concentration and Prandtl number. The bulk temperature increases with volume concentration as higher rates of heat flow takes place which can be observed from **Fig. 5.2**. The increase in Prandtl number indicates higher energy transfer and hence lower bulk temperatures can be expected as can be seen in **Fig. 5.3**. The influence of particle size on Prandtl number at different concentrations and temperatures is shown in **Fig. 5.4**. The Prandtl number increases with volume concentration at a particular temperature and decreases with increase in temperature of the nanofluid. The increase in Prandtl number with particle size is significant at lower temperatures as can be observed from **Fig. 5.4**. It can be observed from the figures that the particle size has a significant influence on the thermo-physical properties, which cannot be precluded in the determination of heat transfer coefficient. This aspect is brought out by a comparison of experimental data of different investigators with theory and the discussion from the results.

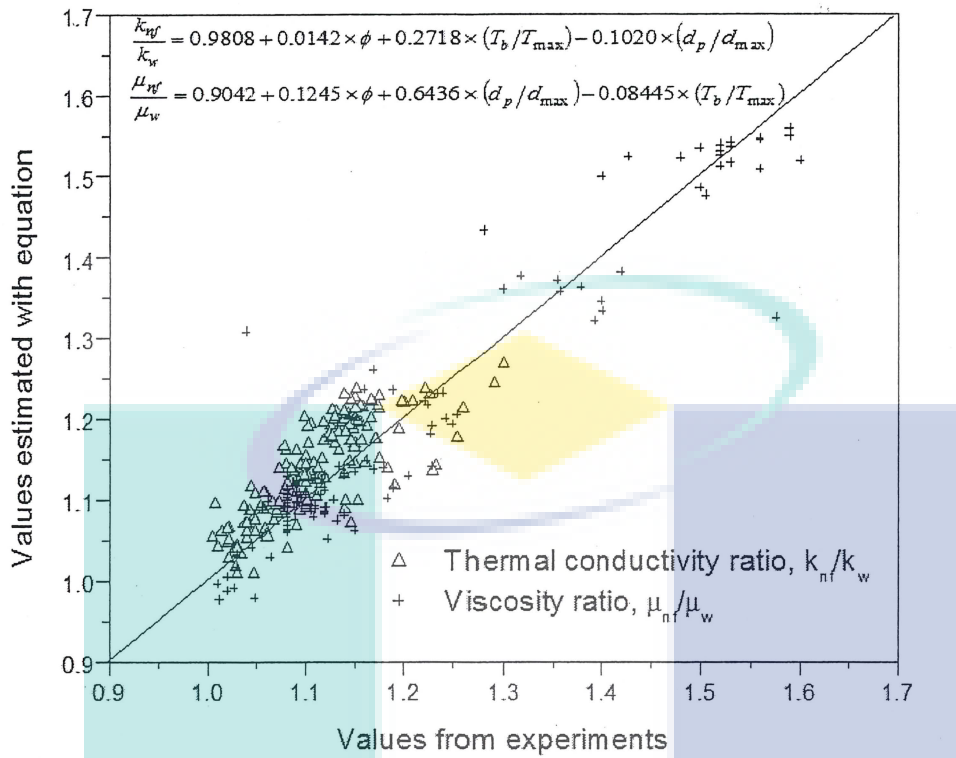


**Figure 5.1:** Validation of experimental data for thermal conductivity and viscosity with equations

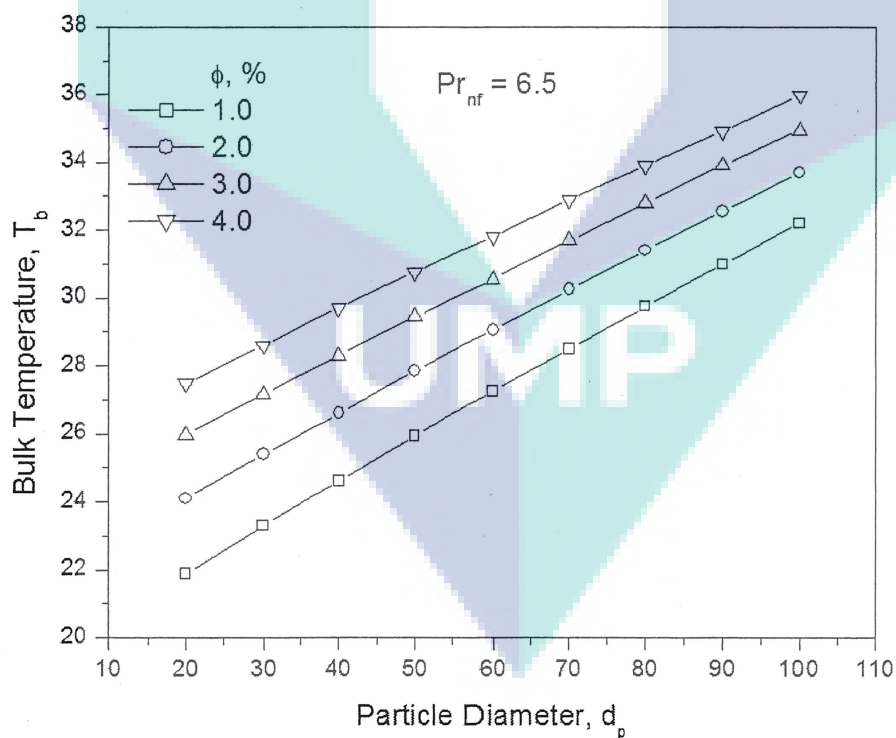


**Figure 5.2:** Variation of bulk temperature with particle diameter – Effect of concentration

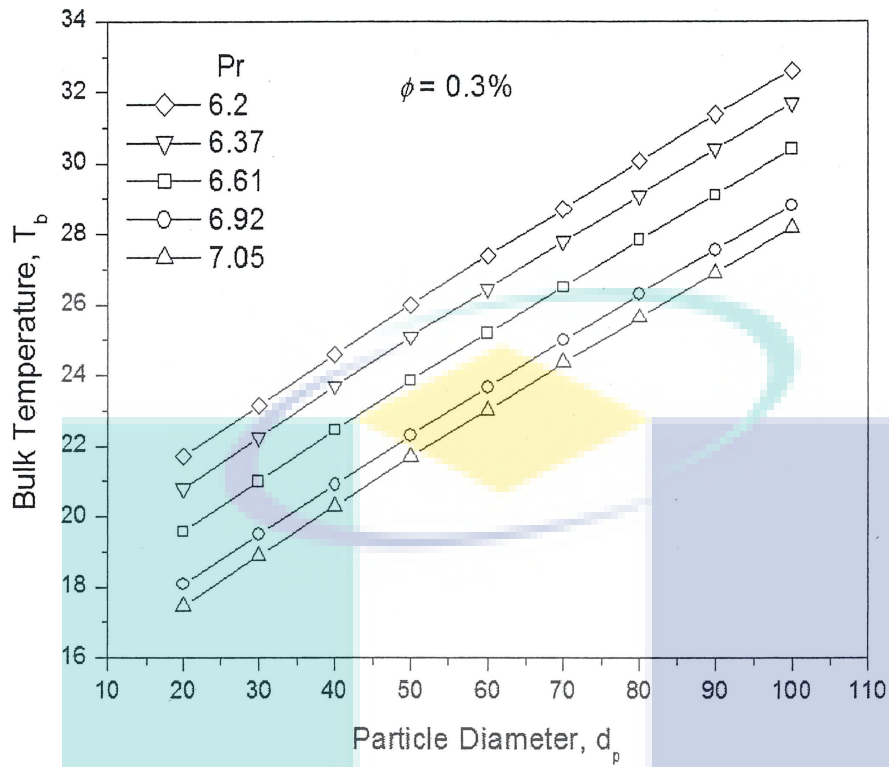


**Figure 5.3:** Variation of bulk temperature with particle diameter – Effect of Prandtl number

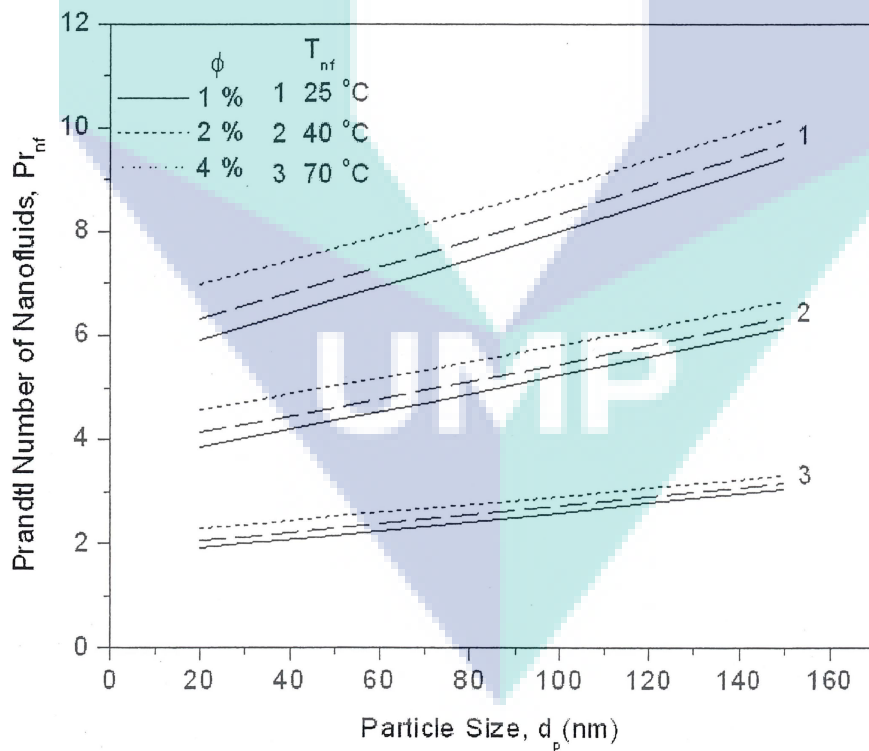


**Figure 5.4:** Variation of Prandtl number with particle diameter – Effect of  $\phi$  and bulk temperature

## 5.2 DEVELOPMENT OF REGRESSION EQUATION OF COLBURN TYPE

The experimental values of Nusselt number for water and nanofluids is shown in **Fig. 5.5** along with the values estimated with Eq. (22). The agreement between the experimental with the estimated values confirms the reliability of the equation proposed. The experimental data of water shown in **Fig. 5.6** is compared with values estimated with different equations available in literature for wide range of experimental Prandtl numbers. A good agreement of the experimental data of water with the equations of Gnielinski (1976), Dittus-Boelter and the proposed equation can be observed.

The experimental data of Fotukian and Esfahany (2010) with CuO nanofluid is shown in comparison with Eq. (22) in **Fig. 5.7**. The authors have stated the particle size to vary between 30 and 50nm. The Prandtl number of the nanofluid estimated with the aid of Eqs. (9) – (16) is observed to vary between 2.4 and 4.9. The Nusselt numbers estimated with Eq. (22) for  $Pr = 2.4$  and  $4.9$  is shown along with the experimental data in **Fig. 5.7**. Experiments with  $Al_2O_3$  nanofluid with 47nm particle size in the volume concentration range of 0.02 to 0.5% have been reported in the transition range by Sharma et al. (2009) and turbulent range by Sundar and Sharma (2010). A comparison of data with the values evaluated with Eq. (22) for extreme values of experimental Prandtl numbers is shown in **Fig. 5.8**. Experiments have been conducted by Yu et al. (2009) with SiC nanofluid of 3.7% volume concentration in the range  $3300 < Re < 13000$ ,  $4.6 < Pr < 7.1$  and  $34 < T_b < 57^\circ C$ . The experimental values of heat transfer coefficients are shown in **Fig. 5.9** along with lines drawn with Eq. (22). The close agreement between the heat transfer coefficients obtained from experiments and the values evaluated using Eqs. (9) – (16), indicate the validity of the thermo-physical property equations developed.

The experimental data of Williams et al. (2008) conducted with Alumina and Zirconia nanofluids in the temperature range of 21 and  $76^\circ C$  is shown plotted between Reynolds and Nusselt at different concentrations in **Fig. 5.10** along with the values estimated with Eq. (22). **Figs. 5.11 and 5.12** shows a comparison of the experimental values of Nusselt number obtained by Xuan and Li (2003) and Duangthongsuk and Wongwises (2010) with Cu and  $TiO_2$  nanofluids with values estimated with Eq. (22).

The data of water and nanofluid in the experimental range of Prandtl number evaluated using Eqs. (9) – (16) is shown enclosed by the extreme values of Prandtl numbers 5.0 and 7.3. The marginal deviation of the experimental data with the lines drawn with Eq. (22) in Figs. 5.7 to 5.12 can be due to variation in the property values employed in the analysis.

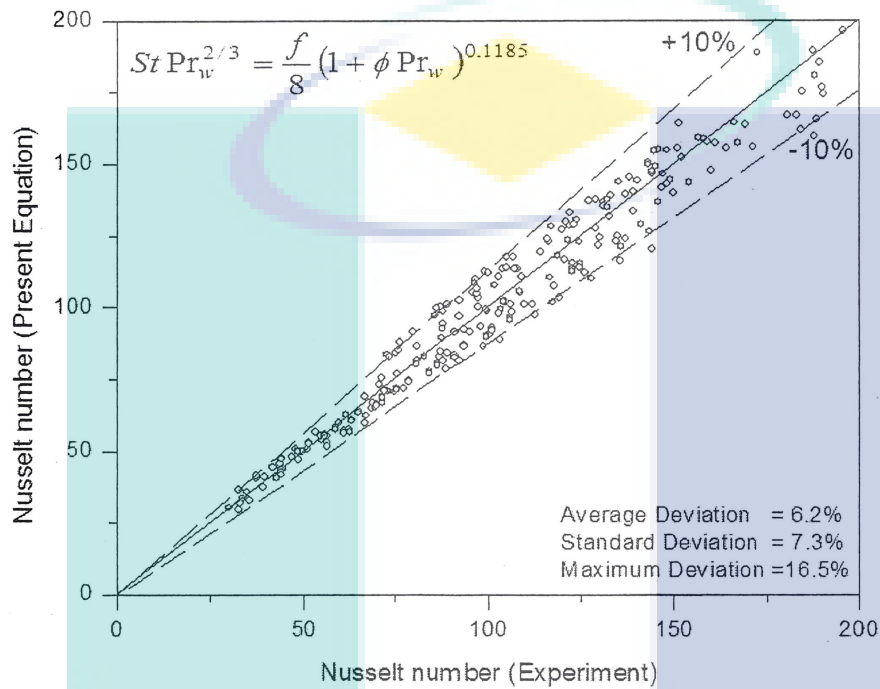


**Figure 5.5:** Comparison of experimental data with present equation for Nusselt number

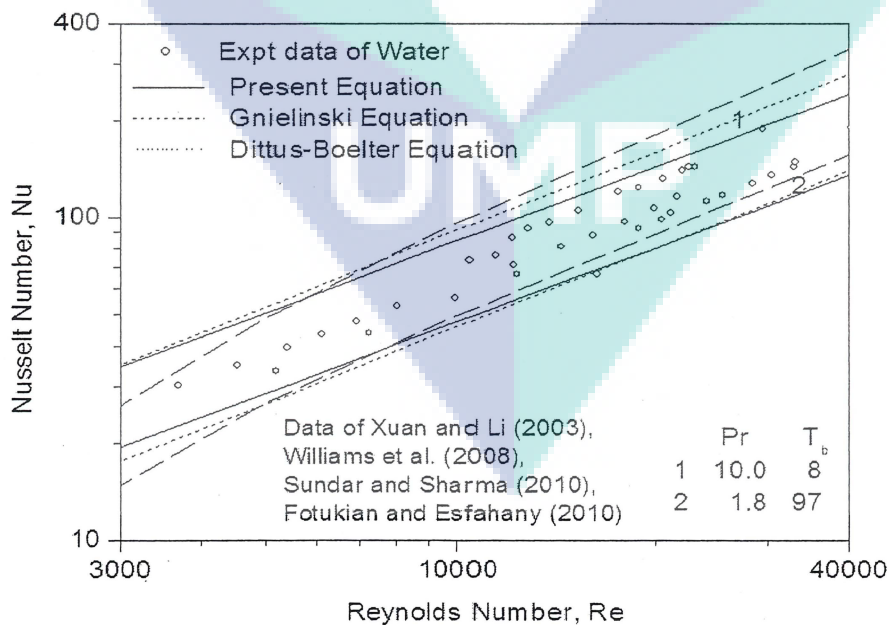


**Figure 5.6:** Comparison of experimental data with present equation and other equations for water

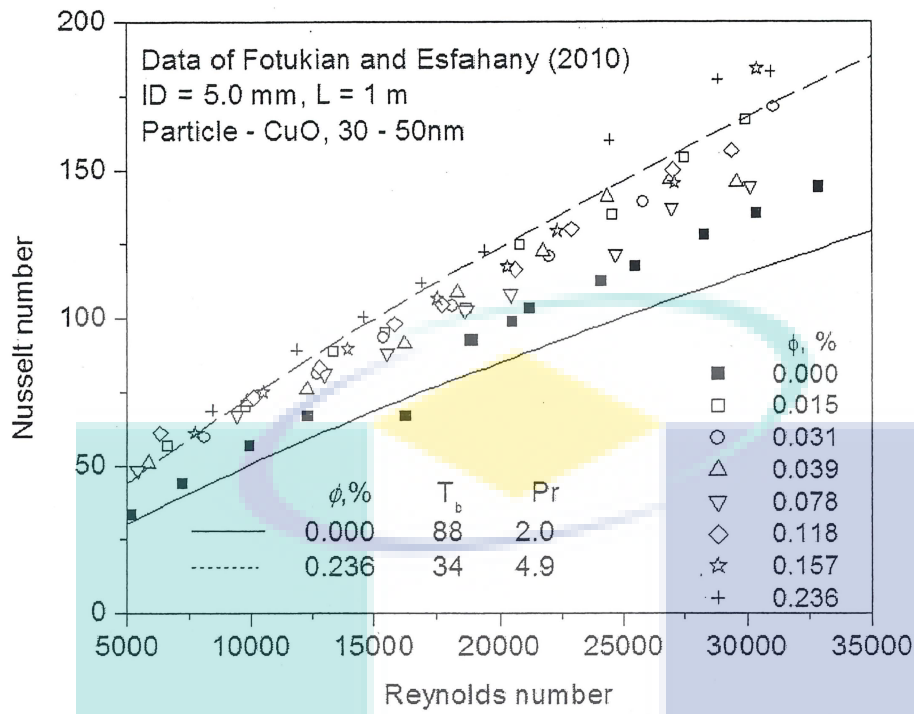


Figure 5.7: Comparison of experimental Nusselt number with present equation for CuO/water nanofluid

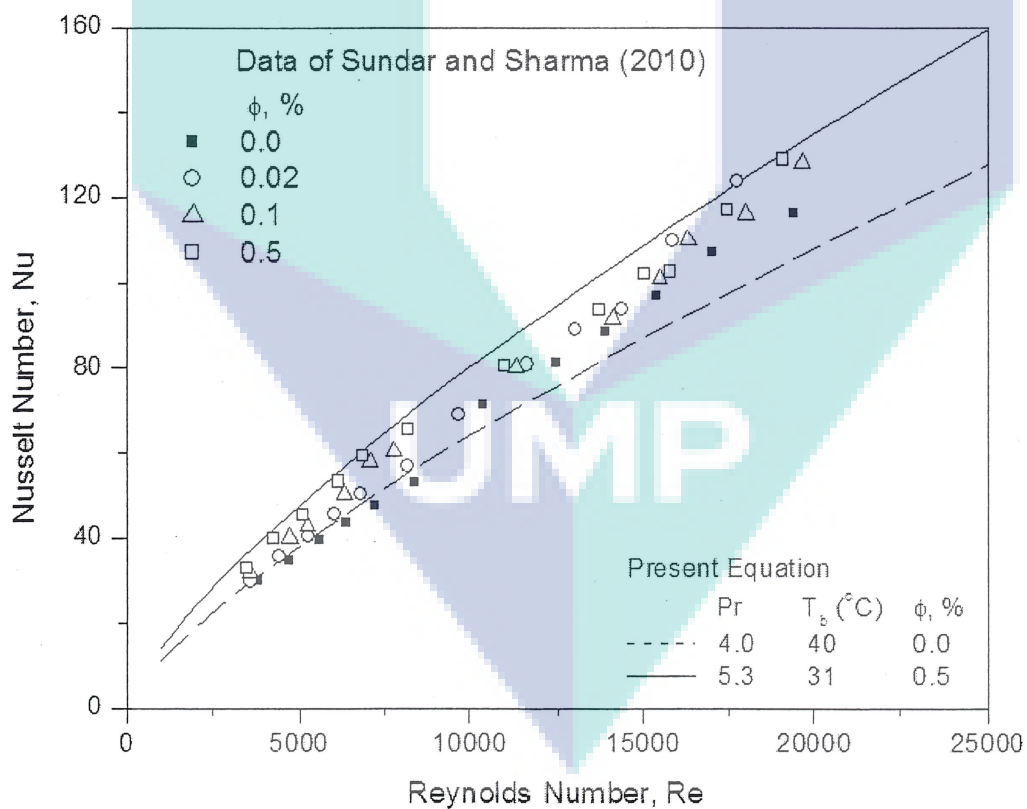
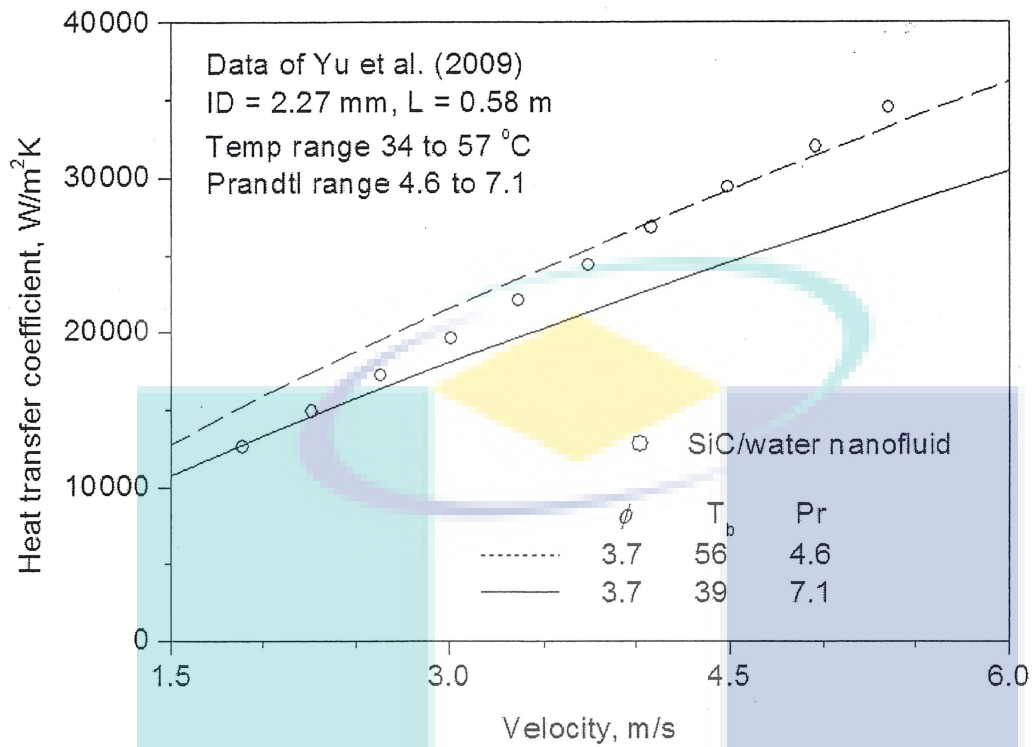
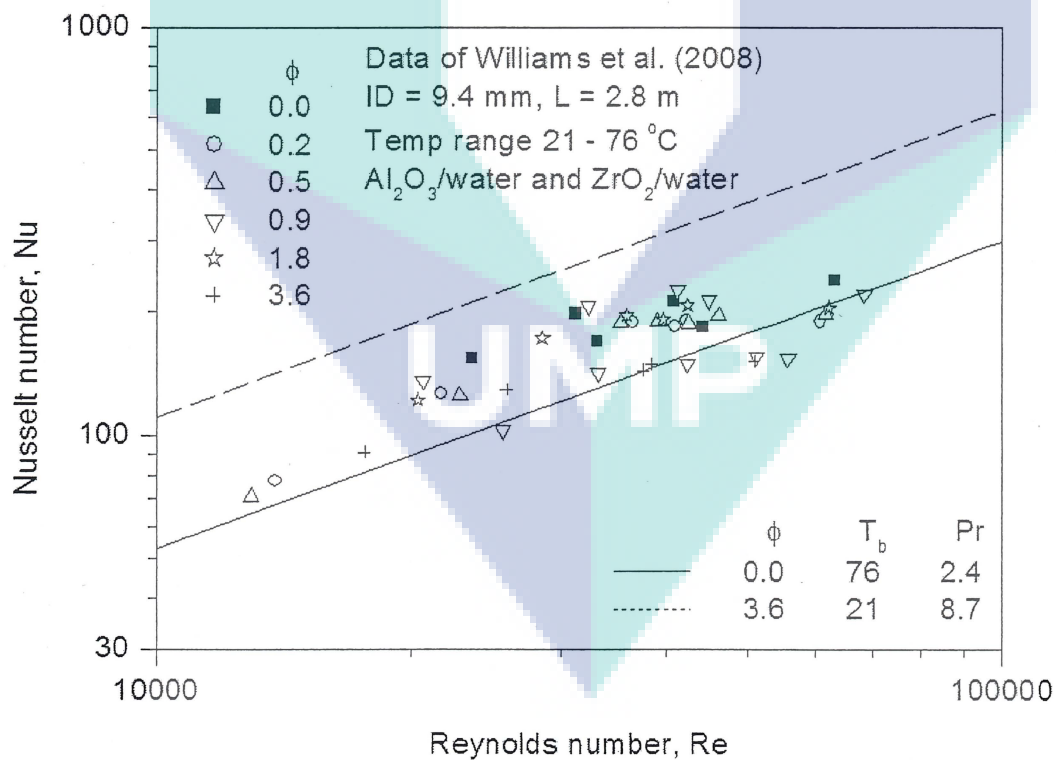


Figure 5.8: Comparison of experimental Nusselt number with present equation for  $\text{Al}_2\text{O}_3$ /water nanofluids



**Figure 5.9:** Comparison of experimental Nusselt number with present equation for SiC/water nanofluids



**Figure 5.10:** Comparison of experimental Nusselt number with present equation for Al<sub>2</sub>O<sub>3</sub>/water and ZrO<sub>2</sub>/water nanofluids

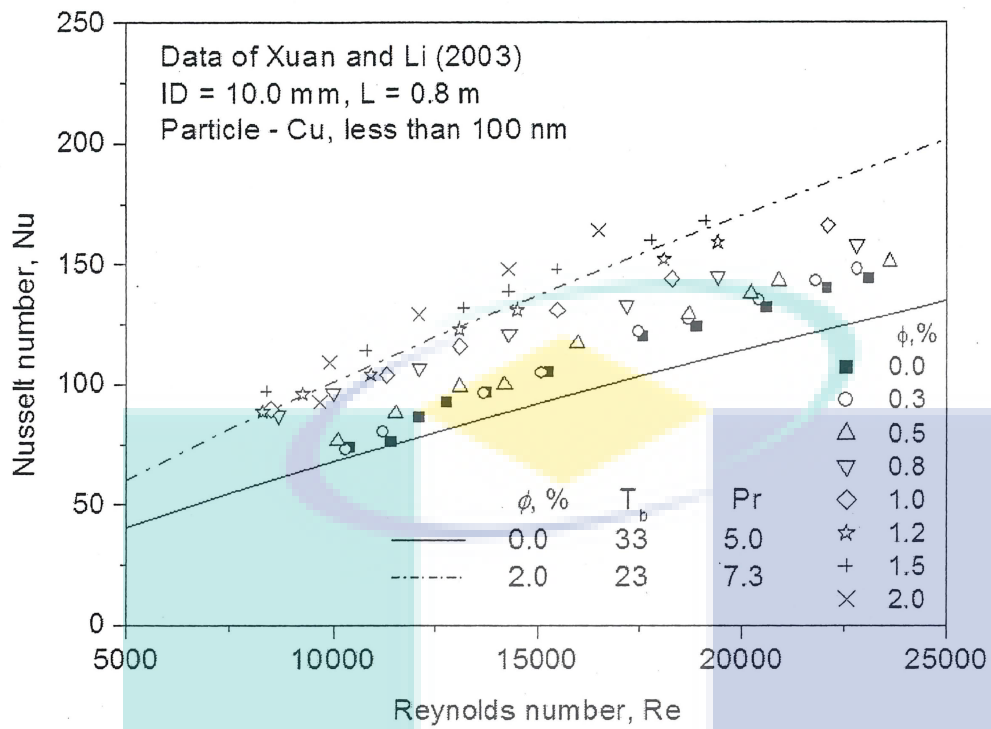


**Figure 5.11:** Comparison of experimental Nusselt number with present equation for Cu/water nanofluids

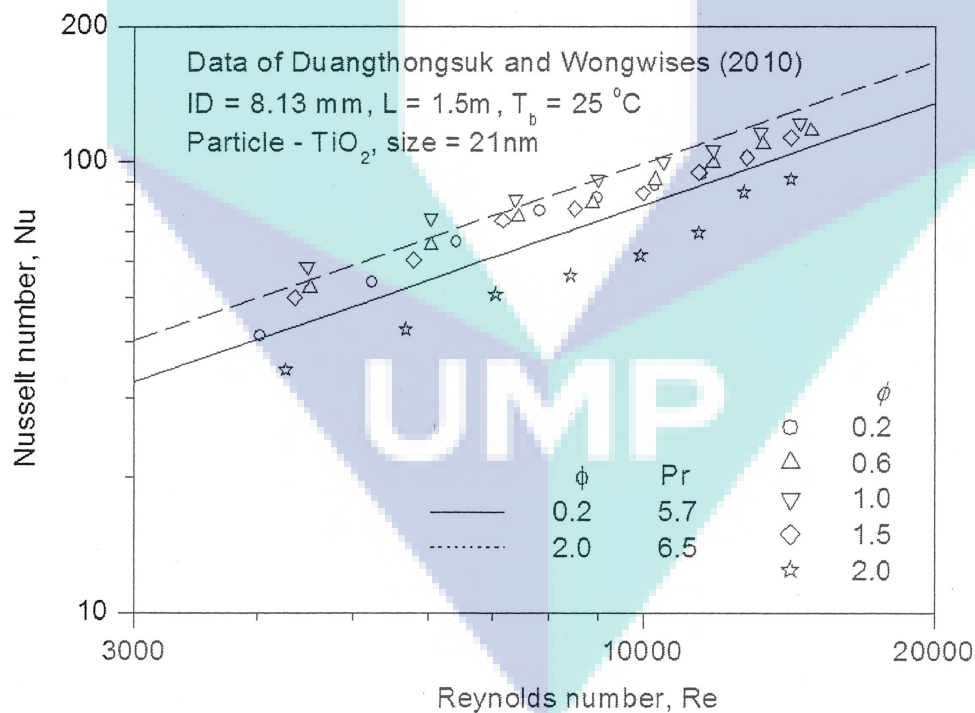


**Figure 5.12:** Comparison of experimental Nusselt number with present equation for  $\text{TiO}_2$ /water nanofluid



### 5.3 THEORETICAL ANALYSIS: NANOFLUID FLOW IN A TUBE

Theoretical model for the determination of nanofluid Nusselt number under turbulent flow has been presented by Sarma et al. (2010). The theoretical Nusselt numbers estimated with the eddy diffusivity equations is observed to be in good agreement with the experimental data of  $\text{Al}_2\text{O}_3$  nanofluid for concentrations up to  $\phi \leq 0.5\%$ .

Experimental data for water base nanofluids with different nano materials and particle sizes have been reported recently in literature for volume concentrations up to 4.0%. Hence, for determining the influence of various parameters affecting heat transfer coefficients, regression equations are developed for estimating the thermo physical properties which are dependent on particle size, concentration and temperature. The theoretical values of Nusselt numbers obtained from the numerical analysis are compared with the experimental heat transfer coefficients using the property equations (9) – (16) and the results presented in the form of graphs.

The data of water is enclosed with lines drawn from theory for  $\text{Pr}=7.8$  and  $\text{Pr}=5.0$  and compared with Eqs. (18) and (19) of Gnielinski (1976) and Dittus-Boelter (1930) respectively and shown as **Fig. 5.13**. The experimental data of water and nanofluid at different concentrations is shown enclosed by the theoretical lines in **Fig. 5.14**. It can be observed that the data lies between the theoretical lines drawn with  $\text{Pr}=5.0$  and  $\text{Pr}=9.1$ . A similar observation can also be made from **Fig. 5.15** drawn between fluid velocity and heat transfer coefficient for two values of Prandtl number.

The viscosity and thermal conductivity of nanofluid at a volume concentration is considered constant by Xuan and Li (2003), whereas the present analysis considers the properties to be dependent on temperature and particle size, in addition to concentration. The theoretical Nusselt number/heat transfer coefficient for the estimated value of  $\text{Pr}=7.3$  under predicts the experimental data presented in **Figs. 5.14 and 5.15**.

Experimental data of Fotukian and Esfahany (2010) is shown in comparison with the theoretical values for  $\text{CuO}$  nanofluid in **Figs. 5.16 and 5.17**. The authors have stated the particle size to vary between 30 and 50nm. The equation of Buongiorno (2006) is used to determine the Prandtl number with a value of 8.75 instead of 12.7 for laminar sublayer thickness. The Prandtl number of the nanofluid estimated is observed

to vary between 2.0 and 4.7. The Nusselt number in the volume concentration range of experimental data is shown to encompass with  $Pr = 2.4$  and  $4.9$ .

The variation of heat transfer coefficient/Nusselt number with Reynolds number of Alumina and Zirconia nanofluids at different concentrations obtained by Williams et al. (2008) is shown in **Figs. 5.18 and 5.19**. The theoretical values of heat transfer coefficient/Nusselt number estimated at temperatures undertaken by the investigators are shown to encompass the experimental data in **Figs. 5.18 and 5.19**. The deviation of the experimental data with the theoretical predictions in **Figs. 5.16 – 5.19** is due to the consideration of variable properties.

Experimental data of Yu et al. (2009) with SiC dispersed in water at 3.7% volume concentration in the range  $3300 < Re < 13000$  is shown along with the theoretical values in **Fig. 5.20**. The experimental data is shown with the theoretical values for heat transfer coefficient with Prandtl number of 4.6 and 7.1. The authors have stated the experimental range of temperature as 34 to 57°C, the theory has predicted to vary between 39 and 56°C.

Duangthongsuk and Wongwises (2010) conducted experiments with  $TiO_2$  dispersed in water and presented a regression equation for the evaluation of Nusselt number valid for the range  $3000 < Re < 18000$  and  $\phi \leq 1.0$  with a deviation of less than 1.0% as

$$Nu_{nf} = 0.07 Re_{nf}^{0.707} Pr_{nf}^{0.385} \phi^{0.074} \quad (36)$$

Equation (36) is shown in comparison with the values obtained from theory in **Fig. 5.21** for  $\phi = 0.2$  and  $\phi = 1.0$ . The agreement between the values from theory and the regression equation (36) is satisfactory.

Experiments are conducted at 25°C in the volume concentration range  $0.2 \leq \phi \leq 2.0$  with 21nm size  $TiO_2$  nanoparticles by Duangthongsuk and Wongwises (2010) and the data presented as **Fig. 5.22**. The theory is in satisfactory agreement with the experimental data in the turbulent range for up to  $\phi = 1.0\%$ . The experimental heat transfer coefficients with  $\phi = 2.0\%$  are lower than the values obtained with  $\phi = 1.0\%$ . To explain this unusual observation of decrease in Nusselt number with increase in  $\phi$ ,

the ratio of Prandtl number of nanofluid to that of water is estimated and presented as **Table 5.1**. **Fig. 5.23** shows the variation of Prandtl number of nanofluid and water with fluid temperature. It can be observed for  $\phi = 1.0\%$ , the Prandtl number of nanofluid is greater than water for temperatures below  $20^\circ\text{C}$  and decreases thereafter for 20nm particle size. Since the experiments by Duangthongsuk and Wongwises (2010) are undertaken at  $25^\circ\text{C}$  with 21nm particle size, no enhancements in heat transfer coefficients could be obtained. The reduction in heat transfer coefficients observed by Pak and Cho (1998) with  $\text{Al}_2\text{O}_3$  nanoparticles of 13nm size can be due to the reasons stated.

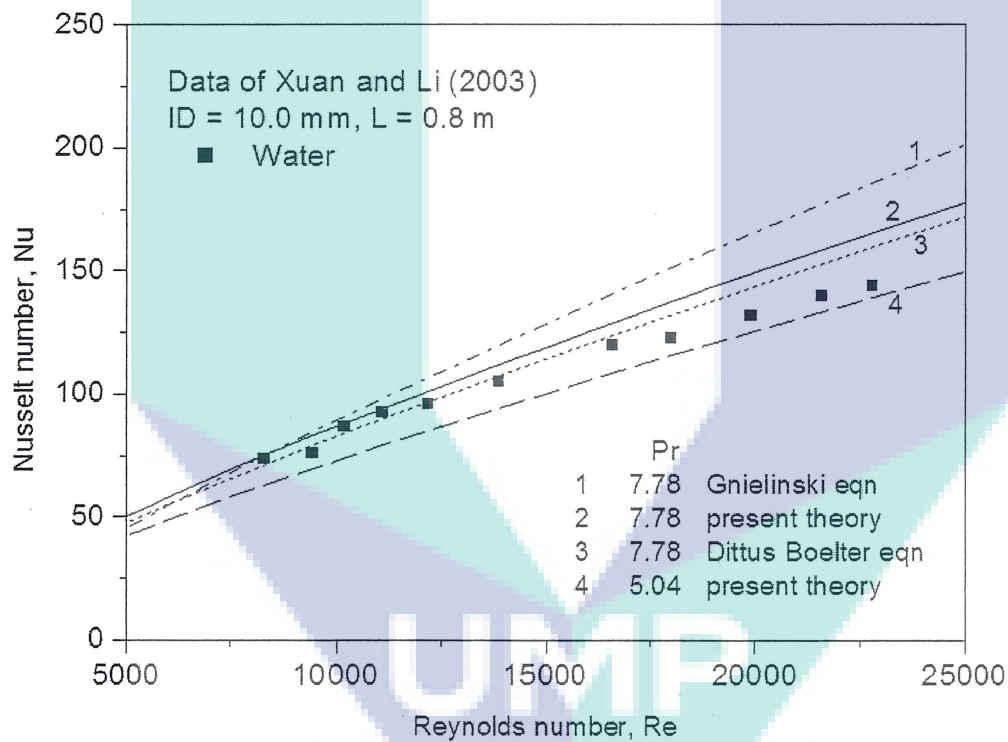


**Figure 5.13:** Comparison of experimental data with theory and other equations for water

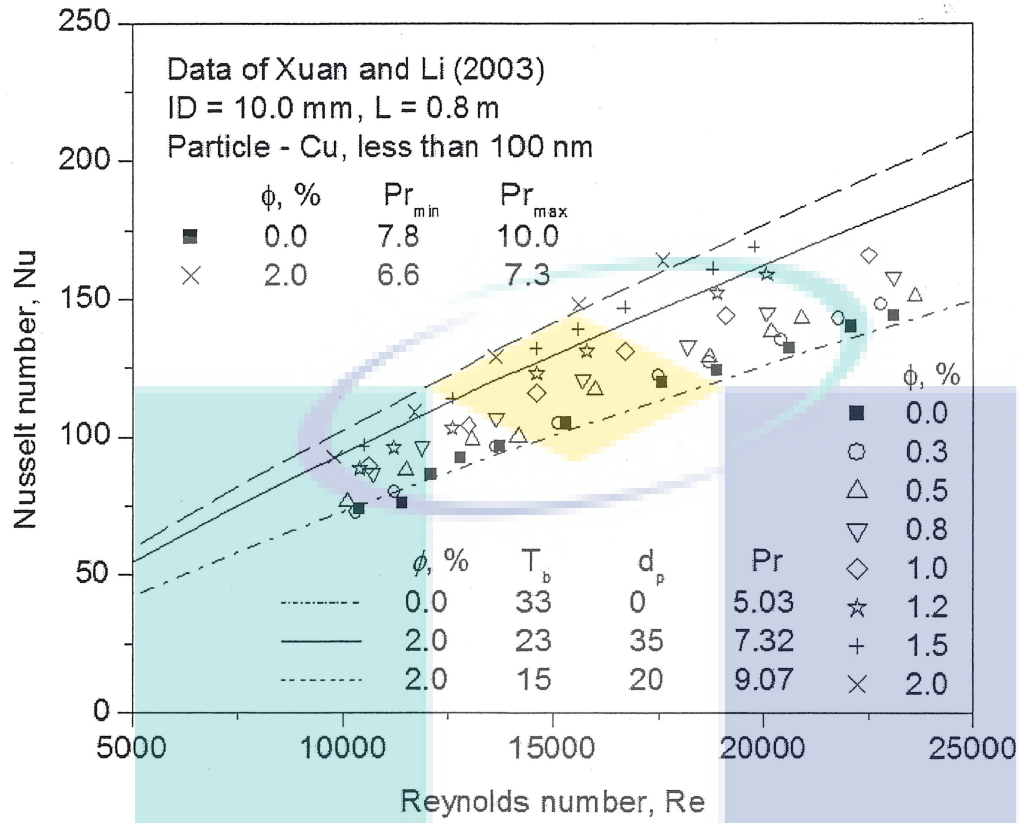


Figure 5.14: Comparison of experimental Nusselt number with theory for Cu/water nanofluid

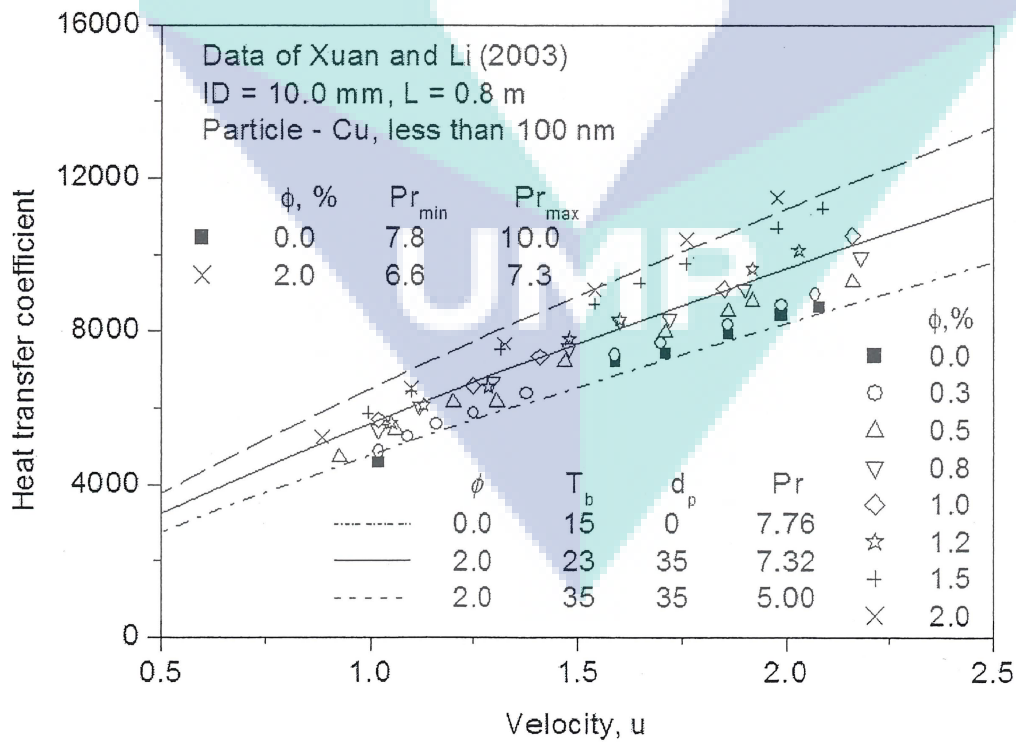


Figure 5.15: Comparison of experimental heat transfer coefficients with theory for Cu/water nanofluid

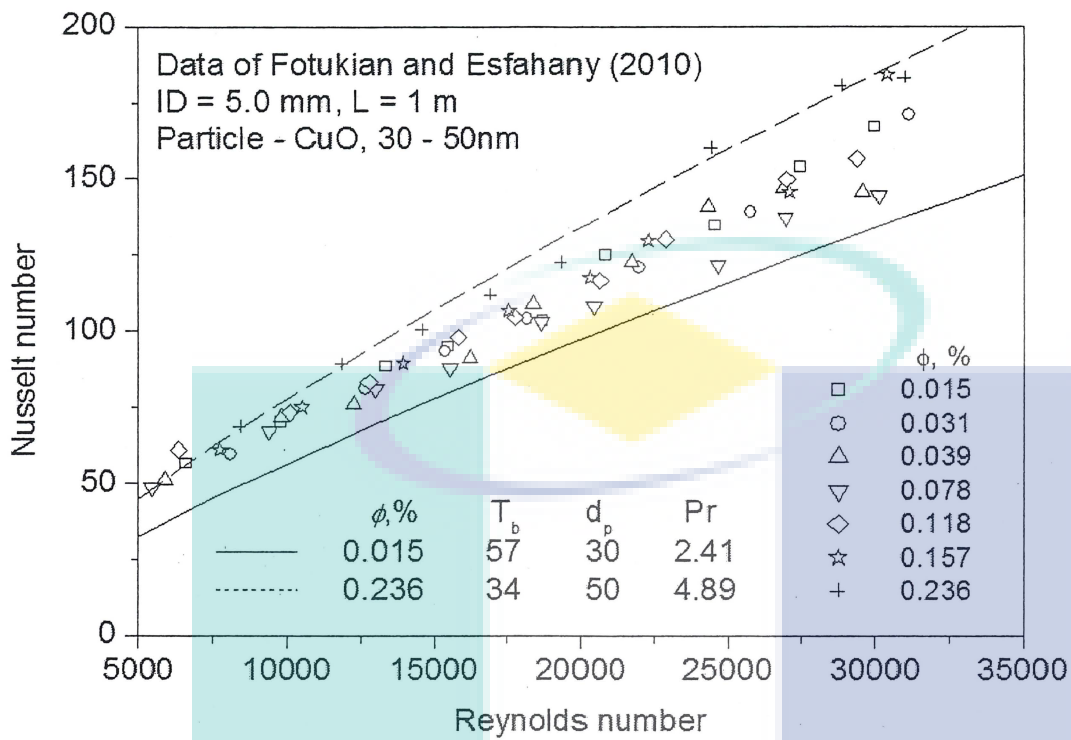


Figure 5.16: Comparison of experimental Nusselt number with theory for CuO/water nanofluid

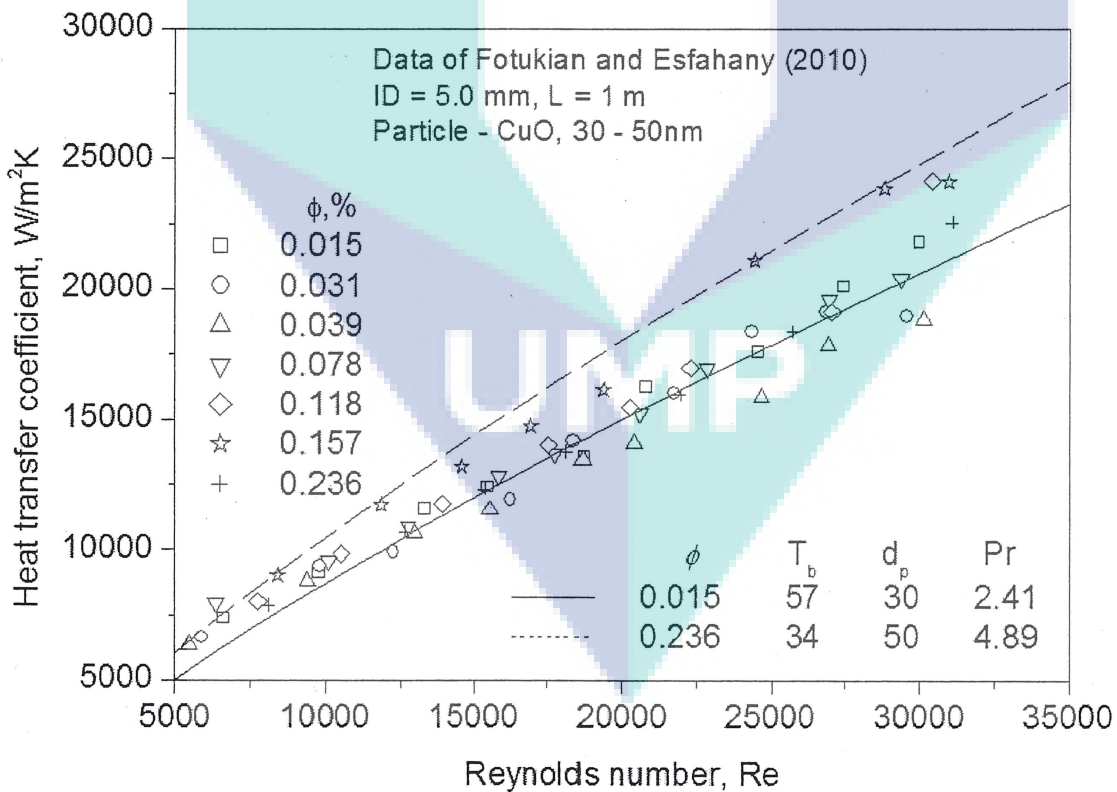
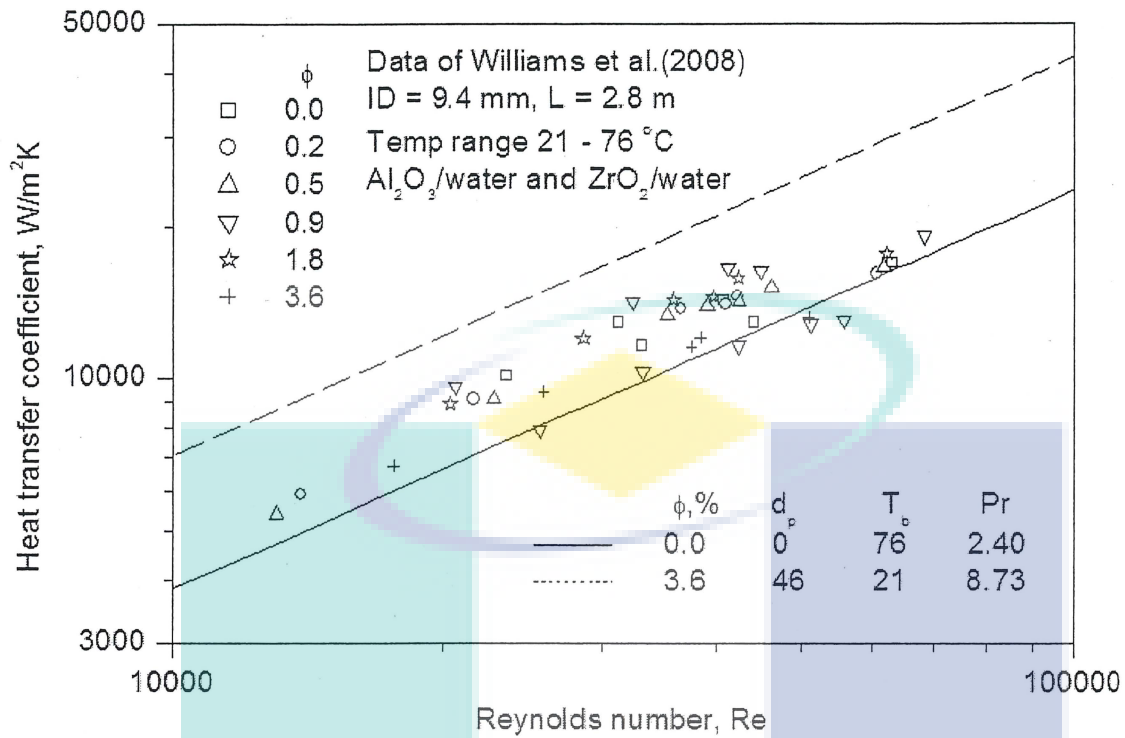
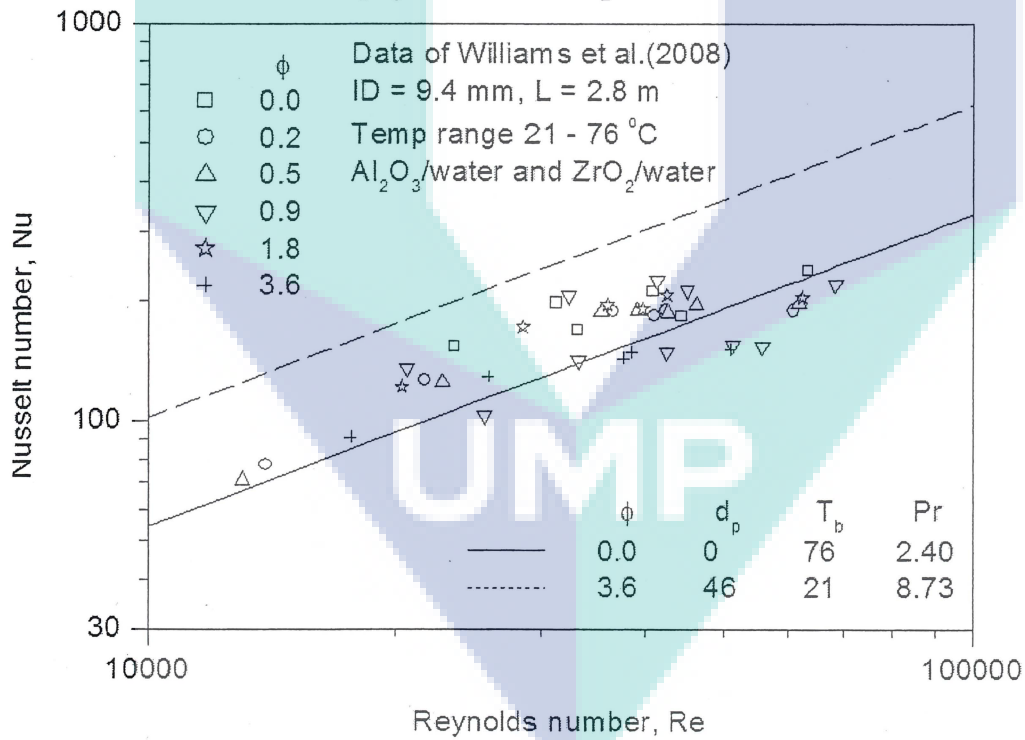


Figure 5.17: Comparison of experimental heat transfer coefficients with theory for CuO/water nanofluid



**Figure 5.18:** Comparison of experimental heat transfer coefficients with theory for  $Al_2O_3/water$  and  $ZrO_2/water$  nanofluids



**Figure 5.19:** Comparison of experimental Nusselt number with theory for  $Al_2O_3/water$  and  $ZrO_2/water$  nanofluids

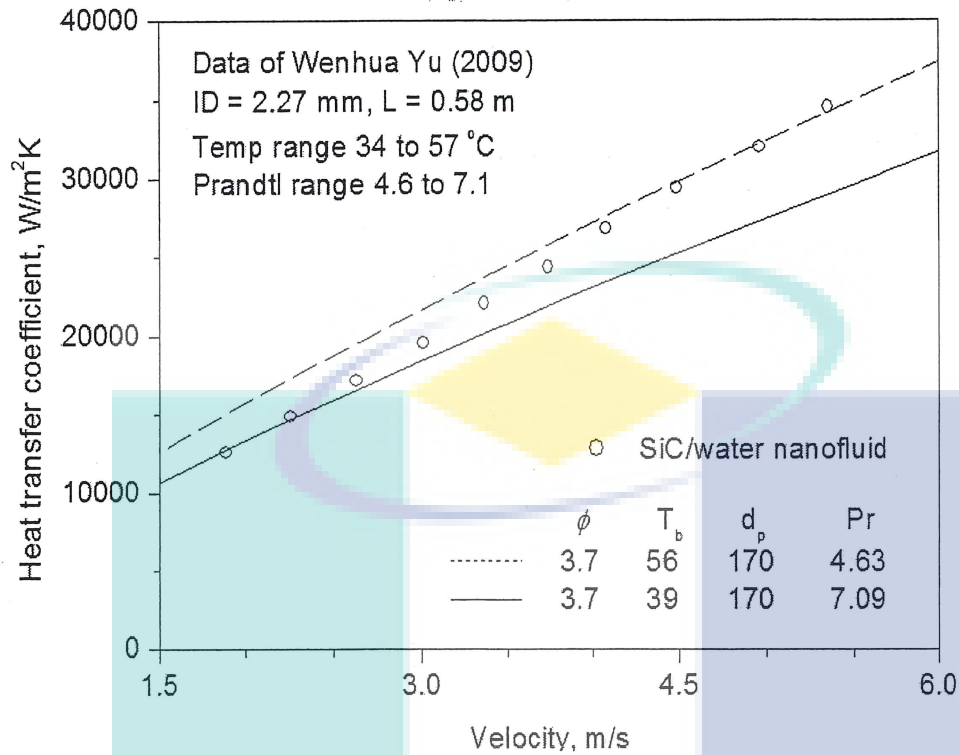


**Figure 5.20:** Comparison of experimental heat transfer coefficients with theory for SiC/water nanofluid

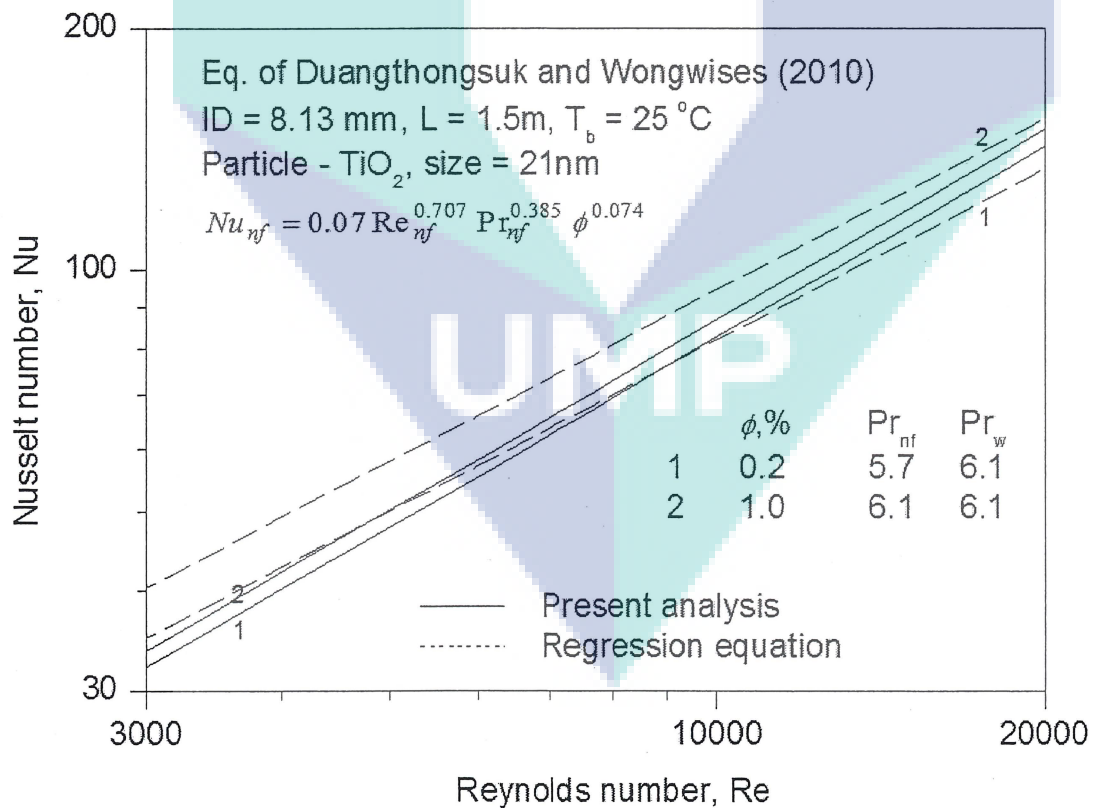


**Figure 5.21:** Comparison of theory with Eq.(13) of Duangthongsuk and Wongwises (2010)

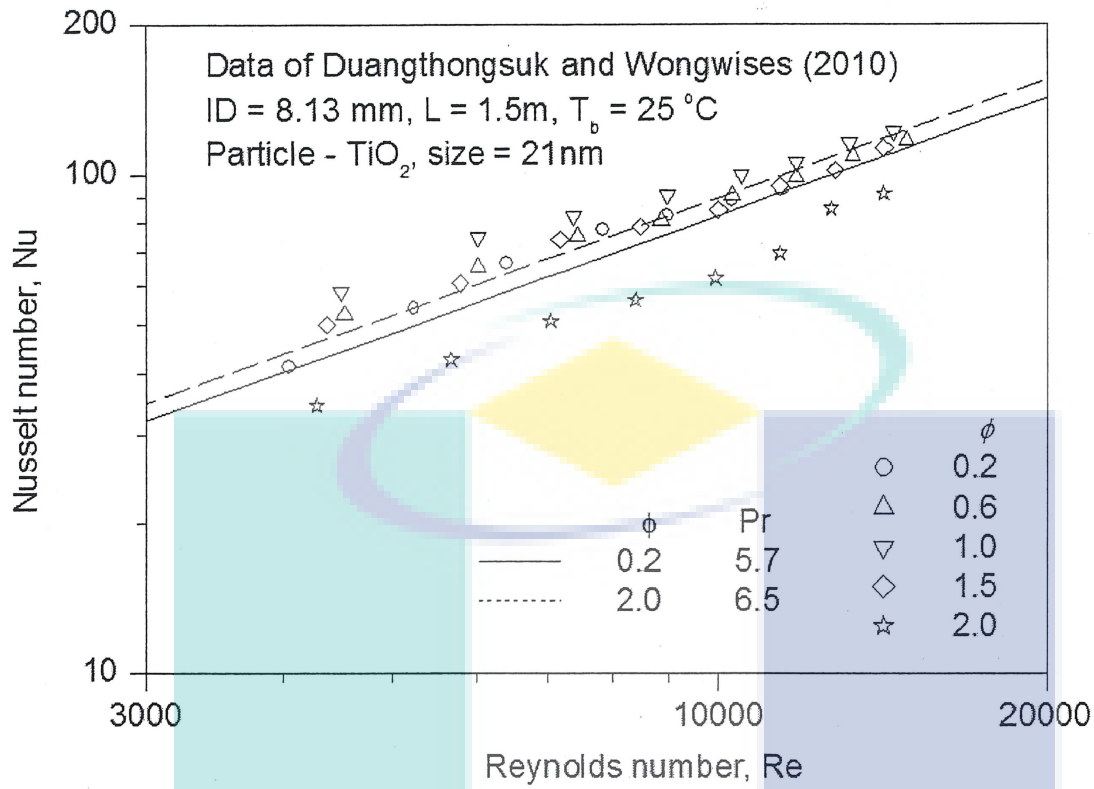


**Figure 5.22:** Comparison of experimental Nusselt number with theory for  $\text{TiO}_2$ /water nanofluid

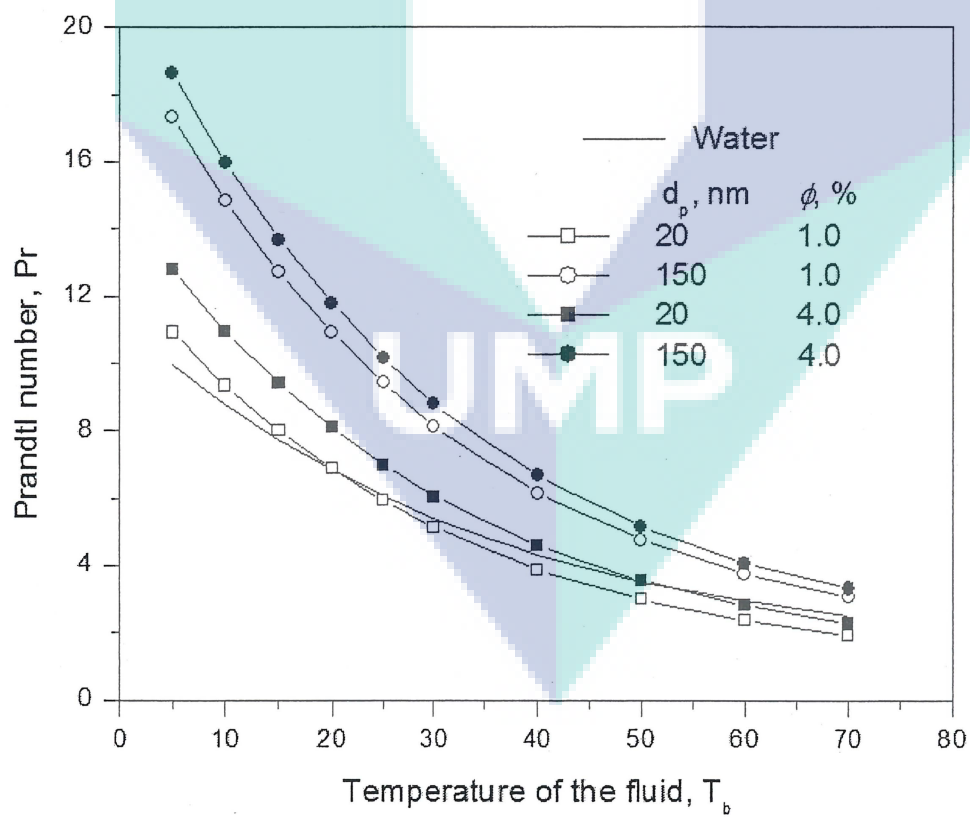


**Figure 5.23:** Variation of Prandtl number with temperature for different particle size and  $\phi$



**Table 5.1:** Estimation of Prandtl ratio of various nanofluids of different investigators

No	Nanoparticle	$D_p$ , nm	$T_b$	$\phi$ , (%)	$Pr_w$	$Pr_{nf}$	$Pr_{nf}/Pr_w$	Authors
1	Al <sub>2</sub> O <sub>3</sub>	13	27	1.34	5.89	5.66	0.96	Pak and Cho (1998)
		13	27	2.78	5.89	6.19	1.05	
2	TiO <sub>2</sub>	21	25	0.2	6.21	5.73	0.92	Duangthongsuk and Wongwises (2010)
		21	25	1.0	6.21	6.10	0.98	
		21	25	2.0	6.21	6.51	1.05	
3	TiO <sub>2</sub>	27	27	0.99	5.89	5.85	0.99	Pak and Cho (1998)
		27	27	2.04	5.89	6.25	1.06	
		27	27	3.16	5.89	6.62	1.12	
4	Cu	20	15	2.0	8.21	9.07	1.10	Xuan and Li (2003)
		20	23	2.0	6.56	6.92	1.06	
		35	15	2.0	8.21	9.59	1.17	
		35	23	2.0	6.56	7.32	1.12	
5	CuO	30	34	0.015	4.92	4.41	0.90	Fotukian and Esfahany (2010)
		30	57	0.236	3.07	2.46	0.80	
		50	34	0.015	4.92	4.81	0.98	
		50	57	0.236	3.07	2.68	0.87	
6	Al <sub>2</sub> O <sub>3</sub>	46	21	0.9	6.93	7.65	1.10	Williams et al. (2008)
		46	76	0.9	2.40	1.96	0.81	
		46	21	3.6	6.93	8.73	1.26	
		46	76	3.6	2.40	2.26	0.94	
7	Al <sub>2</sub> O <sub>3</sub>	47	30	0.5	5.44	5.57	1.02	Sundar and Sharma (2010)
		47	43	0.5	3.99	3.79	0.95	
8	ZrO <sub>2</sub>	60	21	0.2	6.93	7.72	1.11	Williams et al. (2008)
		60	76	0.2	2.40	1.97	0.82	
		60	21	0.9	6.93	8.07	1.16	
		60	76	0.9	2.40	2.07	0.86	

9	SiC	170	56	3.7	3.12	4.63	1.49	Yu et al. (2009)
		170	39	3.7	4.36	7.09	1.63	

#### 5.4 THEORETICAL ANALYSIS: NANOFLUID FLOW WITH TAPE INSERTS

The values of Nusselt number evaluated from theory for water are shown plotted in **Fig. 5.24** for two values of Prandtl number and twist ratios ( $H/D$ ). It can be observed that the influence of fluid properties on Nusselt are more pronounced than the twist ratio for water.

A comparison of Nusselt number for water and nanofluid for volume concentration  $\phi = 0.5\%$  is shown for two twist ratios in **Fig. 5.25**. It can be observed that the values of Nu are greater for nanofluid than for water for the same value of  $Pr = 6.2$ . Comparison of the Nusselt number obtained by various investigators for  $(H/D) = 6.0$  and  $Pr = 5.0$  at different Reynolds is shown in **Fig. 5.26**.

The agreement between the experimental data of Chiu and Jang (2009) for air with the present theory is satisfactory for different twist ratios as shown in **Fig. 5.27**. The values of Nusselt number obtained from experiments by Sharma et al. (2009) and Sundar and Sharma (2010) for flow of water and nanofluid in a tube and with tape inserts is shown in **Fig. 5.28**. It can be observed from the figure that the heat transfer rates increase with concentration and decrease with twist ratios. The variation of friction factor with Reynolds number is shown plotted in **Fig. 5.29** along with the experimental values for flow of water and nanofluid in a tube and with tape insert. A good agreement between the experiment and theory can be observed from **Figs. 5.28 and 5.29**.

From the numerical experiments conducted, it is observed that eddy diffusivity coefficient  $B$  varies with Re, twist ratio ( $H/D$ ) and nanofluid volume concentration  $\phi$ . The value of  $B$  employed by Van Driest in his equation is equal to 0.4 when the damping constant  $A = 26$  which is applicable to pure fluids. However, Sarma et al. (2010) observed that for nanofluids  $B$  attains a constant value of 0.023 when  $A = 15$ . However, for the case of nanofluid flow with tape insert,  $B$  decreases

monotonically with  $Re$  for different values of  $(H/D)$  as can be seen from **Fig 5.30**.

The theoretical data is subjected to regression and the equation is obtained as

$$B = 1.649 (R^+)^{-0.26} (0.001 + \phi)^{0.00103} (0.001 + D/H)^{0.05} \quad (37a)$$

$$B = 2.384 (Re)^{-0.2248} (0.001 + \phi)^{0.00095} (0.001 + D/H)^{0.04634} \quad (37b)$$

obtained with a  $AD = 0.4$  and  $SD = 0.6$  and valid in the range  $3 \times 10^3 < Re < 10^5$ ,  $4.0 \leq Pr \leq 5.8$   $0 \leq \phi \leq 4.0\%$  ( $\phi = 0$  refers to water) and  $5 \leq (H/D) \leq 83$

Numerical computations in the Reynolds number range of  $3 \times 10^3 < Re < 10^5$  are carried out to determine the parameters influencing  $\zeta$  the index of Prandtl in the eddy diffusivity equation. Based on the earlier assumption that  $\zeta = F \{ \phi, R^+, (H/D), Pr \}$ , the values obtained from the computer runs is subjected to regression and the equation obtained is obtained as

$$\zeta = -7.723 (R^+)^{-0.0649} (0.001 + \phi)^{-0.1544} (0.001 + D/H)^{-0.0384} (Pr)^{-1.242} \quad (38a)$$

$$\zeta = -8.47 (Re)^{-0.0561} (0.001 + \phi)^{-0.1545} (0.001 + D/H)^{-0.0394} (Pr)^{-1.242} \quad (38b)$$

The equation is valid for water and nanofluids for volume concentration  $\phi \leq 4.0\%$  with an average deviation of 1.9 % and standard deviation of 2.2 %. The equation has the flexibility to be applied for flow in a plain tube as well as for twisted tapes. **Fig. 5.31** shows the variation of  $\zeta$  with  $Re$  for different values of  $H/D$  and  $\phi$ .

The influence of volume concentration  $\phi$  on temperature and its gradients is shown through **Figs. 5.32 – 5.33**. The plot shown in **Fig. 5.32** indicates that increase in Reynolds for a given  $\phi$  markedly affect the temperature profile and the gradients. Results shown in **Fig. 5.33** depict the modulus of the temperature gradients  $\left| \frac{dT^+}{dy^+} \right|_{y^+=0}$  to increase with  $Re$  and  $\phi$ . However the gradients for flow with twisted taper insert are lower than the values obtained for nanofluid flow in a tube. This is due to the swirling action of the fluid due to tape which lowers the temperature gradient at the wall of the tube. The experimental data of various nanofluids for flow in a plain tube and with twisted tape is shown in **Fig. 5.34** for the equation developed. The close agreement between the line drawn from the equation and the experimental values shows the reliability of the equation proposed.

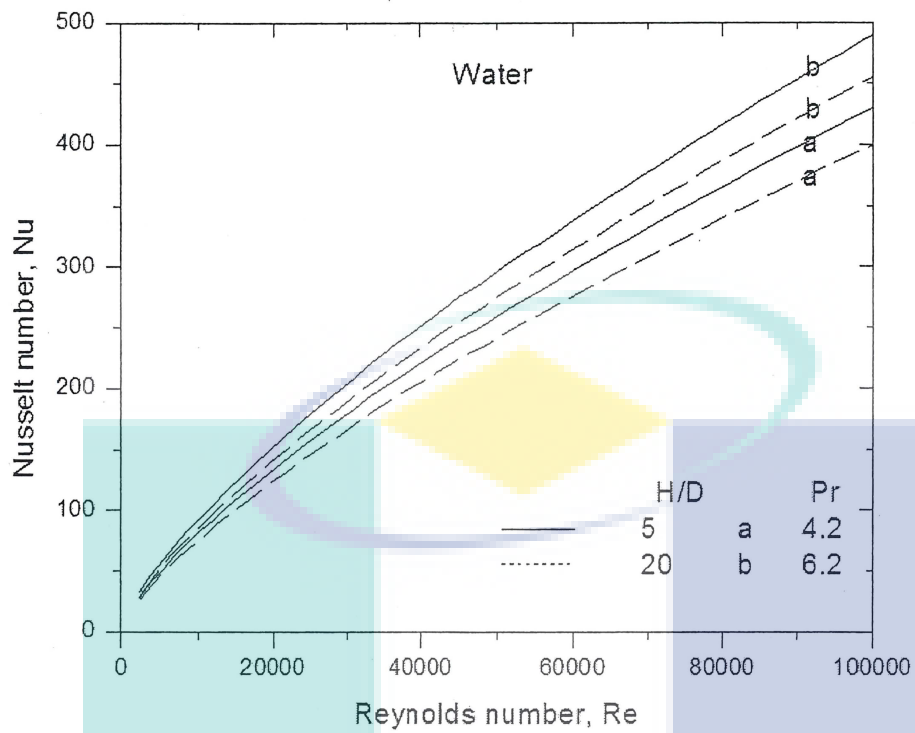


Figure 5.24: Influence of twist ratio and Prandtl number on Nusselt number of water

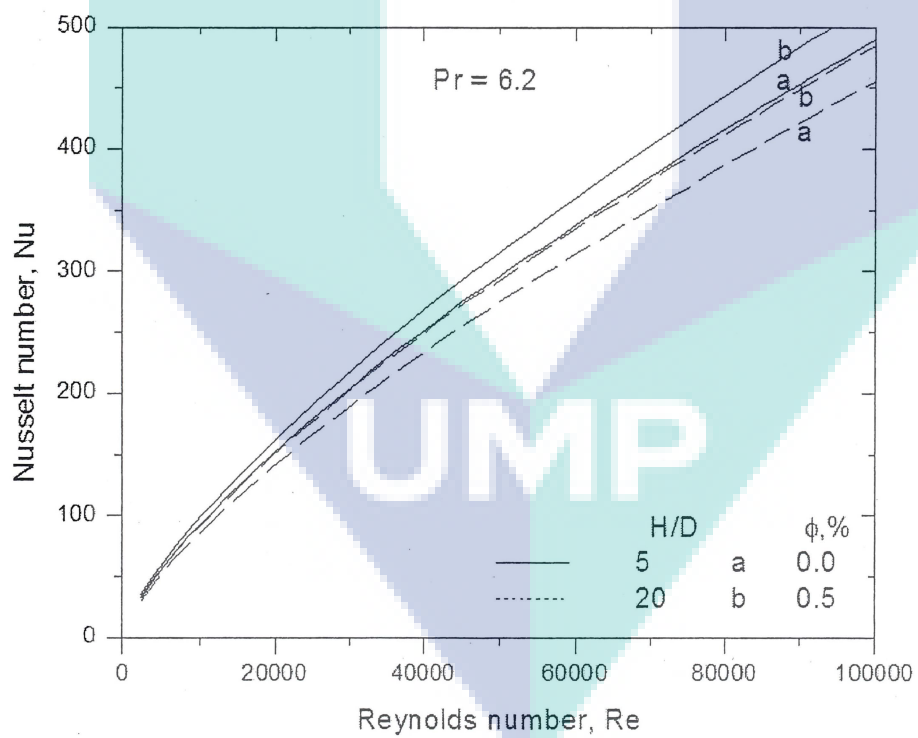
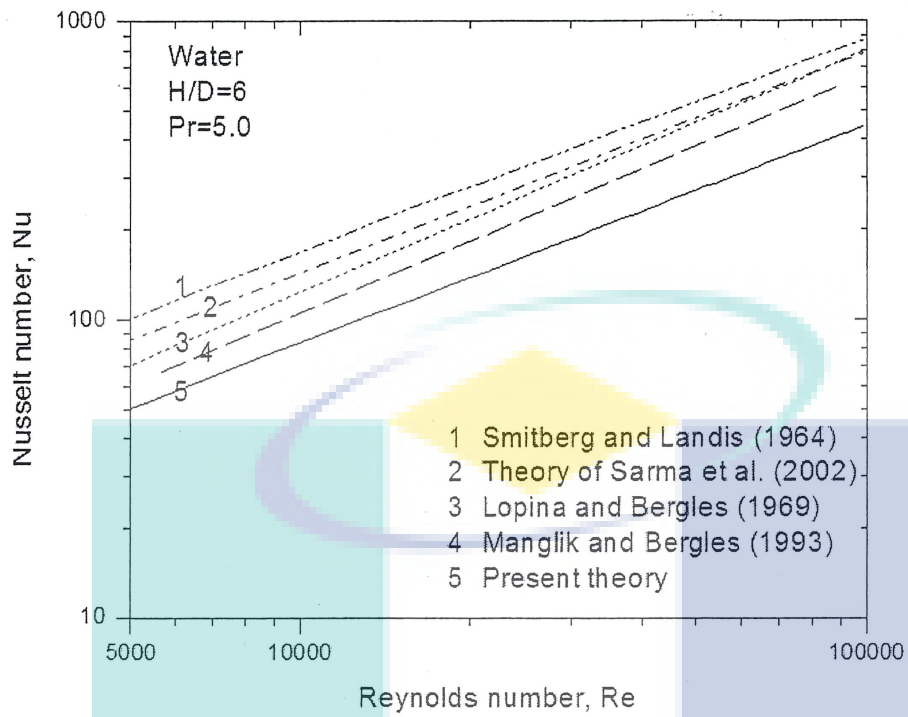
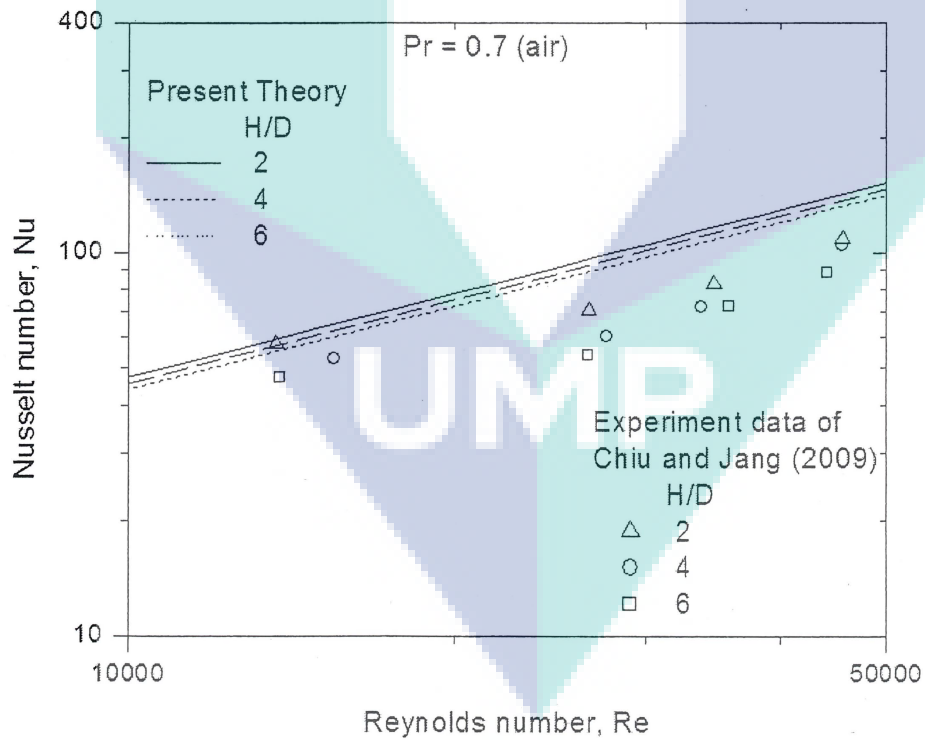


Figure 5.25: Influence of twist ratio and concentration on Nusselt number for Pr=6.2



**Figure 5.26:** Comparison of Nusselt number of various investigators with the present theory



**Figure 5.27:** Comparison of experimental data of air with the present theory for different twist

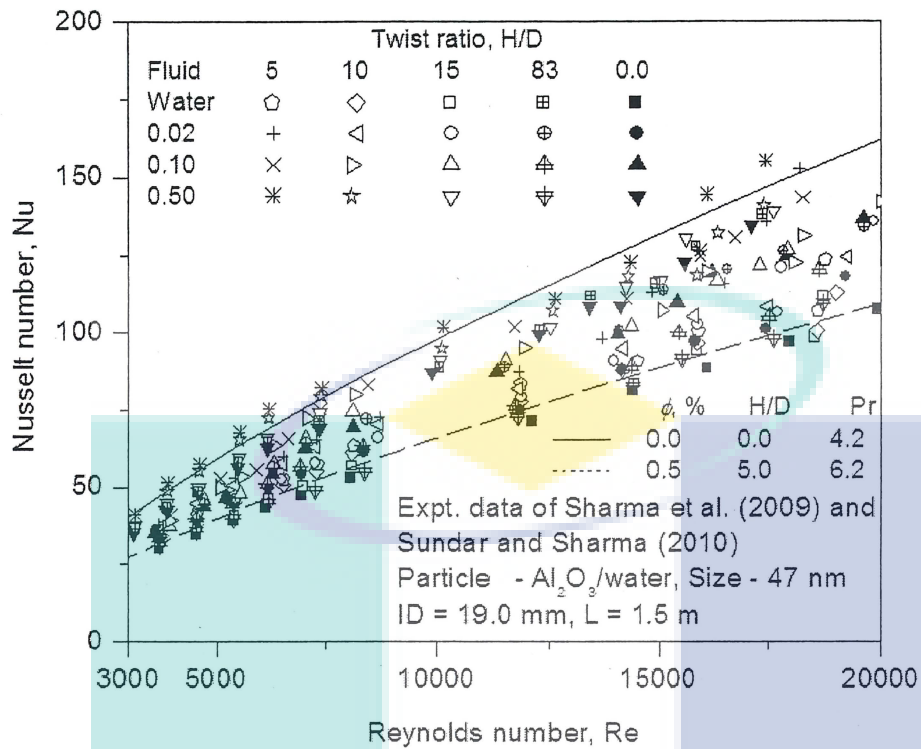


Figure 5.28: Comparison of experimental data of nanofluid at different concentrations and twist ratios

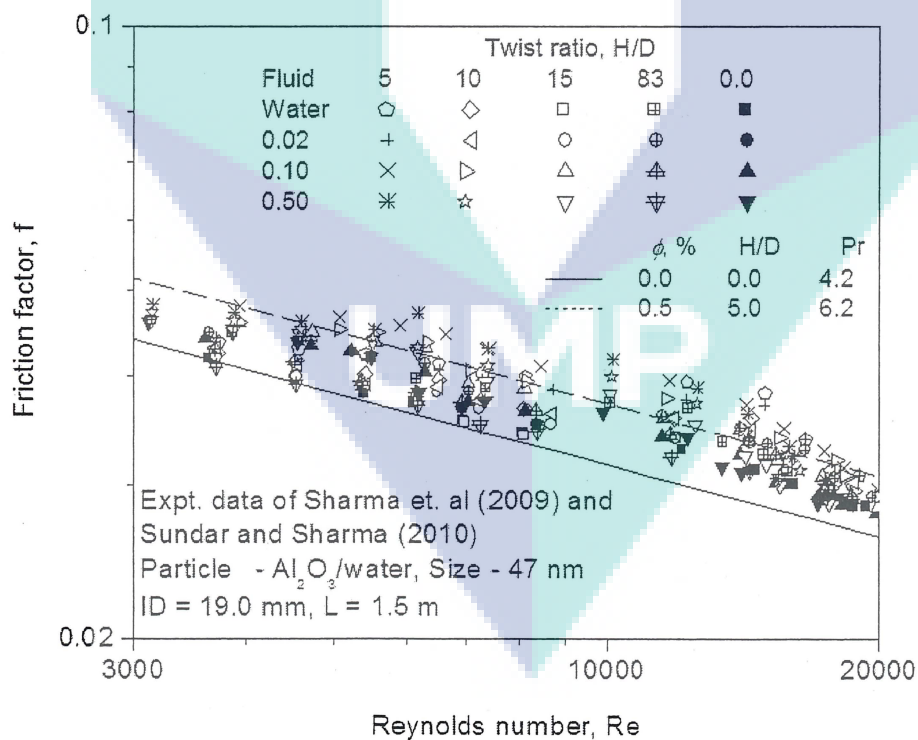


Figure 5.29: Variation of friction factor at different concentrations and twist ratios

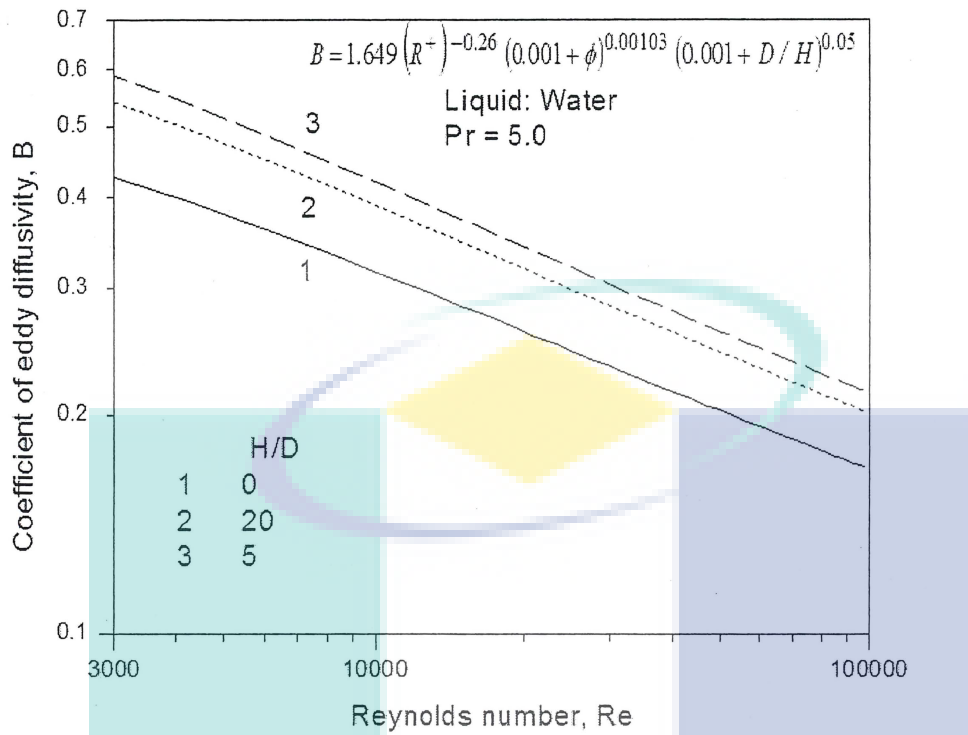


Figure 5.30: Variation of eddy diffusivity coefficient for water at different twist ratios

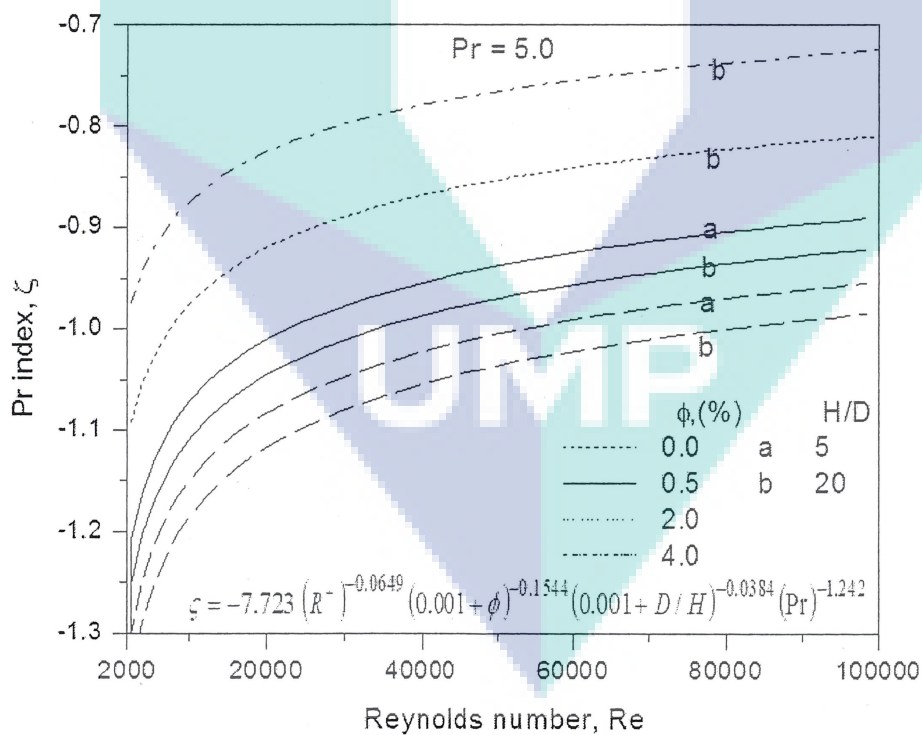


Figure 5.31: Variation of Prandtl index with concentration and twist ratio

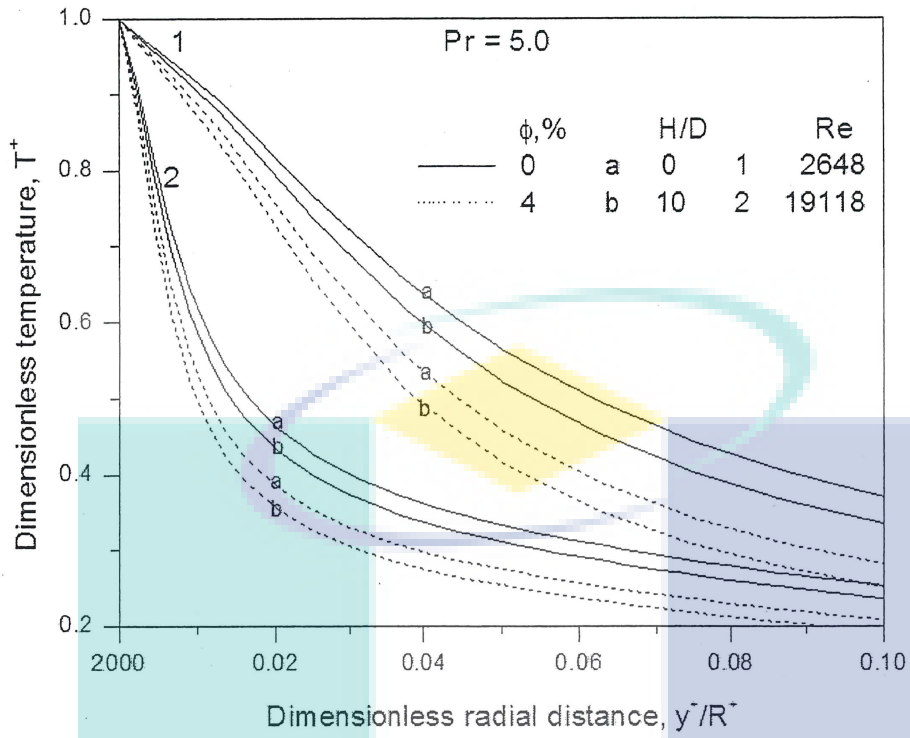


Figure 5.32: Variation of dimensionless temperature with distance

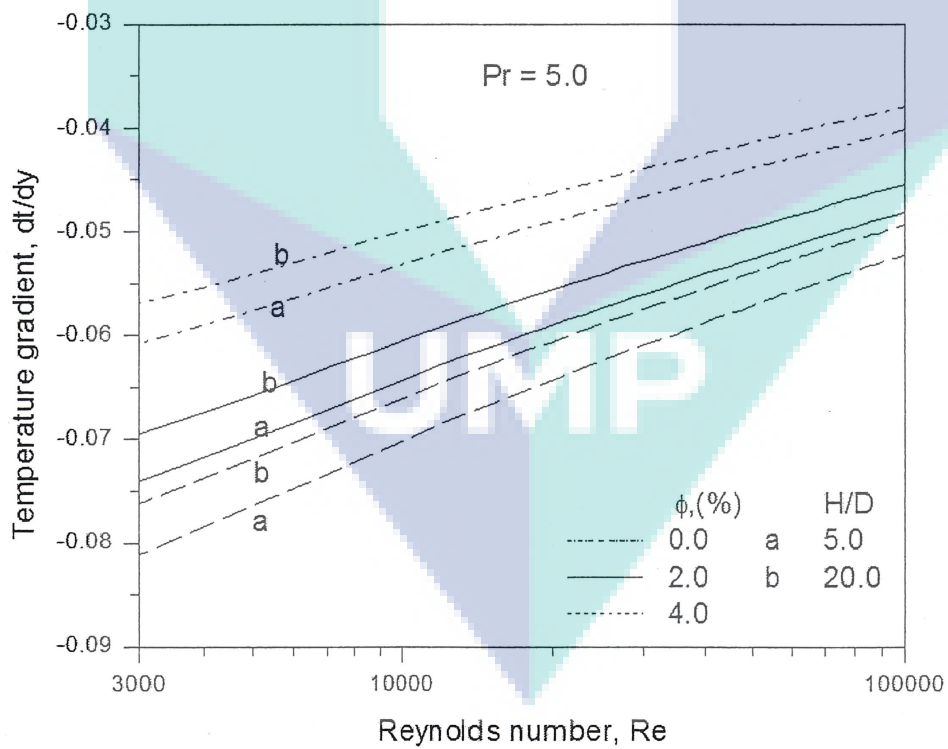
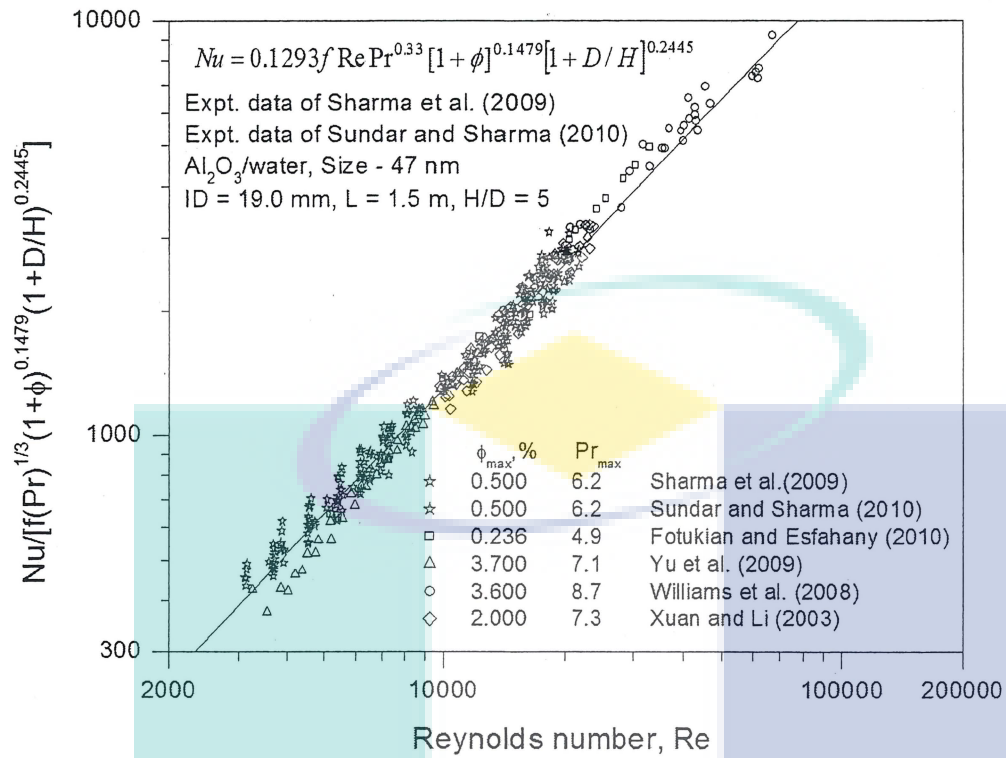


Figure 5.33: Variation of temperature gradient with concentration and twist ratio





**Figure 5.34:** Comparison of experimental data with the proposed equation for flow in a tube and for tape insert

UMP

## CHAPTER 6

### CONCLUSIONS

#### 6.1 SALIENT POINTS

The following conclusions are made from the theoretical and experimental investigations undertaken for flow in a tube and with twisted tape

- i. The viscosity of nanofluid increases with particle size and decreases with temperature. The thermal conductivity of nanofluid decreases with particle size and increases with temperature.
- ii. The nanofluid properties of metal and their oxide nanoparticles dispersed in water can be estimated with Eqs. (9) – (16) for volume concentration less than 4.0%.
- iii. The particle size, concentration and operating temperature are to be considered simultaneously for nanofluid to function as enhanced heat transfer fluid. Nanofluids of volume concentration less than 1.0%, the enhancement ratio increases with particle size and decreases with bulk temperature.
- iv. For particle size of less than 20nm and volume concentration more than 1.0%, the nanofluid bulk temperature less than 20°C predicts heat transfer enhancements.
- v. The Colburn type equation can predict the Nusselt number for a specified nanofluid volume concentration and water

$$St Pr_w^{2/3} = \frac{f}{8} (1 + \phi Pr_w)^{0.1185} \quad (22)$$

Where the friction factors are to be estimated with the Blasius equation

- vi. The equation is observed to predict the experimental data of various investigators.
- vii. The theoretical model of **Sarma et al. [32]** can be employed along with the eddy diffusivity equations to predict nanofluid Nusselt number.

- viii. Nanofluid heat transfer coefficients for volume concentration upto 3.7% in the turbulent range of Reynolds number can be estimated with the equation

$$Nu = 0.0304 Re^{0.7853} Pr^{0.4} [0.001 + \phi]^{0.01398} \quad (21)$$

- ix. The temperature gradients with twisted tapes are lower than obtained in flow in tubes under similar operating conditions

$$St Pr^{2/3} = 1.0344 \left( \frac{f}{8} \right) (1.0 + \phi)^{0.1479} \left( 1.0 + \frac{D}{H} \right)^{0.2445} \quad (27)$$

All the equations has been validated for water based nanofluids for  $\phi \leq 3.7\%$ ,  $3000 \leq Re \leq 70000$  and  $1.4 \leq Pr \leq 10.0$ .

- x. The Nusselt number estimated with the equation predict values close to experimental data for different nanofluids tested.
- xi. The experimental setup for the estimation of forced convection heat transfer coefficients is designed, commissioned and in working condition.
- xii. Thus the objectives envisaged in the project are achieved.

## 6.2 RECOMMENDATION AND FUTURE WORK

- i. Experiments are to be conducted at different particle sizes and temperatures to experimentally validate the analyzed phenomenon.
- ii. Experiments to determine heat transfer coefficients at different particle size are to be investigated.
- iii. Properties and heat transfer coefficients of water based CNT is to be investigated.

## REFERENCES

- Agarwal, S.K. and Raja Rao, M. 1996. Heat transfer augmentation for the flow of a viscous liquid in circular tubes using twisted tape inserts. *Int. J. Heat Mass Transfer*. 39(17): 3547-3557
- Akhavan-Behabadi, M.A., Kumar, R., Rajabi-najar, A. 2008. Augmentation of heat transfer by twisted tape inserts during condensation of R-134a inside a horizontal tube. *Heat Mass Transfer*. 44:651–657
- Ayub, Z.H. and Al-Fahed, S.F. 1993. The effect of gap width between horizontal tube and twisted tape on the pressure drop in turbulent water flow. *Int. J. Heat and Fluid Flow*. 14(1): 64-67
- Bandyopadhyay, P.S., Gaitonde, U.N., Sukhatme, S.P. 1991. Influence of free convection on heat transfer during laminar flow in tubes with twisted tapes. *Exp. Therm. Fluid Sci*. 4: 577–586
- Behzadmehr, A., Saffar-Avval, M., Galanis, N. 2007. Prediction of turbulent forced convection of a nanofluid in a tube with uniform heat flux using a two phase approach. *International Journal of Heat and Fluid Flow*. 28: 211 – 219
- Bergles, A.E. 1988. Some perspective on enhanced heat transfer-second-generation heat transfer technology. *J. Heat Transfer*. 110: 1082–1096
- Bianco., V., Chiacchio, F., Manca, O., Nardini, S. 2009. Numerical investigation of nanofluids forced convection in circular tubes. *Applied Thermal Engineering*. 29: 3632 – 3542
- Buongiorno, J. 2006. Convective transport in nano fluids. *J. Heat Transfer*. 128: 1-11
- Chang, S.W., Jan, Y.J., Liou, J.S. 2007. Turbulent heat transfer and pressure drop in tube fitted with serrated twisted-tape. *Int. J. Therm. Sci*. 46: 506–518
- Chiu, Yu-Wei and Jang, Jiin-Yuh. 2009. 3D numerical and experimental analysis for thermal–hydraulic characteristics of air flow inside a circular tube with different tube inserts. *Applied Thermal Engineering*. 29: 250–258
- Choi, S.U.S. 1995. Enhancing thermal conductivity of fluids with nanoparticles. In: Siginer, D.A. and Wang, H.P. (Eds). *Developments and Applications of Non-Newtonian Flows*. ASME. FED – Vol. 231/MD – Vol. 66: 99–105.

- Churchill, S.W. and Usagi, R.A. 1972. General expression for the correlation of rates of transfer and other phenomena. *AICHE*. 18(6): 1121-1128
- Colburn, A. P. 1964. A method of correlating forced convection heat transfer data and a comparison with fluid friction. *International Journal of Heat and Mass Transfer*. 7: 1359-1384
- Das, S.K., Putra, N., Thiesen, P., Roetzel, W. 2003. Temperature dependence of thermal conductivity enhancement for nanofluids. *Journal of Heat Transfer*. 125: 567-574
- Date, A.W. 1974. Prediction of fully developed flow in a tube containing a twisted tape. *Internat. J. Heat Mass Transfer*. 17: 845-859
- Dittus, F.W. and Boelter, L.M.K. 1930. Heat transfer in automobile radiators of the tubular type. *University of California Publication in Engineering*. 11: 443-461
- Doohyun Kim, Younghwan Kwon, Yonghyeon Cho, Chengguo Li, Seongir Cheong, Yujin Hwang, Jaekeun Lee, Daeseung Hong, Seongyong Moon. 2009. Convective heat transfer characteristics of nanofluids under laminar and turbulent flow conditions. *Current Applied Physics*. 9: 119-123
- Duangthongsuk, W. and Wongwises, S. 2010. An experimental study on the heat transfer performance and pressure drop of TiO<sub>2</sub>-water nanofluids flowing under a turbulent flow regime. *International Journal of Heat and Mass Transfer*. 53: 334 -344
- DuPlessis, J.P. and Kröger, D.G. 1984. Friction factor prediction for fully developed laminar twisted-tape flow. *International Journal of Heat and Mass Transfer*. 27: 2095-2100
- Eastman, Choi, J., Li, S., Yu, S., Thompson, W.L. 2001. Anomalously increased effective thermal conductivities of ethylene glycol-based nanofluids containing copper nanoparticles. *Appl. Phys. Lett.* 78: 718-720
- Eastman, J.A., Choi, S.U.S., Li, S., Thompson, L.J., Lee, S. 1997. Enhanced thermal conductivity through the development of nanofluids. *Material Research Society Symposium Proceedings*. Pittsburg, PA, Vol. 457: 3-11
- Eckert, E.R.G. and R Drake Jr., M. 1972. *Analysis of Heat and Mass Transfer*, McGraw-Hill. Kogakusha, Japan
- Fotukian S.M. and Esfahany, M.N. 2010. Experimental study of turbulent convective heat transfer and pressure drop of dilute CuO/water nanofluid inside a circular tube. *International Communications in Heat and Mass Transfer*. 37: 214-219
- Gnielinski, V. 1976. New equations for heat and mass transfer in turbulent pipe and channel flow. *International Chemical Engineering*. 16: 359-368

- Gosman, A. D., Pun, W. M., Runchal, A.K., Spalding, D.B., Wolfstein, M. 1969. *Heat and Mass Transfer in Recirculating Flows*. Academic Press, London
- Gwon Hyun Ko, Kyoungyoon Heo, Kyoungjun Lee, Dae Seong Kim, Chongyoun Kim, Yangsoo Sohn, Mansoo Choi. 2007. An experimental study on the pressure drop of nanofluids containing carbon nanotubes in a horizontal tube. *International Journal of Heat and Mass Transfer*. 50: 4749-4753
- Heris, S.Z., Esfahany, M.N., Etemad, S.G. 2007. Experimental investigation of convective heat transfer of  $Al_2O_3$ /water nanofluid in circular tube. *International Journal of Heat and Fluid Flow*. 28: 203-210
- Heris, S.Z., Etemad, S.G., Esfahany, M.N. 2006. Experimental investigation of oxide nanofluids laminar flow convective heat transfer. *International Communications in Heat and Mass Transfer*. 33: 529-535
- Herwig, H. and Kock, F. 2006. Local entropy production in turbulent shear flows: a tool for evaluating heat transfer performance. *Journal of Thermal Science*. 15(2): 159-167, 2006.
- Hong, S.W. and Bergles, A.E. (1976). Augmentation of laminar flow heat transfer in tubes by means of twisted-tape inserts. *Journal of Heat Transfer*. 98: 251-256
- Izadi, M., Behzadmehr, A., Jalali-Vahida, D. 2009. Numerical study of developing laminar forced convection of a nanofluid in an annulus. *International Journal of Thermal Sciences*. 48: 2119 – 2129
- Klaczak, A. 2001. Heat transfer by laminar flow in a vertical pipe and horizontal pipe with twisted-tape inserts. *Heat and Mass Transfer* 37: 443-448
- Kyo Sik Hwang, Seok Pil Jang, Choi, S.U.S. 2009. Flow and convective heat transfer characteristics of water-based  $Al_2O_3$  nanofluids in fully developed laminar flow regime. *International Journal of Heat and Mass Transfer*. 52: 193 – 199
- Lecjaks, Z., Machac, I., Sir, J. 1984a. Druckverlust bei der Stromung einer Fliissigkeit durch ein Rohr mit Schraubeneinbauten. *Chemical Engineering and Processing*. 18: 67-72; also see English translation as; 1987. Pressure loss in fluids' flowing in pipes equipped with helical screws. *International Chemical Engineering*. 27: 205-209
- Lecjaks, Z., Machac, I., Sir, J. 1984b. Warmeiibertragung bei der Stromung Newton'scher Fliissigkeiten in Rohren mit Schraubeneinheiten. *Chemical Engineering and Processing*. 18: 129-136; also see English translation as; 1987. Heat transfer to a newtonian liquid flowing through a tube with an internal helical element. *International Chemical Engineering*. 27: 210-217
- Lee, S., Choi, S.U.S., Li, S., Eastman, J.A. 1999. Measuring thermal conductivity of fluids containing oxide nanoparticles. *Journal of Heat Transfer*. 121: 280-289

- Lopina, R.F. and Bergles, A.E. 1969. Heat transfer and pressure drop in tape generated swirl flow of single phase water. *Trans. ASME J. Heat Transfer*. 91: 434–442
- Maiga, S.E.B., Palm, S.J., Nguyen, C.T., Roy, G., Galanis, N. 2005. Heat transfer enhancement by using nanofluids in forced convection flows. *International Journal of Heat and Fluid Flow*. 26: 530-546
- Manglik, R. M. 1991. *Heat Transfer Enhancement of Intube Flows in Process Heat Exchangers by Means of Twisted-Tape Inserts*. Ph.D. thesis, Department of Mechanical Engineering, Aeronautical Engineering and Mechanics, Rensselaer Polytechnic Institute, Troy, NY
- Manglik, R.M. and Bergles, A.E. 1993. Heat transfer and pressure drop correlations for twisted tape inserts in isothermal tubes: Part I - Laminar flows. *Trans. ASME J. Heat Transfer*. 115: 881–889
- Manglik, R.M. and Bergles, A.E. 1993. Heat transfer and pressure drop correlations for twisted-tape inserts in isothermal tubes: Part II - Transition and turbulent flows. *Trans. ASME J. Heat Transfer*. 115: 890–896
- Marner, W.J. and Bergles, A.E. 1989. Augmentation of highly viscous laminar heat transfer inside tubes with constant wall temperature. *Experimental Thermal and Fluid Science*. 2: 252-267
- Mazen Abu-Khader, M. 2006. Further understanding of twisted tape effects as tube insert for heat transfer enhancement. *Heat Mass Transfer*. 43: 123–134
- Metzner, A.B. and Friend, W.L. 1958. Theoretical analogies between heat, mass and momentum transfer and modifications for fluids of high Prandtl/Schmidt numbers. *Can. J. Chem. Eng.* 36: 235
- Namburu, P.K., Das, D.K., Tanguturi, K.M., Vajjha, R.S. 2008. Numerical Study of Turbulent Flow and Heat Transfer Characteristics of Nanofluids Considering Variable Properties. *International Journal of Thermal Sciences*. In Press, doi: 10.1016/j.ijthermalsci.2008.01.001
- Namburu, P.K., Kulkarni, D.P., Misra, D., Das, D.K. 2007. Viscosity of copper oxide nanoparticles dispersed in ethylene glycol and water mixture. *Experimental Thermal and Fluid Science*. 32: 397–402
- Naphon, P. 2006. Heat transfer and pressure drop in the horizontal double pipes with and without twisted tape insert. *International Communications in Heat and Mass Transfer*. 33: 166–175
- Nguyen, C. T., Desgranges, F., Roy, G., Galanis, N., Mare, T., Boucher, S., Mintsa, H. Angue. 2007. Temperature and particle-size dependent viscosity data for water-based nanofluids – Hysteresis phenomenon. *Int. J. Heat and Fluid Flow*. 28: 1492–1506

- Nguyen, C.T., Roy, G., Christian Gauthier, Galinis, N. 2007. Heat transfer enhancement using  $\text{Al}_2\text{O}_3$ -water nanofluid. *Applied Thermal Engineering*. 27: 1501-1506
- Pak, B.C. and Cho, Y.I. 1998. Hydrodynamic and heat transfer study of dispersed fluids with submicron metallic oxide particles. *Experimental Heat Transfer*. 11(2): 151 – 170
- Palm, S. J., Roy, G., Nguyen, C. T. 2004. Heat transfer enhancement in a radial flow cooling system using nanofluids. *Proceedings of the CHT-04/ICHMT International Symposium Advances Computational Heat Transfer*. April 19–24 Norway. Paper No. CHT-04-121. pp. 18
- Petukhov, B. S. 1970. Heat transfer and friction in turbulent pipe flow with variable physical properties. In *Advances in Heat Transfer*, ed. T. F. Irvine and J. P. Hartnett. Vol. 6. New York: Academic Press.
- Reynolds, O. 1874. On the extent and action of the heating surface for steam boilers. *Proc. Manchester Lit. Phil. Soc.* 14: 7-12
- Roy, G., Nguyen, C.T., Doucet, D., Suiro, S., Mare, T. 2006. Temperature dependent thermal conductivity evaluation of Alumina Based nanofluids. *Proceedings of the 13th IHTC*. 13–18 August 2006. Sydney, Australia
- Saha, S. K. and Dutta, A. 2001. Thermohydraulic study of laminar swirl flow through a circular tube fitted with twisted tapes. *ASME J. Heat Transfer*. 123: 417–427
- Sarma, P.K., Kedarnath Chada, Sharma, K.V., Sundar, L.S., Kishore, P.S., Srinivas, V. 2010. Experimental study to predict momentum and thermal diffusivities from convective heat transfer data of nano fluid with  $\text{Al}_2\text{O}_3$  dispersion. *International Journal of Heat and Technology*. Vol.28
- Sarma, P.K., Kishore, P.S., Rao, V.D., Subrahmanyam, T. 2005. A combined approach to predict friction coefficients and convective heat transfer characteristics in A tube with twisted tape inserts for a wide range of Re and Pr. *International Journal of Thermal Sciences*. 44: 393–398
- Sarma, P.K., Subramanyam, T., Kishore, P.S., Rao, V.D., Kakac, S. 2002. A new method to predict convective heat transfer in a tube with twisted tape inserts for turbulent flow. *International Journal of Thermal Sciences*. 41: 955–960
- Sharma, K.V. Sundar, L.S., Sarma, P.K. 2009. Estimation of heat transfer coefficient and friction factor in the transition flow with low volume concentration of  $\text{Al}_2\text{O}_3$  nanofluid flowing in a circular tube and with twisted tape insert. *International Communications in Heat and Mass Transfer*. 36: 503–507
- Smithberg, E. and Landis, F. 1964. Friction and forced convection heat transfer characteristics in tubes with twisted-tape swirl generators. *Trans. ASME J. Heat Transfer*. 86: 39–49



- Sundar, L.S. and Sharma, K.V. 2010. Turbulent heat transfer and friction factor of  $\text{Al}_2\text{O}_3$  Nanofluid in circular tube with twisted tape inserts. *International Journal of Heat and Mass Transfer*. 53: 1409–1416
- Tam, L.M. and Ghajar, A.J. 2006. Transitional heat transfer in plain horizontal tubes. *Heat Transfer Engineering*. 27: 23-38
- Thorsen, R. and Landis, F. 1968. Friction and heat transfer characteristics in turbulent swirl flow subjected to large transverse temperature gradients. *Trans. ASME J. Heat Transfer*. 90: 87–98
- Trinh, K.T. 1969. *A boundary layer theory for turbulent transport phenomena*. M.E. Thesis,, New Zealand, University of Canterbury.
- Trinh, K.T. 2010. Reflections on a Penetration Theory of Turbulent Heat Transfer. arXiv.org [physics.flu-dyn] [Online]. Available: <http://arxiv.org/abs/1009.2280>
- Tsai, C.Y., Chien, H.T., Ding, P.P., Chan, B., Luh, T.Y., Chen, P.H. 2003. Effect of structural character of gold nanoparticles in nanofluid on heat pipe thermal performance. *Materials Letters*. 58: 1461-1465
- Vajjha, R.S. and Das, D.K. 2009. Experimental determination of thermal conductivity of three nanofluids and development of new correlations. *International Journal of Heat and Mass Transfer*. 52: 4675-4682
- Vassallo, P., Kumar, R., Damico, S. 2004. Pool boiling heat transfer experiments in silica-water nanofluids. *International Journal of Heat and Mass Transfer*. 13: 474-480
- Wang, X., Xu, X., Choi, S.U.S. 1999. Thermal Conductivity of Nanoparticle–Fluid Mixture. *Journal of Thermophysics and Heat Transfer*. 13(4): 474-480
- Watanabe, K., Taira, T., Mori, Y. 1983. Heat transfer augmentation in tubular flow by twisted tapes at high temperatures and optimum performance. *Heat Transfer—Japanese Research*. 12(3): 1-31
- Wen, D. and Ding, Y. 2004. Experimental investigation into convective heat transfer of nanofluids at the entrance region under laminar flow conditions. *International Journal of Heat and Mass Transfer*. 47: 5181–5188
- Williams, W., Buongiorno, J., Lin-Wen Hu. 2008. Experimental investigation of turbulent convective heat transfer and pressure loss of alumina/water and Zirconia/water nanoparticle colloids (nanofluids) in horizontal tubes. *Journal of Heat Transfer*. 130: 042412(1-7)
- Xuan, Y., and Li, Q. 2000. Heat transfer enhancement of nanofluids. *International Journal of Heat and Fluid Flow*. 21: 58-64

- Xuan, Y. and Li, Q. 2003. Investigation on convective heat transfer and flow features of nanofluids. *Journal of Heat Transfer*. 125: 151–155
- Xuan, Y. and Roetzel, W. 2000. Conceptions for Heat Transfer Correlation of Nanofluids. *Int. J. Heat Mass Transf.* 43: 3701–3707
- Yang, Y., Zhang, Z.G., Grulke, E.A., Anderson, W.B., Wu, G. 2005. Heat transfer properties of nanoparticle-in-fluid dispersions (nanofluids) in laminar flow. *International Journal of Heat and Mass Transfer*. 48: 1107–1116
- You, S.M., Kim, J.H., Kim, K.H. 2003. Effect of nanoparticles on critical heat flux of water in pool boiling heat transfer. *Appl. Phys. Lett.* 83: 3374-3376
- Yu, W., France, D.M., Smith, D.S., Singh, D., Timofeeva, E.V., Routbort, J.L. 2009. Heat transfer to a silicon carbide/water nanofluid. *International Journal of Heat and Mass Transfer*. 52: 3606-3612
- Yulong Ding, Haisheng Chen, Yurong He, Alexei Lapkin, Mahboubeh Yeganeh, Lidija Šiller, Yuriy V. Butenko. 2007. *Advanced Powder Technology*, 18(6): 813-824
- Yulong Ding, Hajar Alias, Dongsheng Wen, Richard A. Williams. 2006. Heat transfer of aqueous suspensions of carbon nanotubes (CNT nanofluids). *International Journal of Heat and Mass Transfer*. 49: 240-250
- Yurong He, Yi Jin, Haisheng Chen, Yulong Ding, Daqiang Cang, Huilin Lu. 2007. Heat transfer and flow behaviour of aqueous suspensions of TiO<sub>2</sub> nanoparticles (nanofluids) flowing upward through a vertical pipe. *International Journal of Heat and Mass Transfer*. 50: 2272 – 2281
- Yurong He, Yubin Men, Yunhua Zhao, Huilin Lu, Yulong Ding. 2009. Numerical investigation into the convective heat transfer of TiO<sub>2</sub> nanofluids flowing through a straight tube under the laminar flow conditions. *Applied Thermal Engineering*. 29: 1965 – 1972

UMP

## LIST OF PUBLICATIONS

The list of publications based on this project is as follows:

1. Sharma, K.V., Sundar, L.S., Sarma, P.K. 2009. Estimation of heat transfer coefficient and friction factor in the transition flow with low volume concentration of  $Al_2O_3$  nanofluid flowing in a circular tube and with twisted tape insert. *International Communications in Heat and Mass Transfer*. 36: 503–507
2. Sharma, K.V., Sarma, P.K., Noor, M.M., Kadirgama, K., Wan Azmi Wan Hamzah, Rosli A.Bakar. 2009. Thermal conductivity estimation of oxide nanofluids in water – Influence of particle properties. Accepted for presentation at the *International Conference on Nano Technology (ICONT-2009)*. 14-17 December, Bayview Hotel, Langkawi, Malaysia
3. Wan Azmi Wan Hamzah, Sharma, K.V., Mohd Hanif Md Saad. 2009. Estimation of nanofluid heat transfer coefficient using Artificial Neural Network (ANN). Accepted for presentation at the *International Conference on Nano Technology (ICONT 2009)*. 14 – 17 December, Bayview Hotel, Langkawi, Malaysia
4. Sundar, L.S. and Sharma, K.V. 2010. Turbulent heat transfer and friction factor of  $Al_2O_3$  Nanofluid in circular tube with twisted tape inserts. *International Journal of Heat and Mass Transfer*. 53: 1409–1416
5. Sarma, P.K., Kedarnath Chada, Sharma, K.V., Sundar, L.S., Kishore, P.S., Srinivas, V. 2010. Experimental study to predict momentum and thermal diffusivities from convective heat transfer data of nano fluid with  $Al_2O_3$  dispersion. *International Journal of Heat and Technology*. Vol.28
6. Sharma, K.V., Sarma, P.K., Azmi, W. H., Noor, M.M., Kadirgama, K., Rizalman Mamat. 2010. Validation of turbulent flow heat transfer data of water based nanofluids, 18 *International Conference on Composites/Nano Engineering*. July 4-10, Anchorage, Alaska, USA
7. Azmi, W. H., Sharma, K.V., Rizalman Mamat, Zuhairi, S. M., Hisham, M. A. 2010. Estimation of Forced Convection Heat Transfer Coefficient of Nanofluids Using the Concept of Colburn Analogy. *The 2<sup>nd</sup> National Conference In Mechanical Engineering For Research & Post Graduate Studies (NCMER 2010)*. December 3-4, UMP, Pahang, Malaysia

8. Azmi, W. H., Sharma, K.V., Sarma, P.K., and Rizalman Mamat. 2010. Influence of Certain Thermo-Physical Properties on Prandtl Number of Water Based Nanofluids. *National Conference in Mechanical Engineering Research and Postgraduate Students (1<sup>st</sup> NCMER 2010)*. 26-27 MAY 2010, FKM Conference Hall, UMP, Kuantan, Pahang, Malaysia; pp. 502-515 ISBN: 978-967-5080-9501

